NEW, ENVIRONMENTALLY FRIENDLY, NON-TOXIC CORROSION INHIBITORS

A Dissertation

by

NG JUN HONG CLARENCE

Submitted to the Graduate and Professional School of
Texas A&M University
in partial fulfillment of the requirements for the degree of

DOCTOR OF PHILOSOPHY

Chair of Committee,	Nobuo Morita
Committee Members,	Hadi Nasrabadi
	Mahmoud El-Halwagi
	John Lee
Head of Department,	Jeff Spath

December 2021

Major Subject: Petroleum Engineering

ABSTRACT

Acid treatments are commonly used in the oilfield to remove inorganic scale or to stimulate formations. These treatments typically consist of mineral acids such as hydrochloric acid (HCl), organic acids, or chelating agents. At elevated temperatures, these acids are highly corrosive and can cause severe damage to tubulars and downhole equipment. In order to mitigate some of the damage from these acids, corrosion inhibitors are added to the treatment solution.

Corrosion inhibitors used in the oil and gas industry are typically quaternary amines or sulfur-containing compounds. These compounds adsorb to the surface of the metal, thereby reducing contact between the metal surface and the corrosive substance. However, these corrosion inhibitors are damaging to the environment and harmful to human health. Alternative new environmentally-friendly corrosion inhibitors are also either toxic to the human body or face performance limitations at higher temperature field applications.

In this work, new, environmentally friendly, non-toxic corrosion inhibitors will be investigated. These corrosion inhibitors will be developed from commonly eaten foods, spices, and aromatics in order to ensure their environmental friendliness and non-toxicity. Deriving them from commonly eaten foods also ensures that they will be widely available. Firstly, potential candidates will be obtained from local grocery stores or online retailers. They will then be ground to increase the surface area and immersed in HCl in order to allow for the extraction of any possible inhibiting molecules into the solution. N-80 metal

coupons will then be immersed in the extracted solution, and the corrosion rates can be determined. This will be carried out at room temperature conditions for 6h. Following this, the most successful candidates will be tested at temperatures up to 300°F. They will then be tested in the presence of other additives to determine the influence of external additives on their performance. Finally, extracts of these chemicals will be determined and tested in order to verify the chemical compound that is providing the corrosion resistance.

Initial work shows that out of the 99 different samples tested, several showed promising results. This was determined by comparing the results from these tests to a control case where no corrosion inhibitor was used. 9 of these promising samples were then tested at 150°F where 3 were further eliminated. By obtaining the corrosion rate for all cases, the inhibition efficiency of each sample can be determined. Only samples with inhibition efficiency of 90% and higher will be tested at higher temperatures.

DEDICATION

This work is dedicated to my parents, siblings, friends, and my late advisor Dr. Hisham Nasr-El-Din for their continuous support and encouragement all the way.

ACKNOWLEDGEMENTS

I would like to express my sincere thanks to my committee chair, Dr. Morita for taking me under his wing during this trying time. I would also like to thank my committee members for their guidance and advice throughout the course of my research.

I would also like to thank my friends and colleagues who have provided immense help in my research. Special thanks to my friends Tariq Almubarak, Kenta Nakajima, 'Jude' and 'Aya' Elric for their efforts and encouragement throughout my PhD program.

Finally, thank you to my parents, and all my brothers for their financial and emotional support all these years.

CONTRIBUTORS

I would like to thank my committee chair Dr. Morita and my other committee members for their input to better my work. I would also like to extend special thanks to Dr. Tariq Almubarak who has been a source of inspiration for me during my Ph.D.

FUNDING SOURCES

No financial support was used during this work.

NOMENCLATURE

H_2S – Hydrogen Sulfide

HCl – Hydrochloric Acid

PEEK – Polyether Ether Ketone

Room temperature – 77°F

NMR – Nuclear Magnetic Resonance

LC-MS – Liquid Chromatography Mass Spectrometry

gpt – gallon of chemical per thousand gallons of water

DCl – Deuterium Chloride

CDCl3 – Deuterated Chloroform

TMS – Tetramethyl Silane

MeOD – Deuterated Methanol

ACS – American Chemical Society

TABLE OF CONTENTS

Page

LIST OF FIGURES

Page

LIST OF TABLES

Page

CHAPTER I

INTRODUCTION

Hydrochloric acid (HCl) is commonly used in stimulation treatments such as matrix acidizing, acid fracturing, scale removal, and mud filtercake removal due to its strong dissolving capabilities as well as low cost (Chang et al. 2008; Rafie et al. 2014; Almubarak et al. 2020; Ramanathan et al. 2020). However, at high temperatures, HCl becomes highly corrosive and will therefore result in severe corrosion of well tubulars and equipment downhole (Buijse et al. 2004; Mahmoud et al. 2010; Almubarak et al. 2017). To reduce the damage from corrosion, corrosion inhibitors are required. In addition, at temperatures above 200°F, corrosion inhibitor intensifiers such as potassium iodide (KI) and formic acid are required (Al-Katheeri et al. 2002; Cassidy et al. 2007; Al-Taq et al. 2012; Khadom et al. 2018). Commonly used corrosion inhibitors, however, are usually harmful to the environment as well as to human health (Raja and Sethuraman 2008; Rani and Basu 2012; Chigondo and Chigondo 2016). The objective of this paper is to present an alternative variety of corrosion inhibitors that are environmentally friendly and non-toxic.

There are eight main types of corrosion (Fontana and Greene 1967): uniform corrosion, galvanic corrosion, crevice corrosion, pitting, intergranular corrosion, selective leaching, erosion, and stress-corrosion cracking. Each of these corrosion types involves a unique mechanism and thus requires a different method of protection. In the petroleum industry, the use of mineral acids such as HCl, organic acids such as formic acid, and the presence of chloride ions causes uniform corrosion, crevice corrosion, and pitting to be

the most prevalent forms of corrosion present (Finsgar and Jackson 2014). Under specific conditions, other forms of corrosion have also been observed in the oil field, such as stress-corrosion cracking in the presence of hydrogen sulfide (H_2S).

Many commonly used corrosion inhibitors act by adsorbing to the surface of the metal to create a protective layer that reduces contact between the metal surface and the corrosive substance. This inhibits the cathodic/anodic reactions or poisons the production of H_2 on the surface of the metal (Rostami and Nasr-El-Din 2009). There are a variety of organic compounds that have been used as corrosion inhibitors such as acetylenic alcohols (Foster et al. 1959; Bockris 1991; Barmatov et al 2015), imidazolines (Chen et al. 2000; Durnie et al. 2002; Yang et al. 2016), Mannich bases (Elewady and Mostafa 2009; Tang et al. 2019), and quartenary ammonium salts (El Dahan et al. 1999; Hegazy et al. 2014). In general, the most common types of corrosion inhibitors used in the oil and gas industry are typically quaternary amines or sulfur-containing compounds (Son 2007; Ng et al. 2018). These corrosion inhibitors usually contain sulfur, nitrogen, and oxygen atoms as they help the molecule better adsorb to the surface of the metal. Since many naturally occurring chemicals also have these groups, it is no wonder they would also possess corrosion-inhibiting properties.

Many authors have examined plant extracts and products as corrosion inhibitors. Khamis and Alandis (2002) tested the corrosion inhibiting properties of thyme, coriander, hibiscus, anise, black cumin, and garden cress in 0.3 wt.% sulfuric acid on steel at 77°F. They found thyme showed the best corrosion inhibition efficiency at 93.8% and the remaining herbs showing various inhibition efficiencies between 37.4% and 85.9%.

Ginger extract was also studied as a corrosion inhibitor in 1.0 M HCl on mild steel at room temperature over 22 hours (Fidrulsli et al. 2018). The authors observed an inhibition efficiency ranging between 86% and 91% depending on the concentration of extract used. Parthipan et al. (2018) tested the effect of garlic extract as a corrosion inhibitor on carbon steel and stainless steel in produced water. They showed an 81% inhibition efficiency for carbon steel and 75% inhibition efficiency for stainless steel as well as antibacterial properties over the 20 day long test at 98.6°F. Elmsellem et al. (2014) showed that curcumin, a major component in turmeric, had a corrosion rate of 0.0001 lb/ft^2 per hour, which was a 93% inhibition efficiency compared to the control solution. The experiment was carried out using 3.6 to 7.2 wt.% HCl at 95°F. Zucchi and Omar (1985) investigated the corrosion inhibition properties of papaya, peacock flower, coffee senna, and devil's snare seeds, as well as those of papaya, giant milkweed, neem tree and Auforpio turkiale sap on mild steel. The authors showed that the inhibitors had corrosion rates from 0.0002 to 0.00055 lb/ft2 per hour in 3.6 wt.% HCl solutions and 0.0003 to 0.0008 lb/ft2 per hour in the 7.2 wt.% HCl solutions at 84°F. The corrosion inhibition properties of jasmine tea extract were also tested on Q235 carbon steel in 3.6 wt.% HCl between 68°F and 176°F over 5 hours by Tang et al. (2018). Using electrochemical methods, the authors determined that the inhibition efficiency ranged between 41.6% and 97.4%. Yaro et al. (2011) tested peach juice as a corrosion inhibitor for mild steel in 3.6 wt.% HCl between 86°F and 140°F. They found that the peach juice showed a corrosion rate of 0.00094 lb/ft2 per hour. Sedik et al. (2020) examined the effect of dardagan fruit extract with 3.6 wt.% HCl as a corrosion inhibitor for mild steel at 77°F and observed a 92% corrosion inhibition

efficiency over 1 hour of testing. da Rocha (2010) tested aqueous extracts of mango, orange, passion fruit, and cashew peels as corrosion inhibitors on mild steel in 3.6 wt.% HCl at 77°F for up to 24h. They observed a range of inhibition efficiencies of 67% to 86% over 1h and 93% to 96% over 24h. Zhao et al. (2019) used bitter gourd in 3.6 wt.% HCl to determine its effectiveness as a corrosion inhibitor on mild steel at 77°F and observed inhibition efficiencies between 55% and 96%. Umoren et al. (2015) tested red apple juice as a corrosion inhibitor for mild steel at temperatures between 86°F and 140°F in 1.8 wt.% HCl and found inhibition efficiencies of up to 90%. However, these corrosion inhibitors derived from natural products have not been tested extensively at temperatures above 150°F and higher acid concentrations. As can be observed, these tests are generally carried out at low temperatures and with HCl concentrations much lower than in acidizing fluids.

Metals used in the oil industry can generally be divided into 2 categories: low-carbon steel and corrosion resistant alloys (CRAs). Low-carbon steels such as C-90, N-80 and L-80 are iron based metals alloyed with carbon and low manganese content. Examples of typical compositions of these steels are shown in Table 1 below.

Table 1: Material composition of some API grade low carbon steel metals commonly used in the oil and gas industry (API Spec 5CT 2005).

Metal	Composition (wt.%)								
	Fe	C	Mn	Cr	Ni	Cu	S	P	Si
C-90	Bal.	-	-	-	-	-	<.03	<.03	-
N-80	Bal.	-	-	-	-	-	<.03	<.03	-
L-80	Bal.	0.43	1.9	-	0.25	0.35	0.03	0.03	0.45
P-110	Bal.	-	-	-	-	-	<.03	<.03	-

These steels are relatively cheap and are thus a popular choice for casing and tubing material. CRAs refer to metals such as stainless steels and other non-iron based alloys such as Hastelloy or Incoloy. These metals usually contain chrome, nickel, and molybdenum to enhance their corrosion resistance. Table 2 shows the composition of several CRAs that have been widely used in industry.

Table 2: Material composition of some CRAs commonly used in the oil and gas industry (Craig and Smith 2001)

Metal	Composition (wt.%)							
	Cr	Ni	Mo	Fe	Mn	C	N	Other
13Cr	13	-	-	Bal.	0.8	0.2	-	-
S13Cr	11-13	1-6	1-2	Bal.	0.2-0.5	0.025	-	0 - 2.0 Cu, Ti
22Cr Duplex	22	5	3	Bal.	1	0.02	0.15	-
316L	17	12	2.5	Bal.	1	0.02	-	-

Due to its widespread usage in the oil and gas industry, N-80 was chosen as the sample material for these tests (Finsgar and Jackson 2014). S13Cr was also used to determine the effectiveness of the corrosion inhibitor on CRAs.

Corrosion inhibitors are additives that must be included in acidizing treatments in order to minimize damage to the tubulars and other downhole equipment. However, these inhibitors are also typically environmentally damaging and harmful to human health (Singh and Bockris 1996). Therefore, this paper seeks to examine the corrosion inhibiting properties of several edible seed extracts at downhole conditions with high concentrations of HCl.

CHAPTER II

MATERIALS

Coupons

N-80 and S13Cr coupons with a surface area of approximately 3.62 in2, and centered holes of 0.15 in diameter were prepared according ASTM G31. A single coupon was used per corrosion test. They were washed with DI water followed by acetone and allowed to air dry. The coupons were polished by the manufacturer with a 600 grit finish and therefore no further polishing was required. After drying, the coupons were weighed on a scale with 1 mg accuracy to determine the mass of the coupon prior to the corrosion test.

Chemicals

15 wt.% HCl solution was used for all the corrosion tests and emulsified acid experiments. This acid solution was prepared by diluting a stock solution of 36.5 wt.% ACS grade HCl using College Station tap water (<500 ppm). In order to prepare the emulsified acid, diesel was obtained from a nearby gas station using a 1 gallon gas can. The emulsifier used was obtained from a service company.

Solvents were also used to dissolve the sample to test its effectiveness in a solvent. Acetone and isopropyl alcohol were obtained from hardware stores. 99% purity methanol was obtained from a chemical company and 95% purity ethanol was obtained from a local liquor store.

CHAPTER III EQUIPMENT

HPHT Corrosion Reactor

Room temperature tests were carried out by suspending the coupon in a 150 mL beaker containing the HCl solution. Teflon tape was passed through the holes on the top of the coupon and the ends tied around a beaker cover and held together with a bread clip. This would allow the coupon to be suspended in the acidic solution. An example of the setup used can be seen in Figure 1 below.

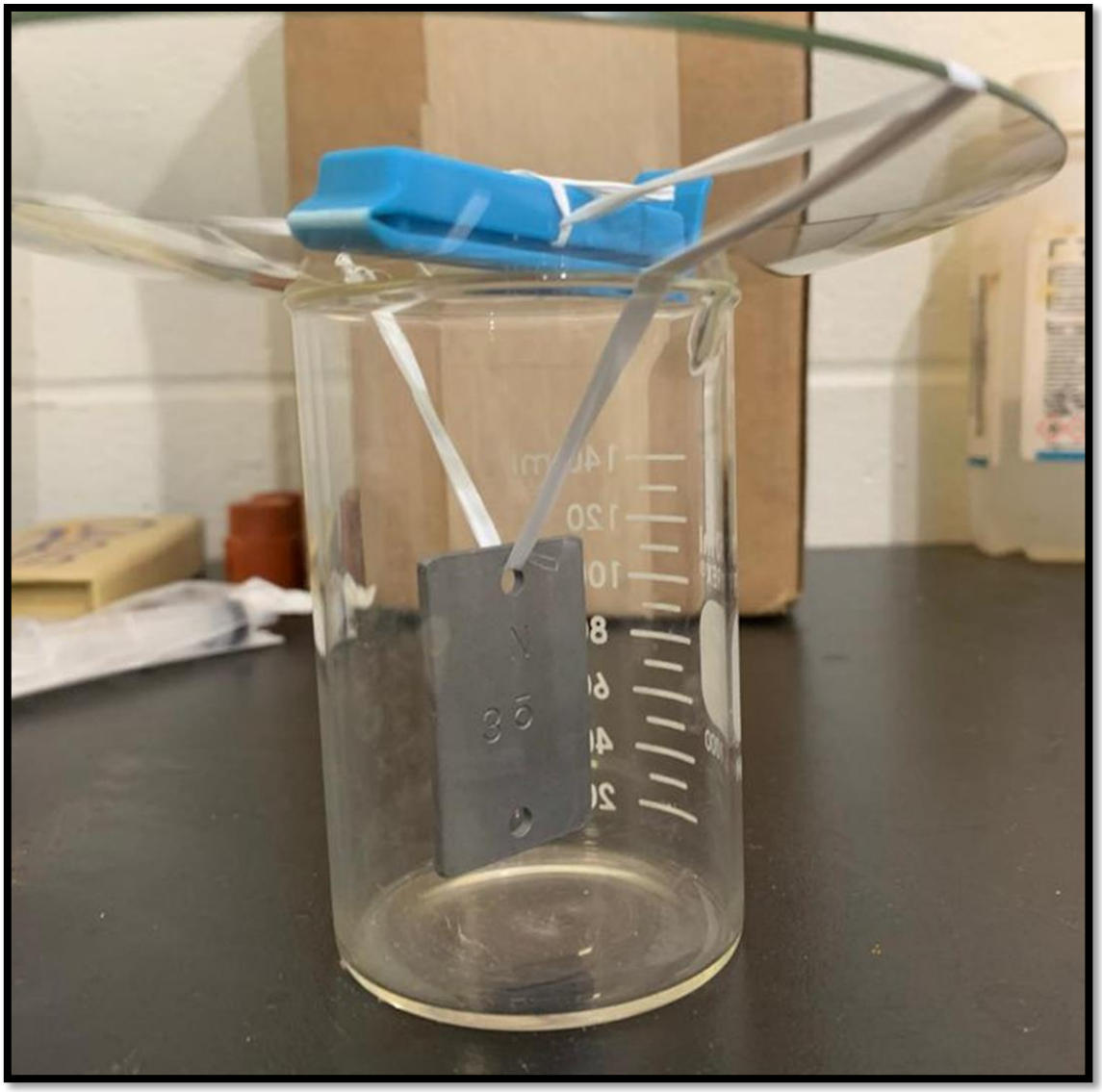

Figure 1: Setup for room temperature tests.

High temperature corrosion tests were carried out in a Series 4523 1 liter Hastelloy B benchtop reactor with a maximum temperature and pressure rating of 662°F and 1,800 psi purchased from Parr Instruments. The set-up is shown in Figure 2. The prepared coupons will be mounted on the coupon holder using PEEK (Polyether ether ketone) screws and washers to prevent galvanic corrosion with the Hastelloy B holder. The coupon and

solution were placed into the reactor autoclave which is sealed by 2 C-clamps. N_2 gas is supplied to the reactor from a tank connected to the reactor using a series of rubber hoses and check valves. Gas from the reactor was released into a scrubber containing 400 ml DI water to remove any harmful vapors before releasing it into a fumehood.

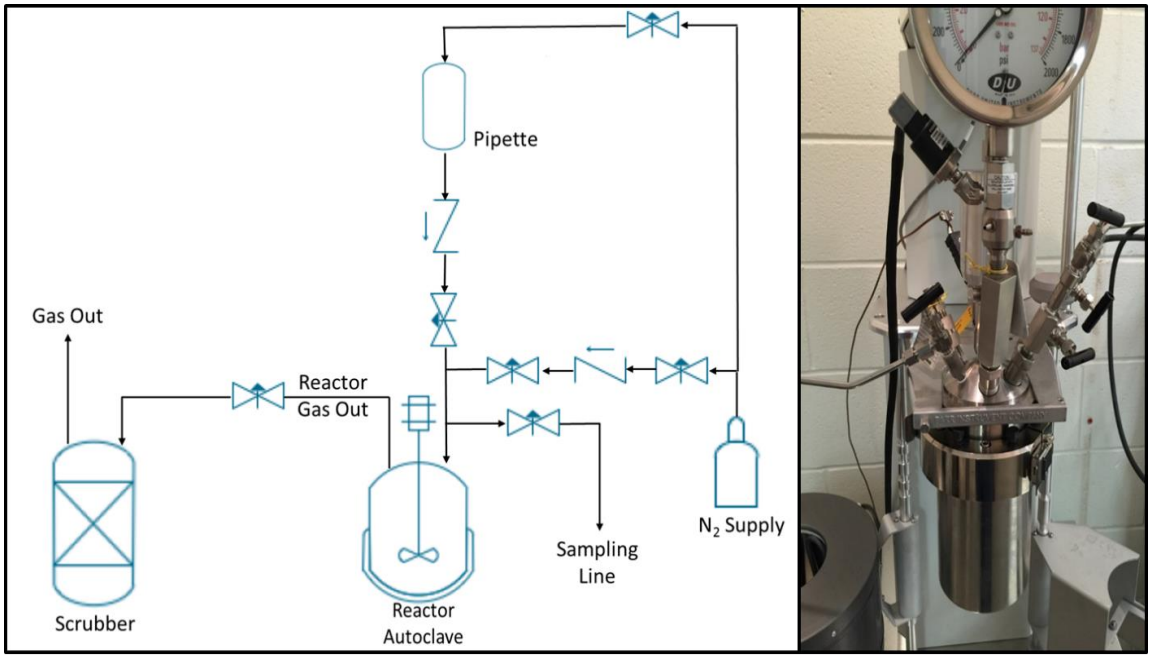

Figure 2: Schematic of autoclave used for corrosion tests.

Nuclear Magnetic Resonance (NMR)

A 5 mm thin wall precision NMR sample tube (Wilmad 528PP-8) was charged with 600 µl of filtered solution and the NMR spectra recorded on a Bruker Avance 500 MHz NMR spectrometer. The spectra were processed using MestReNova version 11.0.2-17801.

Liquid Chromatography Mass Spectroscopy (LC-MS)

20 µL of the filtrated sample (diluted 1 to 10 with methanol) was separated on a Waters Xbridge BEH C18 column (130Å, 5 µm, 4.6 x 100 mm) using a 20% to 100% acetonitrile + 0.1% formic acid gradient over 12 minutes at a flow rate of 0.750 mL/min and subjected to electrospray ionization. Ions were detected using a MSQ Plus single quadrupole mass spectrometer in positive mode.

CHAPTER IV

EXPERIMENTAL PROCEDURES

Room Temperature Tests

For each of the room temperature tests, 140g of 15 wt.% HCl solution was prepared from a 36.4 wt.% HCl stock solution diluted with tap water (<500 ppm). 2 wt.% of each sample was then added to the beaker containing the solution and mixed thoroughly before lowering the coupon in. The coupon was then soaked for 6 hours in the mixture. After the 6 hours, the coupon was removed from the solution and tap water was used to rinse the coupon of the acid solution. Acetone was then used to wash the coupon in order to remove any corrosion inhibitor layer that had formed on the coupon's surface as well as to remove excess water on the surface. The coupon was then weighed on a 1 mg scale to determine its final mass. A control test was carried out to present a baseline corrosion rate for comparison in the absence of a corrosion inhibitor.

Autoclave Corrosion Tests

For the high-temperature tests, 700g of 15 wt.% HCl solution was prepared using the stock solution in a similar manner to that of the room temperature tests. 2 wt.% of seed extract was then added to each test at all temperatures and the resulting solution thoroughly mixed with a magnetic stirrer and stir bar. The temperatures tested were between 150 to 300°F to determine the maximum effective temperature of the corrosion inhibitor. For the tests at 200°F, 1 corrosion inhibitor intensifier was used while at temperatures at 250°F

and above, 2 corrosion inhibitor intensifiers were used. All tests were carried out over a duration of 6 hours. As before, a control test was also carried out to determine a base corrosion rate.

Pressure in the autoclave was kept at 400 PSI using inert N_2 gas to prevent excessive evaporation of the acid solution. The N_2 gas was passed through the solution for about 10 minutes before the start of the test in order to deaerate the solution. This is to prevent the effects of O_2 on the test. Dimensions and weight of the coupon were taken before and after each test to determine the corrosion rate using the weight loss method according to equation 1:

$$\frac{Initial\ Weight - Final\ Weight}{Surface\ Area} = Corrosion\ Rate\ (\frac{lb}{ft^2}) \quad \text{..... (1)}$$

This equation was also used to calculate the corrosion rate of the coupons for the room temperature tests. For the tests at room temperature, the effectiveness of the sample was determined by the corrosion inhibitor efficiency that was calculated as shown in equation 2:

$$\frac{Base\ Corrosion\ Rate - Sample\ Corrosion\ Rate}{Base\ Corrosion\ Rate} \text{ x } 100 = Corrosion\ Inhibition\ Efficiency\ (\%) \text{... (2)}$$

Emulsified Acid Preparation

For the tests involving emulsified acid, the 15 wt.% HCl solution was first prepared from a 36.4 wt.% HCl stock solution and diluted with tap water (<500 ppm) to meet the desired acid cocnentration. The corrosion inhibitor and corrosion inhibitor intensifier were added to the acid and thoroughly mixed before being placed in a 2 L separatory funnel which was suspended over a 1 L Waring blender as shown in Figure 3 below.

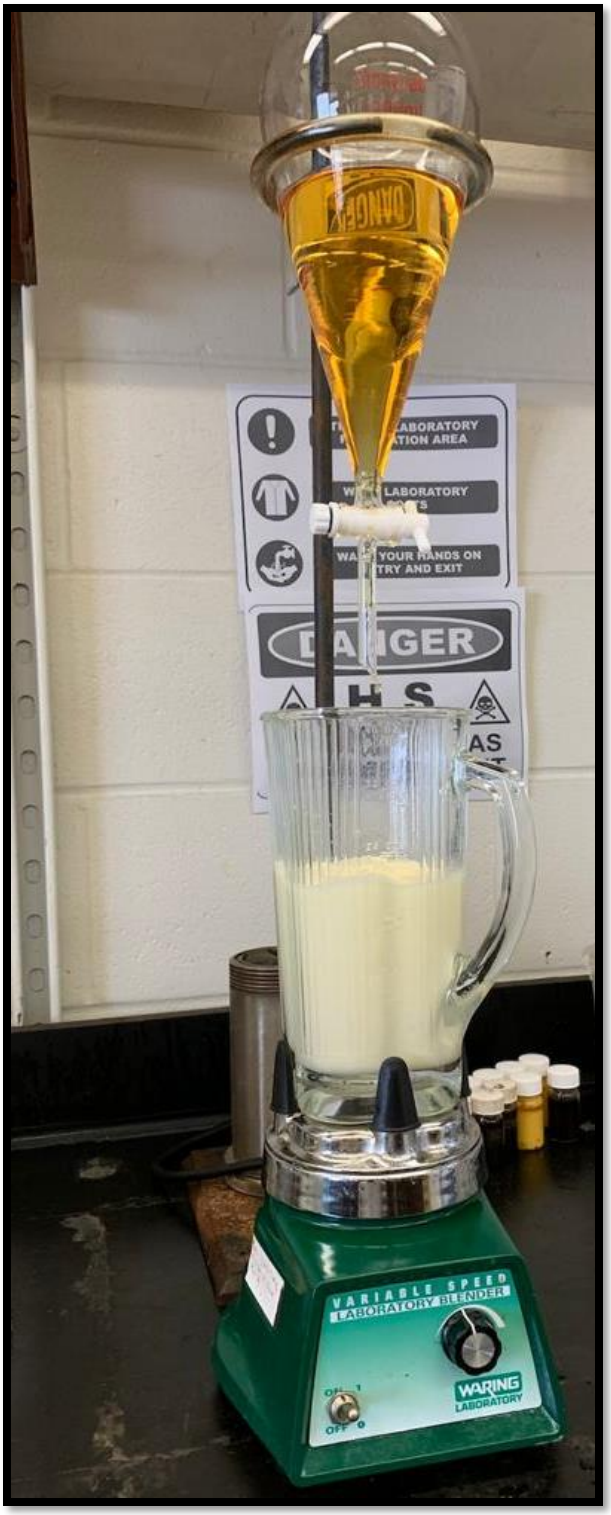

Figure 3: Setup to mix emulsified acid.

Diesel was then added to the blender and subsequently, the desired volume of emulsifier was added, and the mixture was blended at a medium shear rate for 10 minutes to ensure proper mixing. Before adding the acid, care was taken to ensure a proper vortex was present, which indicated adequate shear rate and ensure proper mixing of the acid and diesel phases. After the 10 minutes, the acid was then added dropwise into the center of the vortex and was allowed to drip until all of the acid was added. Throughout the mixing process, care was taken to ensure that the vortex did not close as a result of the increasing viscosity of the emulsified acid. After all the acid was added, the mixture was allowed to mix for a further 30 minutes. The resulting emulsion was then tested using a drop test and a conductivity test to verify the stability and ratio of the emulsion. 1 L of emulsified acid was prepared per batch in a 70:30 acid to diesel ratio.

Preparation for Chemical Analysis

In order to identify the chemicals responsible for corrosion inhibition, chemical analysis using NMR and LC-MS were carried out. The samples were tested before and after degradation at high temperature to determine if they would maintain their chemical structure during the high temperature corrosion tests.

For the chemical analysis of samples prior to degradation, they were first dissolved in 2 ml deuterated choloroform ($CDCl_3$) containing a reference of 0.05% tetramethylsilane (TMS) (99.8% purity) and subsequently filtered through a 0.2 micron polytetrafluoroethylene syringe filter. This was to remove the excess, undissolved

particles from the $CDCl_3$ solution. The filtrate was then used for the NMR and LC-MS analyses.

To prepare a solution of the degraded products, a 20 ml scintillation vial was charged with a stir bar and 100 mg of each sample was resuspended with 4 ml of 15 wt.% DCl (deuterium chloride). This DCl solution was created by diluting 35 wt.% DCl with D_2O (Deuterium Oxide). The scintillation vial was then tightly sealed, stirred, and heated to 200°F. After 10 minutes, the vessel was vented and resealed. After 6 hours, the samples were allowed to cool before concentration *in vacuo* and further drying overnight under high vacuum. The degraded products were resuspended in 2 ml deuterated methanol (MeOD) containing a reference of 0.05% tetramethylsilane (99.8% purity) and filtered through a 0.2 micron polytetrafluoroethylene syringe filter prior to NMR and LC-MS analysis.

CHAPTER V

ROOM TEMPERATURE TESTS

Seed Samples

In order to determine the type of samples to buy, a cursory survey of various foods was carried out. This focused on strong-smelling spices and aromatics since many of these foods contain molecules fitting the criteria of corrosion inhibitors. The corrosion rate observed for the room temperature control test was 0.0142 lb/ft^2 over the 6 hours of testing. This rate is shown in each table of results to provide a basis for comparison. The 85 different foods tested could be divided into 5 main categories: seeds, flowers, stems, fruits, and leaves. Any other sample that did not fall into this category was placed into the miscellaneous category.

Table 3: Corrosion rates for seed samples tested in 15 wt.% HCl over 6 hours.

Seed	Corrosion Rate (lb/ft^2)	Inhibition Efficiency %
Base	0.0142	-
1	0.00008	99.4
2	0.00428	69.9
3	0.00169	88.1
4	0.00184	87.0
5	0.00251	82.3
6	0.0013	90.8
7	0.00359	74.7
8	0.01181	16.8
9	0.00403	71.6
10	0.00245	82.7
11	0.00462	67.5
12	0.00336	76.3
13	0.00336	76.3
14	0.00253	82.2
15	0.00327	77.0
16	0.00263	81.5
17	0.00421	70.4
18	0.00294	79.3
19	0.00385	72.9

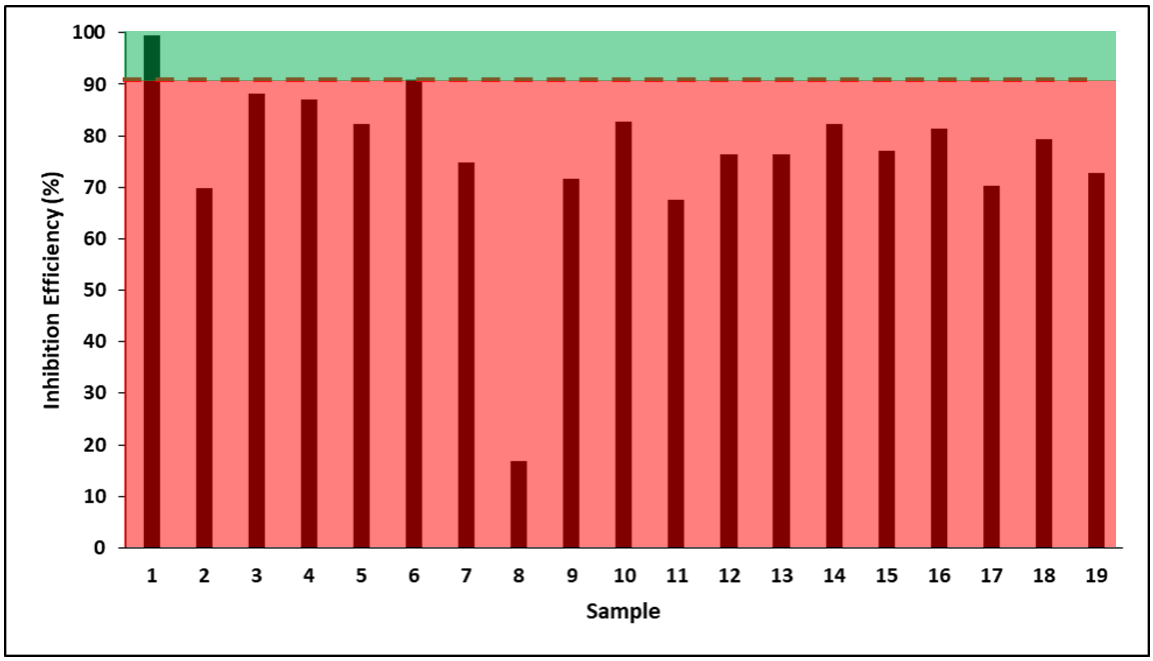

Figure 4: Illustration of corrosion test results for 19 seed samples in 15 wt.% HCl at room temperature (72°F) over 6h. Corrosion inhibition efficiencies lying in the green area represent successful tests.

Table 3 shows the results for the seeds tested. Many of the seed samples did well, averaging a 76.1% corrosion inhibition efficiency across all the samples tested. However, of the seeds tested, only seed samples 1 and 6 were above 90% corrosion inhibition efficiency and would be tested at higher temperatures. These corrosion test results are illustrated in graphical form in Figure 4 above for better visualization.

Flower Samples

Table 4: Corrosion rate of flower samples tested in 15 wt.% HCl over 6 hours.

Sample	Corrosion Rate (lb/ft^2)	Inhibition Efficiency %
Base	0.0142	-
1	0.0109	23.2
2	0.00252	82.3
3	0.01346	5.2
4	0.00017	98.8
5	0.00088	93.8
6	0.01211	14.7
7	0.00347	75.6
8	0.00382	73.1
9	0.0013	90.8
10	0.00231	83.7
11	0.00322	77.3
12	0.00253	82.2
13	0.01503	-5.8

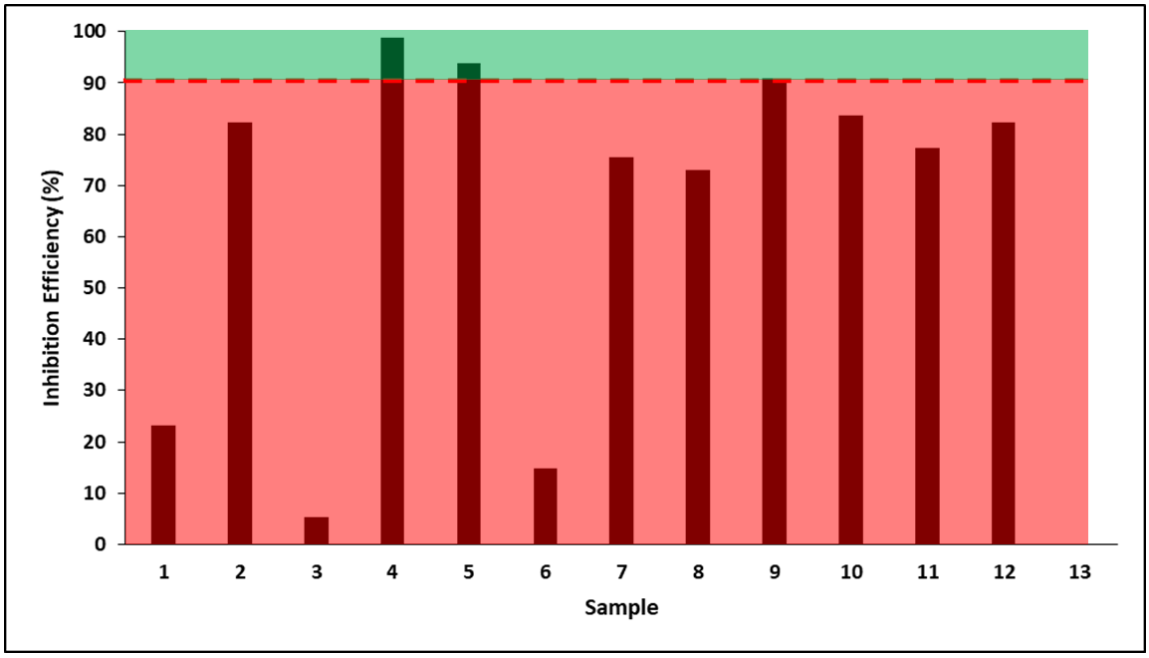

Figure 5: Illustration of corrosion test results for 13 flower samples in 15 wt.% HCl at room temperature (72°F) over 6h. Corrosion inhibition efficiencies lying in the green area represent successful tests.

Table 4 shows the corrosion rates of the flower samples tested. Compared to the seed samples, the flowers did not perform well with a 61.1% corrosion inhibitor efficiency average. Flower 13 was even found to increase the corrosion rate of the solution. These results are again illustrated in Figure 5, which shows the significant difference in corrosion inhibiting properties among the various flower samples.

Stem Samples

Table 5 shows the corrosion rates of the stem samples tested. The average corrosion inhibition efficiency was 78.5%, which is comparable to the results of the seed samples. Stem samples 1 to 3 performed extremely well with samples 1 and 2, providing nearly 100% inhibition efficiency. Figure 6 illustrates these results, showing that samples 1 and 2 did especially well compared to the other seeds tested.

Table 5: Corrosion rate of stem samples tested in 15 wt.% HCl over 6 hours.

Sample	Corrosion Rate (lb/ft^2)	Inhibition Efficiency %
Base	0.0142	-
1	0.00009	99.4
2	0.00001	99.9
3	0.00079	94.4
4	0.00355	75.0
5	0.0045	68.3
6	0.00438	69.2
7	0.00315	77.8
8	0.00265	81.3
9	0.0053	62.7

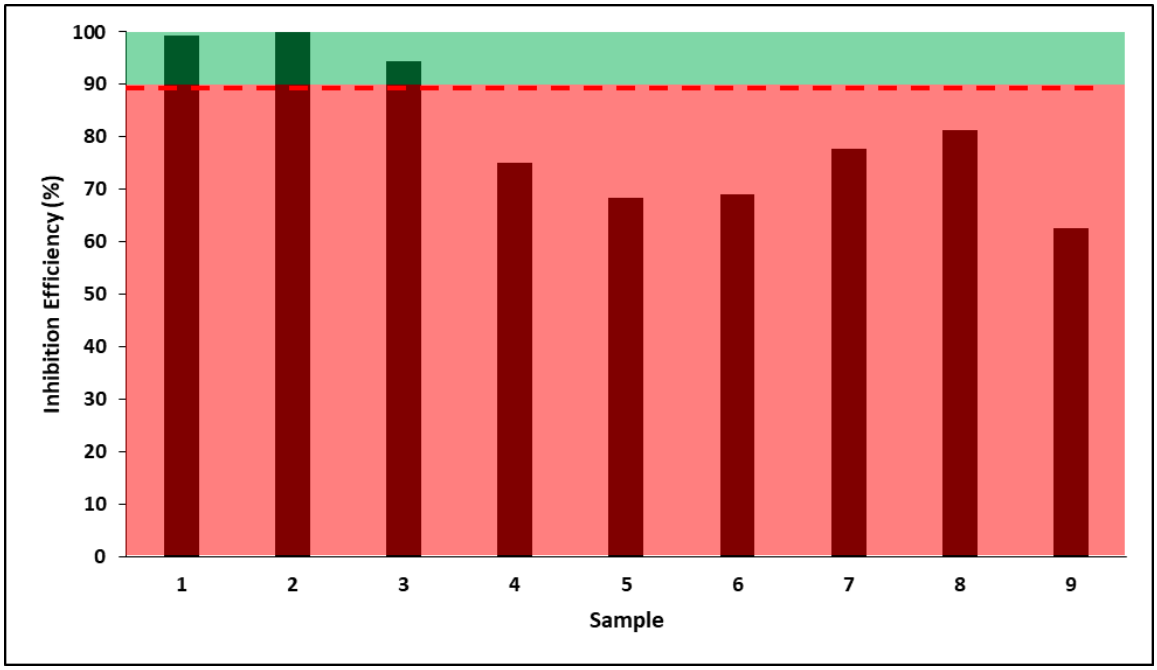

Figure 6: Illustration of corrosion test results for 9 stem samples in 15 wt.% HCl at room temperature (72°F) over 6h. Corrosion inhibition efficiencies lying in the green area represent successful tests.

Fruit Samples

The next set of samples tested were 14 different fruits, as shown in Table 6. The results for this set of samples were mixed, with some giving very good corrosion inhibitor efficiency while others like fruits 11 and 12 end up corroding the metal even more. These results are shown in Figure 7, where the poor performance of fruits 8, 11, and 12 can be seen in contrast to the other fruit samples tested.

Table 6: Corrosion rate of fruit samples tested in 15 wt.% HCl over 6 hours.

Sample	Corrosion Rate (lb/ft^2)	Inhibition Efficiency %
Base	0.0142	-
1	0.00025	98.2
2	0.00009	99.4
3	0.0035	75.4
4	0.00614	56.8
5	0.00382	73.1
6	0.00365	74.3
7	0.00617	56.5
8	0.01252	11.8
9	0.00541	61.9
10	0.00644	54.6
11	0.01522	-7.2
12	0.01944	-36.9
13	0.00718	49.4
14	0.00617	56.5

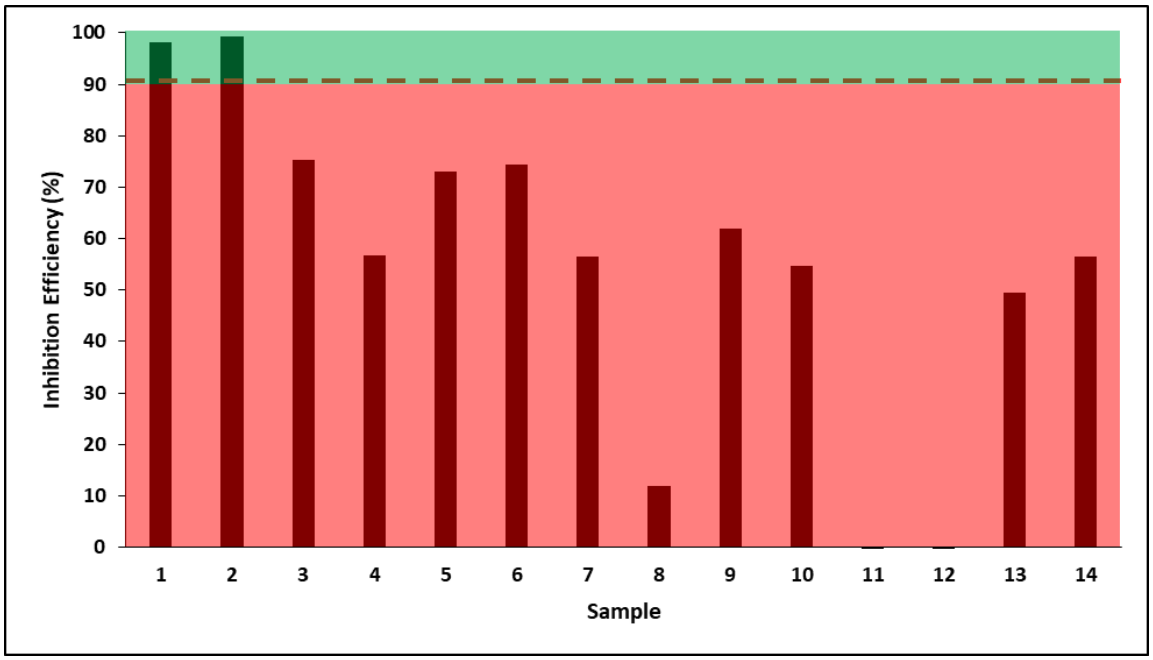

Figure 7: Illustration of corrosion test results for 14 fruit samples in 15 wt.% HCl at room temperature (72°F) over 6h. Corrosion inhibition efficiencies lying in the green area represent successful tests.

Leaf Samples

Table 7 shows the performance of the 20 different leaves tested. The leaves showed an average corrosion inhibition efficiency of 64.9%. Leaf samples 9 and 20 provided the best corrosion inhibition efficiency at 91.7% and 92.7%, respectively. Figure 8 shows that while more leaves were tested than samples in the other categories, most of them were unsuccessful at providing adequate corrosion inhibition.

Table 7: Corrosion rate of leaf samples tested in 15 wt.% HCl over 6 hours.

Sample	Corrosion Rate (lb/ft^2)	Inhibition Efficiency %
Base	0.0142	-
1	0.00607	57.3
2	0.01221	14.0
3	0.00339	76.1
4	0.01107	22.0
5	0.00503	64.6
6	0.00481	66.1
7	0.00756	46.8
8	0.00693	51.2
9	0.00118	91.7
10	0.00196	86.2
11	0.00359	74.7
12	0.00433	69.5
13	0.0026	81.7
14	0.0026	81.7
15	0.00384	73.0
16	0.0035	75.4
17	0.0049	65.5
18	0.01254	11.7
19	0.00267	81.2
20	0.00104	92.7

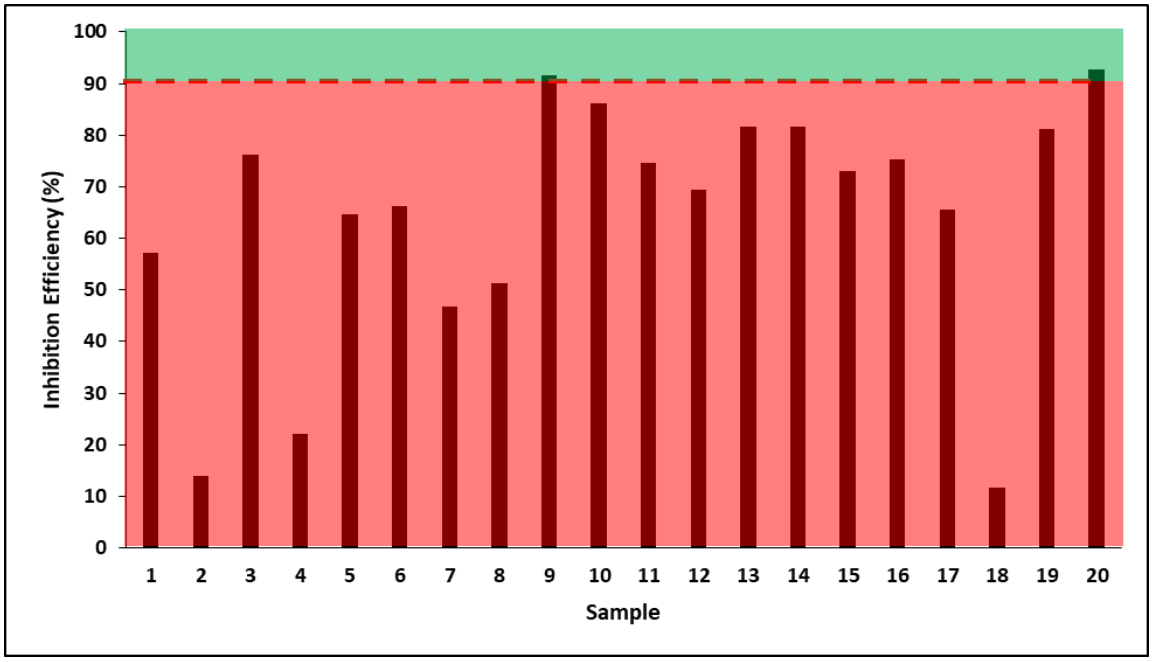

Figure 8: Illustration of corrosion test results for 20 leaf samples in 15 wt.% HCl at room temperature (72°F) over 6h. Corrosion inhibition efficiencies lying in the green area represent successful tests.

Miscellaneous Samples

Finally, the foods falling into the miscellaneous category were tested and the results are shown in Table 8 below. In this category, samples 4 and 13 were found to enhance corrosion rates, while samples 6 to 10 provided excellent corrosion inhibition efficiency. This is better illustrated in Figure 9. With these results, the chemical nature of each sample attaining more than 90% corrosion inhibitor was studied and were tested at 150°F and 200°F.

Table 8: Corrosion rate of the miscellaneous samples tested in 15 wt.% HCl over 6 hours.

Sample	Corrosion Rate (lb/ft^2)	Inhibition Efficiency %
Base	0.0142	-
1	0.0101	28.9
2	0.00426	70.0
3	0.00754	46.9
4	0.01649	-16.1
5	0.0041	71.1
6	0.00036	97.5
7	0.0003	97.9
8	0.01386	2.4
9	0.00467	67.1
10	0.01899	-33.7

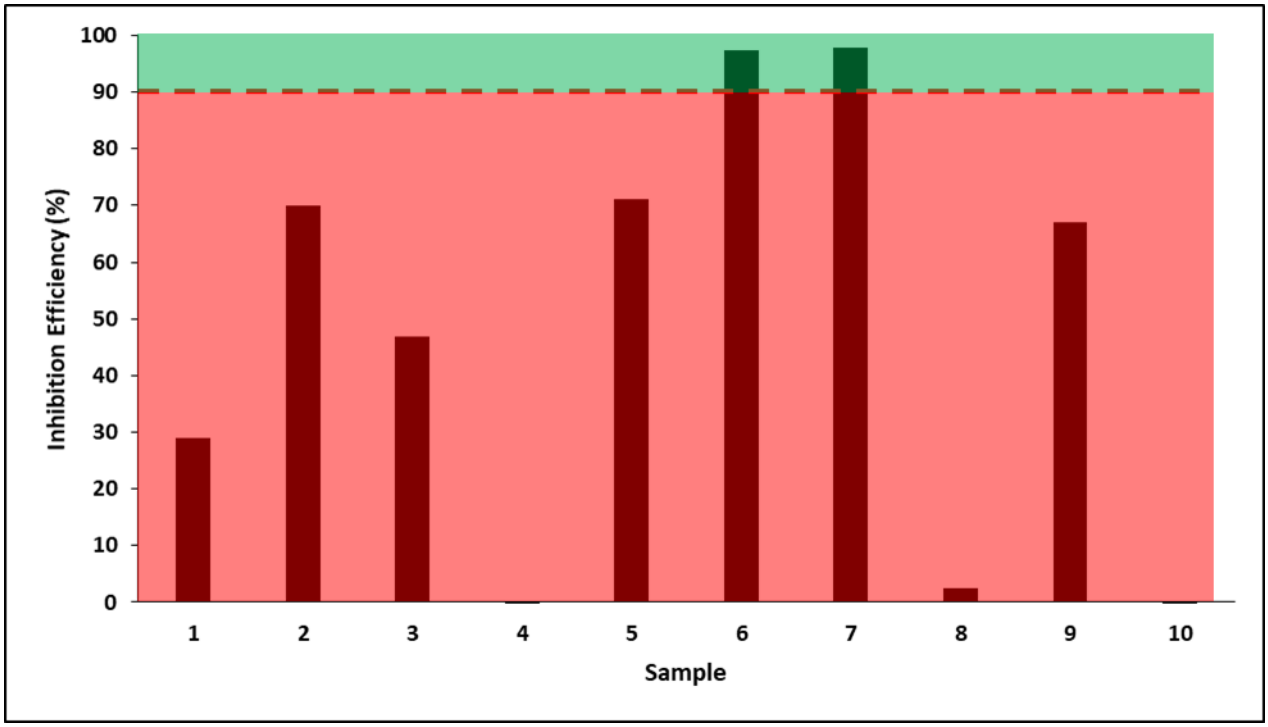

Figure 9: Illustration of corrosion test results for 10 miscellaneous samples in 15 wt.% HCl at room temperature (72°F) over 6h. Corrosion inhibition efficiencies lying in the green area represent successful tests.

Table 9: List of tested plant material and miscellaneous products.

	Seed		Fruits		Stem		Leaves		Flowers		Miscellaneous
Magnoliid	1	Angiosperms	1	Monocot	1	Thymus	1	Syzygium	1	Caffeine	1
Sinapis	2	Solanales	2	Quebracho	2	Salvia	2	Jasmineae	2	Henna	2
Mace	3	Cayenne	3	Aloe Vera	3	Petroselinum	3	Rosebud	3	Coffeemate	3
Papaver	4	Chilli Flakes	4	Allium Sativum	4	Laurus	4	Daisy	4	Cream of Tartar	4
Heracleum	5	Orange	5	Allium Schoenoprasum	5	Coriandrum	5	Nepetoideae	5	Curry	5
Suletteria	6	Lemon	6	Brassica	6	Anethum	6	Rosepetals	6	Melatonin	6
Black Sesame	7	Carica	7	Nepeta	7	Salvia	7	Hibisceae	7	Cigarette Butts	7
Sesame	8	Punica	8	Allium Cepa	8	Origanum Vulgare	8	Chrysanthemum	8	Ascorbic Acid	8
Prunus	9	Sour grapes	9	Cinnamomim	9	Mentha	9	Malpighiale	9	Viagra	9
Illicium	10	Paprika	10			Olea	10	Sambucus	10	Tannic Acid	10
Nutmeg	11	Rhus	11			Ficus	11	Tagetes	11		
Cashew	12	Pimenta	12			Murraya	12	Humulus	12		
Fenugreek	13	Black lemon	13			Origanum Majorana	13	Calluna	13		
Cuminum	14	Ancho Chilli	14			Camellia	14				
Carum	15					Borago	15				
Apium	16					Spinacia	16				
Carya	17					Brassica	17				
Juglans	18					Camellia Sinesis var. assamica	18				
Arachis	19					Nicotiana	19				
						Azadirachta	20				

Table 9 shows the list of products and miscellaneous items tested throughout the course of the room temperature corrosion tests. All these items were readily and cheaply obtained from local grocery shops and online retailers. They were ground into a fine powder using a grinder before being tested.

CHAPTER VI

HIGH TEMPERATURE CORROSION TESTS

Literature studies showed that several of these successful samples had components known as alkaloids. Alkaloids are a class of organic compounds that are derived from amino acids and can be synthesized as secondary metabolites by some plants and animals (Kurek 2019). Alkaloids are often present in many foods consumed by humans with some more well-known alkaloids include quinine, morphine, and nicotine (Figure 10).

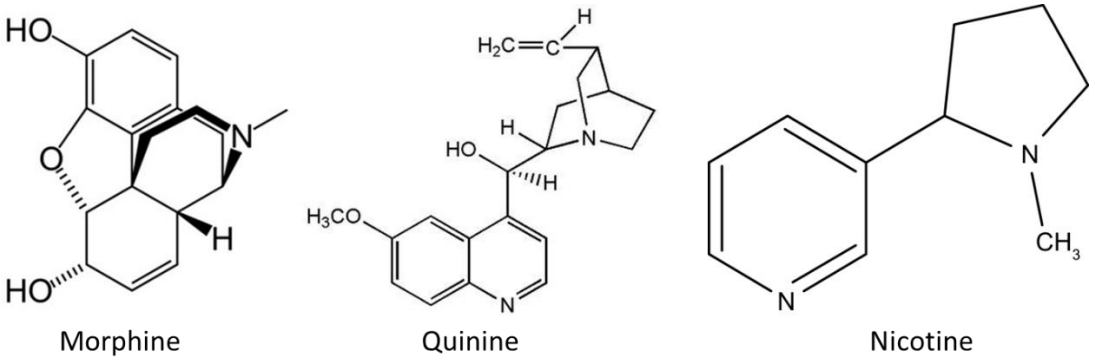

Figure 10: Chemical structures of some common alkaloids.

Alkaloids also tend to contain nitrogen atoms located in a cyclic structure. They can often contain oxygen and sulfur atoms as well, which, as mentioned earlier, are important factors in a good corrosion inhibitor. From the room temperature tests which succeeded, 9 different samples were identified for high temperature testing as shown in Table 10.

Table 10: List of samples used in high temperature tests.

Samples	Compound Name
1	Magnoliid
2	Sinapis
3	Solanales
4	Monocot
5	Quebracho
6	Aloe Vera
7	Malpighiale
8	Daisy
9	Nepetoideae

Corrosion Tests – 150°F

Samples containing these 9 chemicals were tested at 150°F over 6 hours with 15 wt.% HCl and compared to a control test carried out over the same duration under the same conditions. The results from these tests are shown in Table 11 and Figure 11 below. An important point of interest is the significant increase in the corrosion rate of the base test. Compared to the base result at room temperature, the corrosion rate has increased almost 26 times, with a small increase in temperature.

Table 11: Corrosion rates of the 9 chemical containing samples at 150°F in 15 wt.% HCl over 6 hours.

Sample	C.I. Concentration (wt.%)	Corrosion Rate (lb/ft^2)	Inhibition Efficiency %
Base	-	0.371	-
1	2	0.00253	99.3
2	2	0.153	58.8
3	2	0.0277	92.5
4	2	0.0275	92.6
5	2	0.0171	95.4
6	2	0.155	58.2
7	2	0.00206	99.4
8	2	0.03985	89.3
9	2	0.07681	79.3

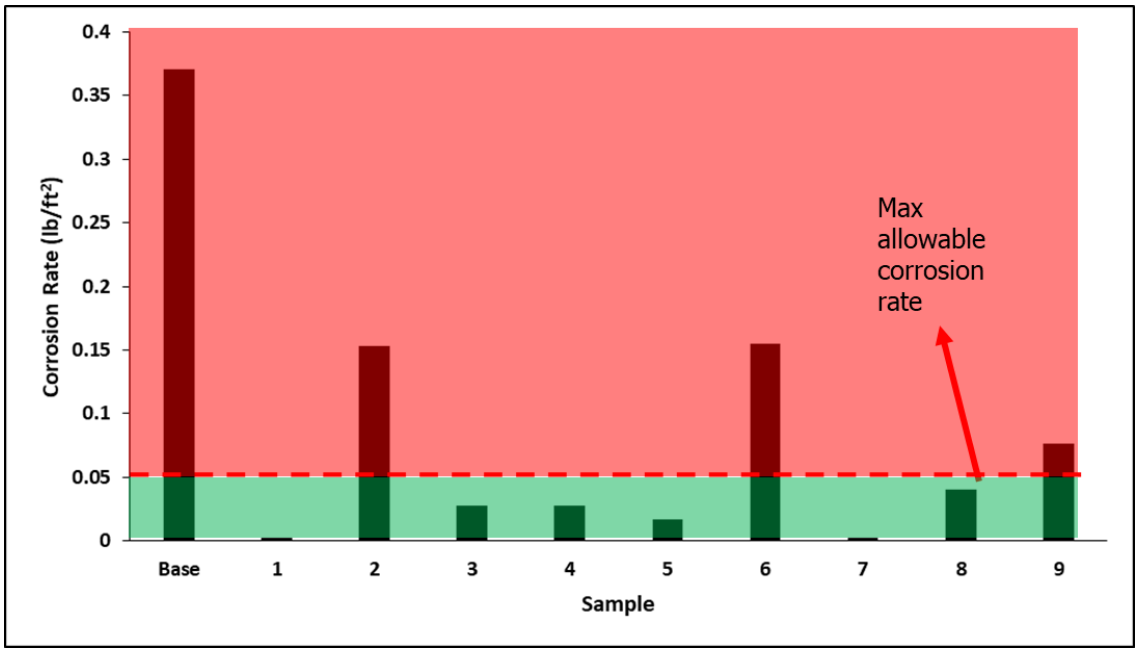

Figure 11: Illustration of corrosion test results for 9 samples in 15 wt.% HCl at 150°F over 6h. Corrosion rates lying in the green area represent successful tests.

In the oil and gas industry, the acceptable corrosion rate of low-carbon steel is less than 0.05 lb/ft^2 over a 6 hour test (Kalfayan 2008). From these results, it is clear that samples 2, 6, and 9 do not meet this criteria. Pictures were taken to document the condition of the coupons used for the corrosion test and can be seen in Figure 12 to Figure 15.

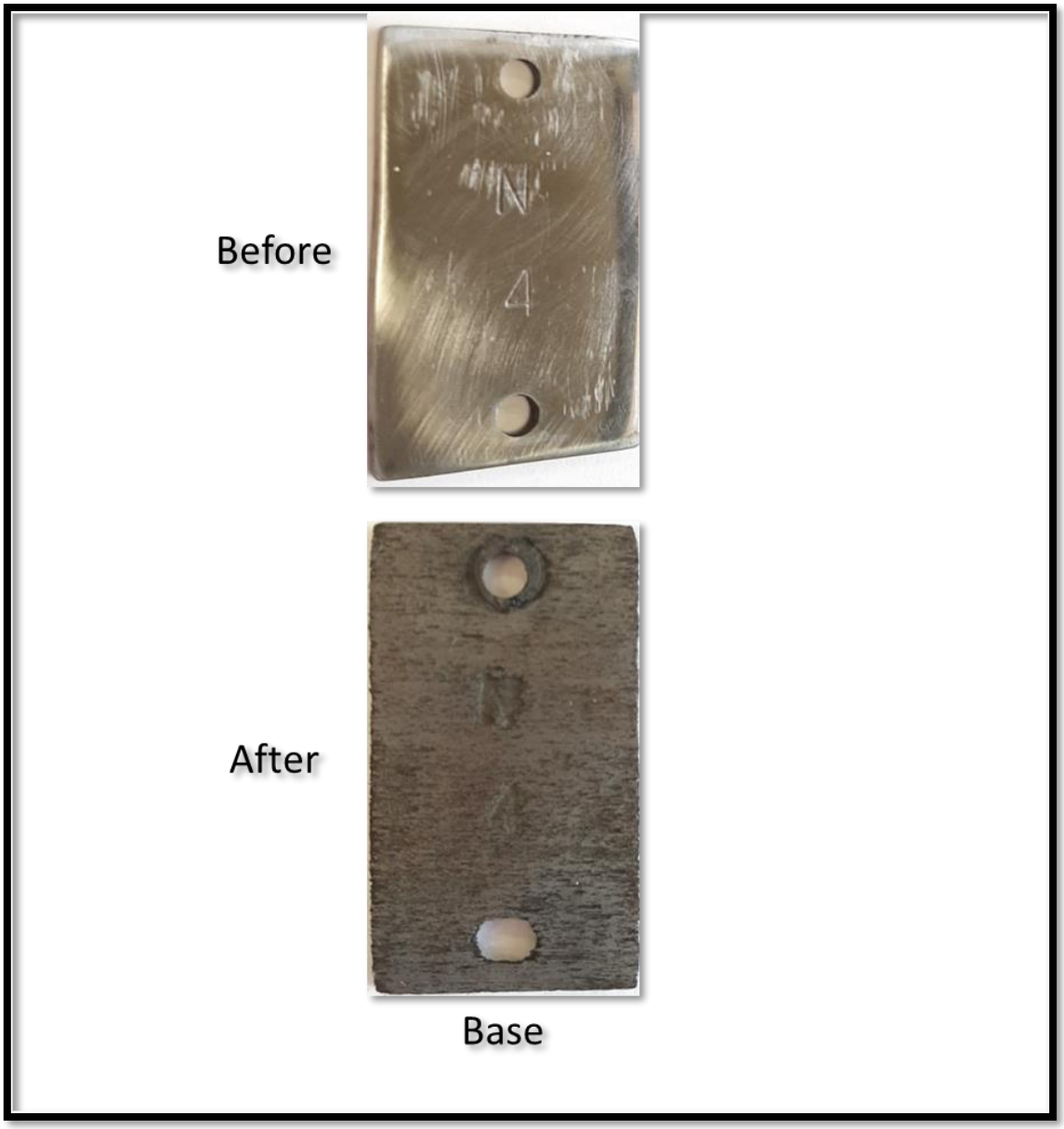

Figure 12: Pictures of N-80 coupon before and after base corrosion test at 150°F in 15 wt.% HCl for 6h.

Figure 12 shows the before and after images of the coupon used for the base corrosion test. The coupon before the test has a shiny appearance due to the 600 grit polish applied to it before the test. After exposure to the HCl solution, however, it can be observed that

the coupon became severely damaged. Severe pitting is also observed with the sides and edges of the coupon becoming frayed and rough. The attachment holes on the coupon also appear to have been widened as a result of the severe corrosion at this temperature.

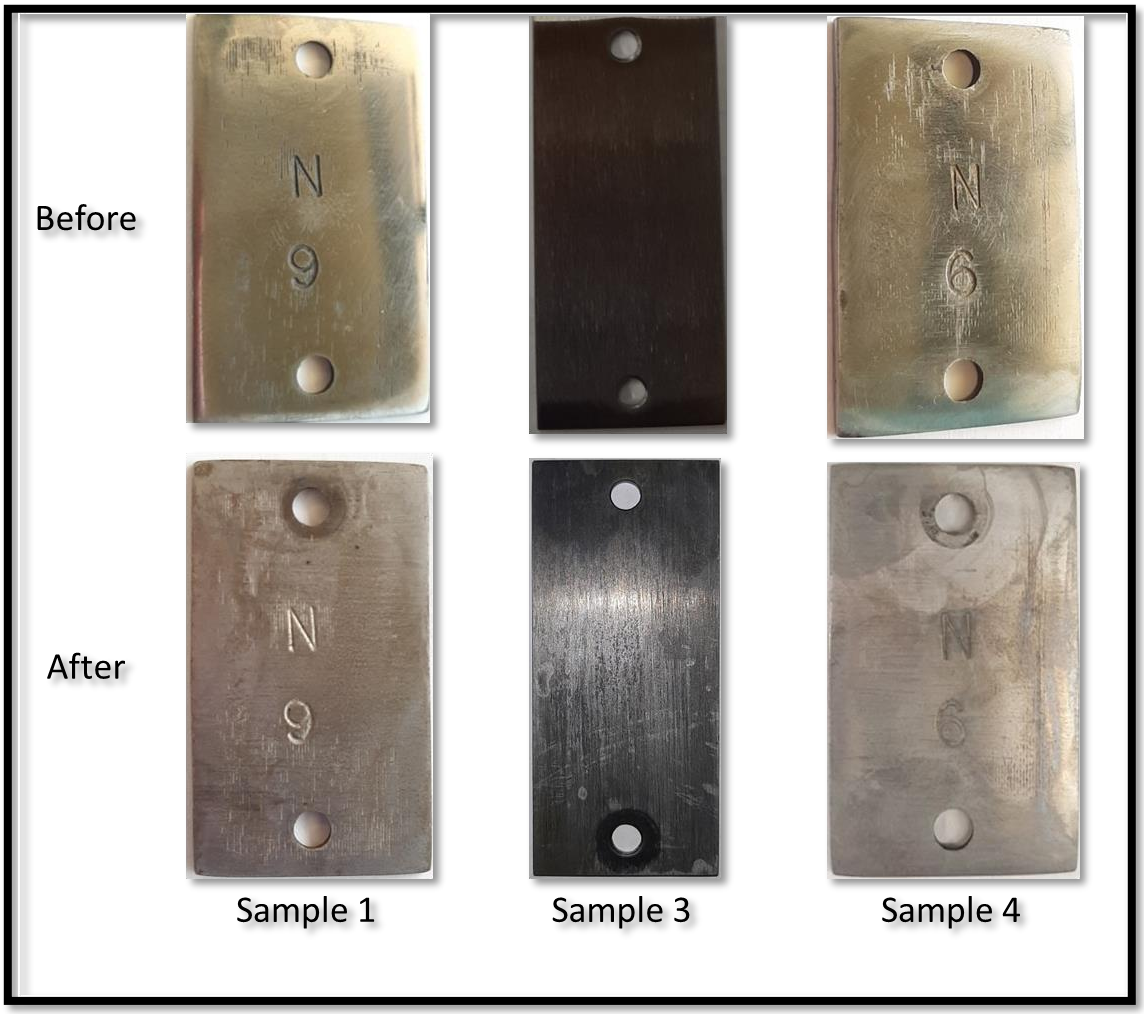

Figure 13: Pictures of N-80 coupons before and after the successful corrosion test at 150°F in 15 wt.% HCl for 6h for samples 1, 3, and 4.

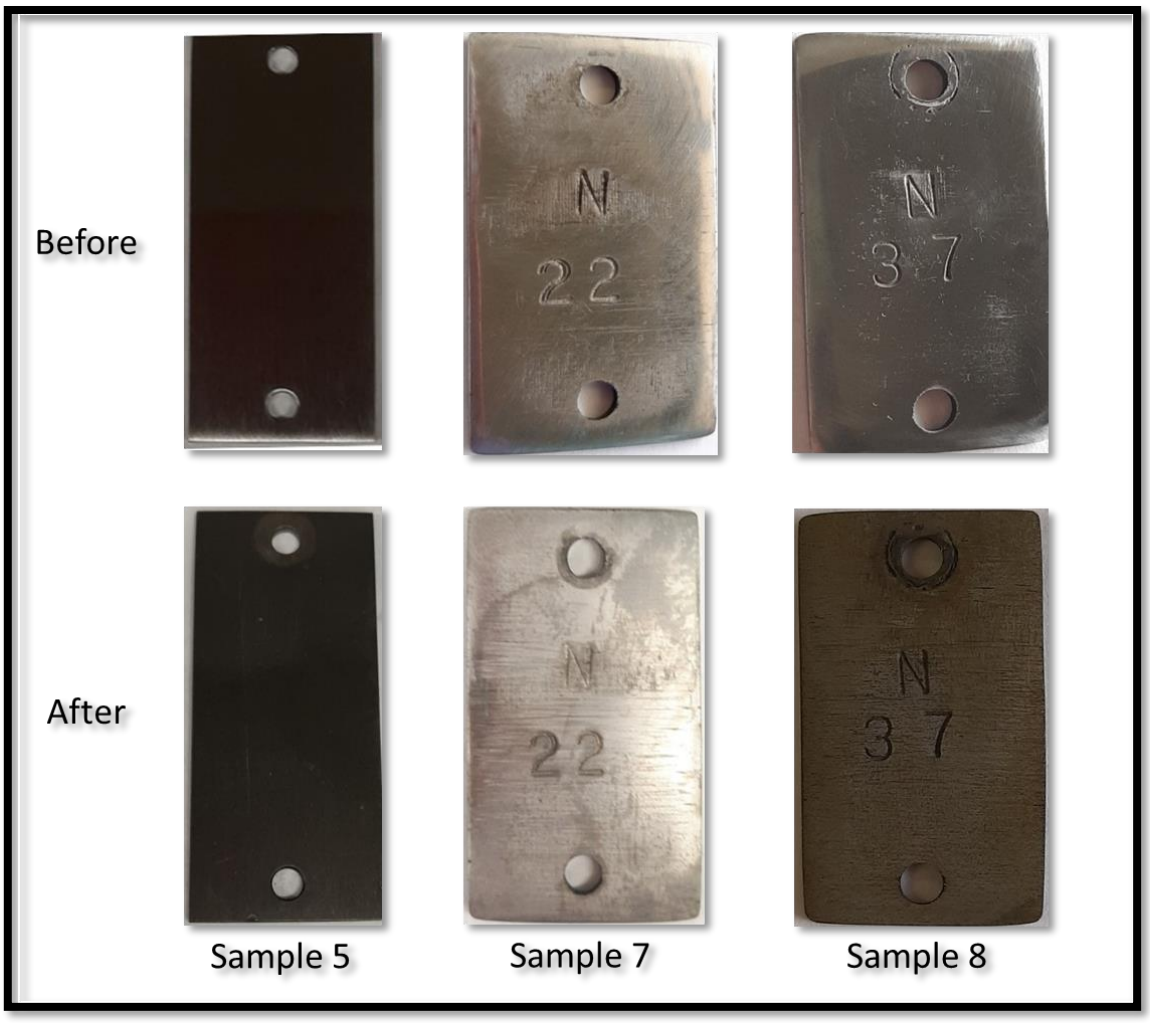

Figure 14: Pictures of N-80 coupons before and after the successful corrosion test at 150°F in 15 wt.% HCl for 6h for samples 5, 7, and 8.

Figure 13 and Figure 14 show the before and after images of the coupons that passed the corrosion test at 150°F. The coupons in these tests appear discolored, but no significant corrosion damage can be observed. Furthermore, some of the coupons even retained some shine to their surface, indicating that hardly any corrosion damage had occurred to the coupon. The coupons also did not sustain any form of pitting damage or other forms of localized corrosion.

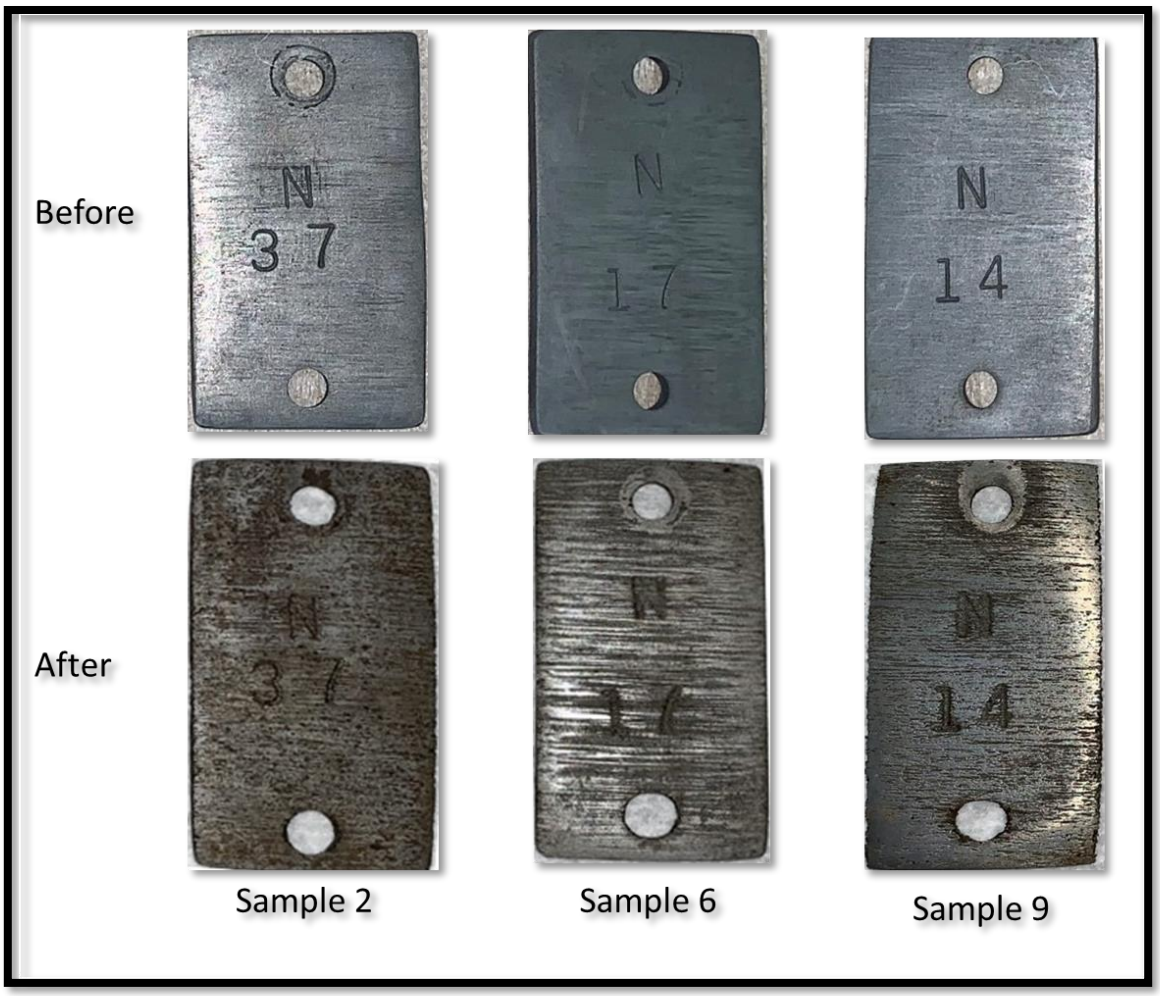

Figure 15: Pictures of N-80 coupons before and after the corrosion test at 150°F in 15 wt.% HCl for 6h for samples 2, 6, and 9. These coupons did not pass the corrosion test.

In Figure 15, it can be seen that the coupons that did not pass the corrosion test were severely damaged though it was not as severe as that of the base test. Similar to the images of the coupon in Figure 12, severe damage to the face of the coupon can be seen. While the stenciling on the coupon was not as severely corroded as that in Figure 12, pitting and edge corrosion are prominent on the surface. The holes on either side of the coupon also

do not appear to have changed significantly, supporting the data in Table 11 that the coupons were less corroded than the base test.

Corrosion Tests – 200°F

With only 6 samples remaining, it was decided to procure high purity food grade extracts of these compounds. The high purity of these extracts would ensure consistent testing due to the lack of impurities and would be used as the testing material in the subsequent tests. With these extracts, the corrosion tests were now carried out at 200°F and the results of these tests are shown in Table 12 and illustrated graphically in Figure 16.

Table 12: Corrosion rates of the 6 chemical containing samples at 200°F in 15 wt.% HCl over 6 hours with 1 wt.% intensifier added.

Sample	C.I. Concentration (wt.%)	C.I. Intensifier Concentration (wt.%)	Corrosion Rate (lb/ft^2)
Base	-	2	0.50969
1	2	1	0.0013
3	2	1	0.01725
4	2	1	0.01358
5	2	1	0.00878
7	2	1	0.0108
8	2	1	0.00823

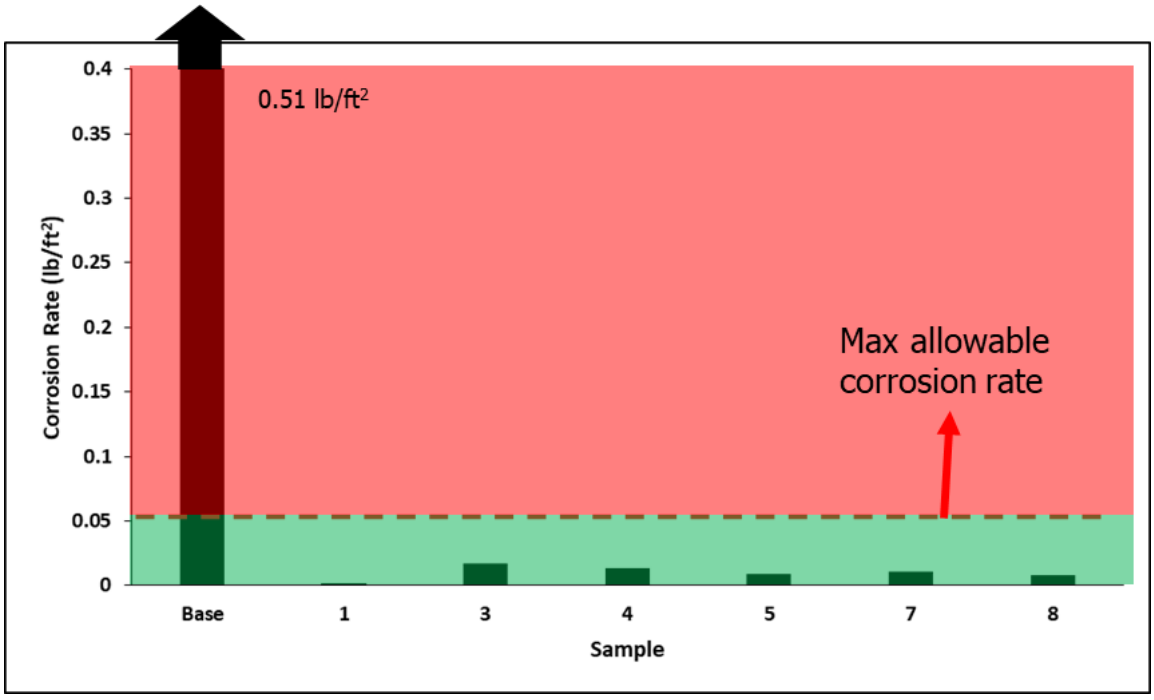

Figure 16: Illustration of corrosion test results for 6 samples in 15 wt.% HCl at 200°F over 6h. Corrosion rates lying in the green area represent successful tests.

At this temperature, corrosion inhibitor intensifiers are typically used to aid the inhibiting capabilities of the corrosion inhibitor. Commonly used corrosion inhibitor intensifiers include KI (potassium iodide) and formic acid. At these conditions, a control test similar to that carried out at 150°F and 77°F was done. However, at this temperature, the coupon was found to dissolve completely before the end of the experiment. This means that a corrosion rate could not be obtained since the exact time it took the coupon to dissolve cannot be known. As a result, a different control test was carried out. The purpose of this altered control test was to determine the effect of the corrosion inhibitor intensifiers on the corrosion test. Therefore, 2 wt.% of corrosion inhibitor intensifier was added to the solution in the absence of any corrosion inhibitor. The corrosion rate was found to be

0.510 lb/ft^2 over 6h with this solution. The presence of the corrosion rate shows that the intensifier is able to protect the coupon from corrosion to an extent though not well.

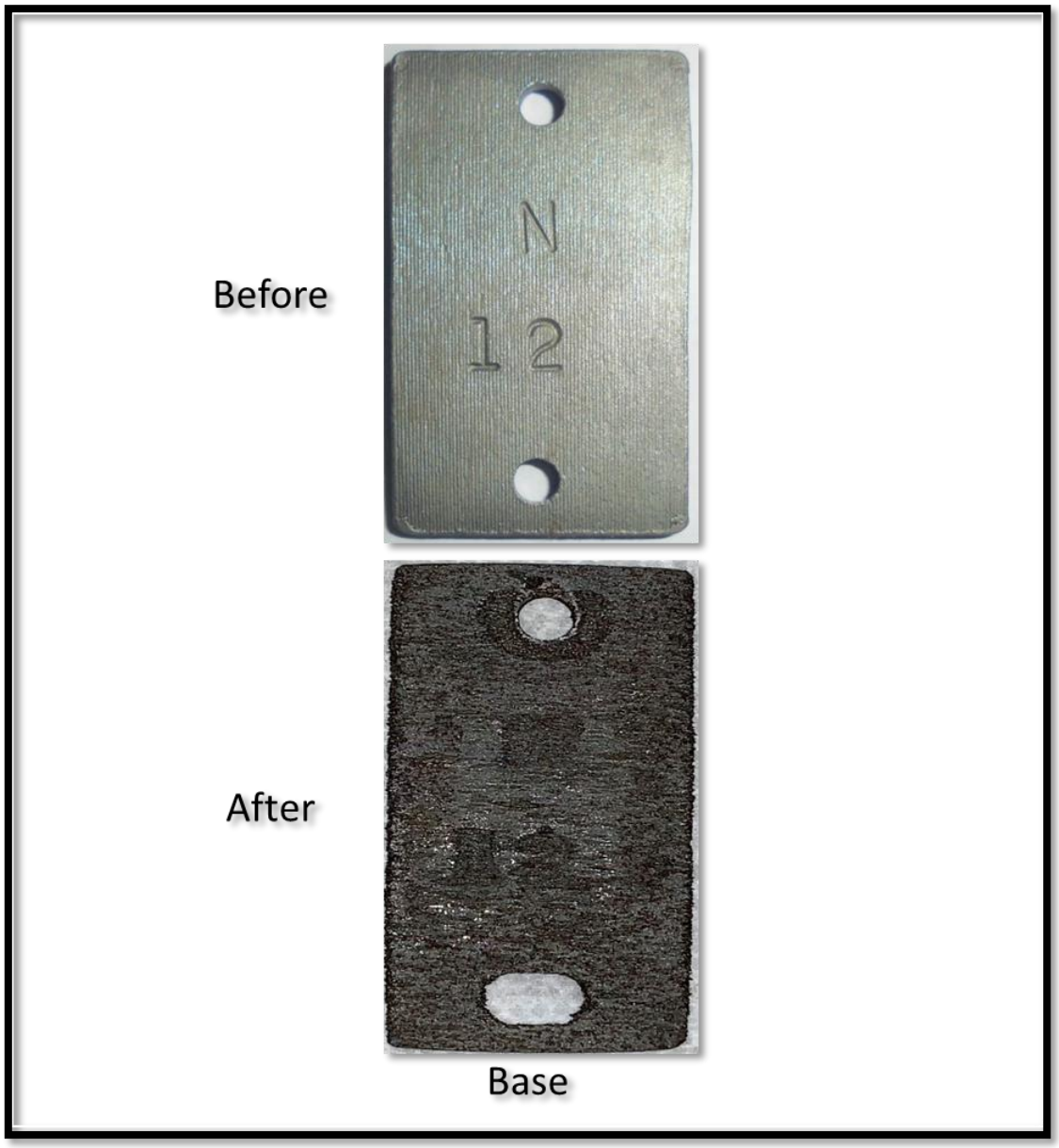

Figure 17: Pictures of N-80 coupon before and after corrosion test at 200°F in 15 wt.% HCl and 2 wt.% corrosion inhibitor intensifier for 6h.

In Figure 17, the damage done to the coupon as a result of the corrosion test can be seen. Due to the high corrosion rate of the base test, it is not surprising to see that the coupon obtained at the end of the test showed severe corrosion damage. The face of the coupon is severely scratched and pitted, with the edges of the coupon also severely corroded. The stenciling on the face of the coupon also appeared to be heavily damaged with the numbers and letters becoming barely readable. Furthermore, the hole at the bottom of the coupon can be observed to have widened significantly. Therefore, it is not surprising that the corrosion rate recorded was 10 times that of the acceptable limit.

Next, a corrosion test containing just 2 wt.% of sample 1 was tested in the absence of corrosion inhibitor intensifiers. This was to determine the extent of the effect of intensifiers in aiding corrosion mitigation. As can be seen, the corrosion rate of this test is 0.248 lb/ft^2. Just like the control test, this corrosion rate is significantly higher than the 0.05 lb/ft^2 limit. From this, it is clear that the corrosion inhibitor will not work alone at temperatures above 200°F. Therefore both chemicals were used together in conjunction to mitigate corrosion.

These corrosion tests were carried out using 1 wt.% of corrosion inhibitor intensifier added to 15 wt.% HCl solution containing along with 2 wt.% of the respective corrosion inhibitors to be tested. The corrosion rates resulting from these tests are shown in Table 12. The results show that the combination of both compounds significantly improves the corrosion rate to values far below the 0.05 lb/ft^2 limit.

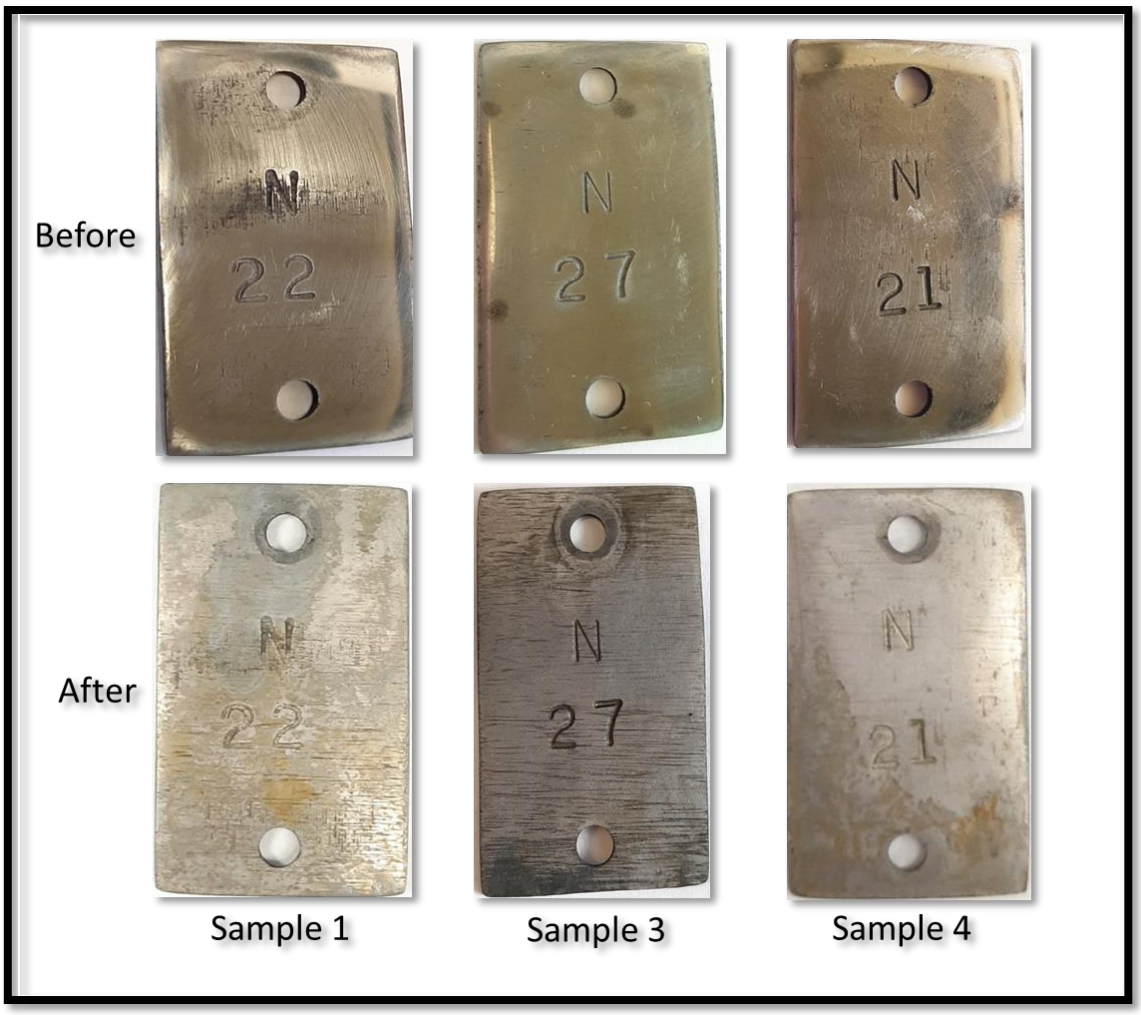

Figure 18: Pictures of N-80 coupons before and after the successful corrosion test at 200°F in 15 wt.% HCl for 6h for samples 1, 3, and 4.

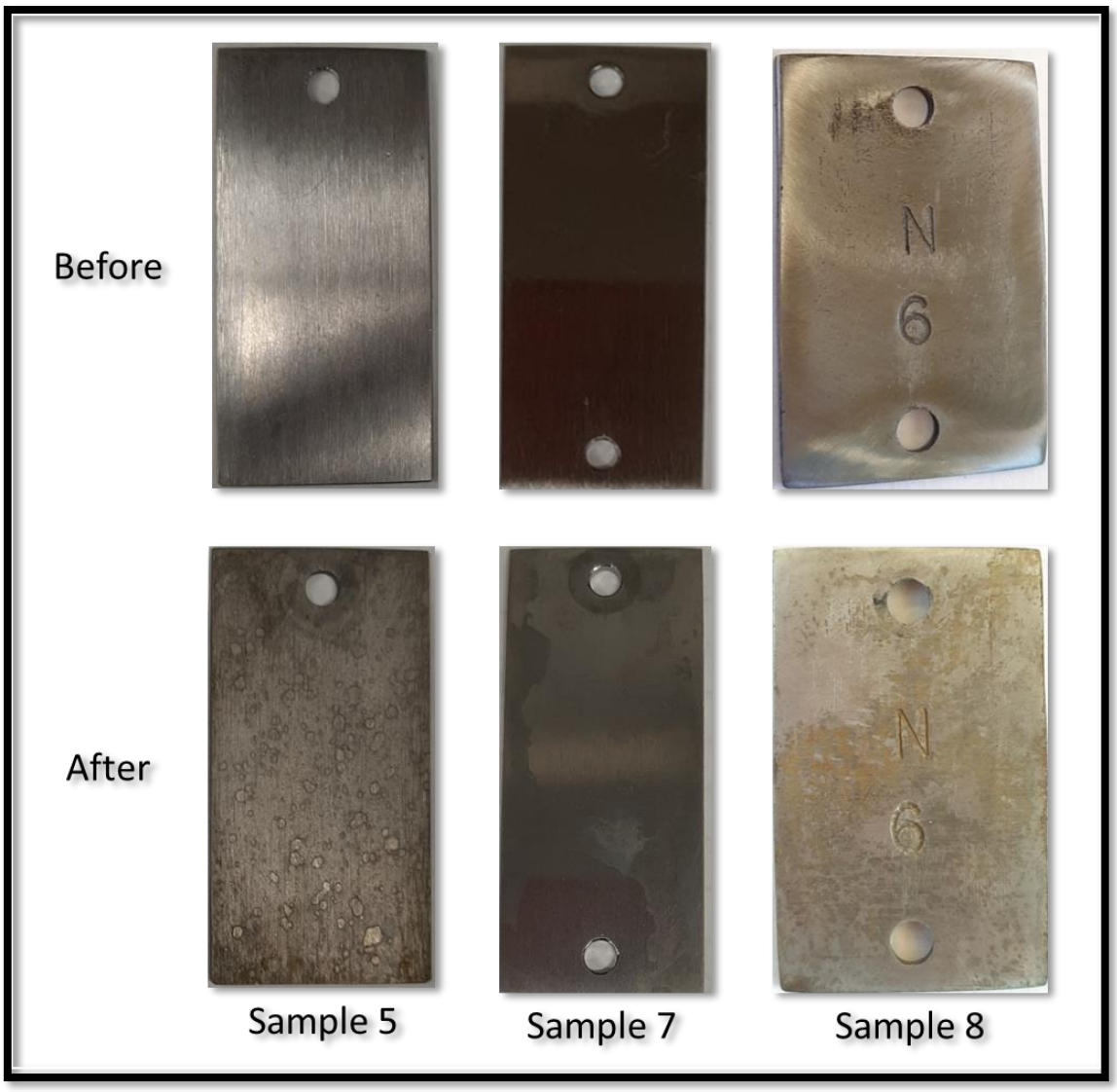

Figure 19: Pictures of N-80 coupons before and after the successful corrosion test at 200°F in 15 wt.% HCl for 6h for samples 5, 7, and 8.

The pictures of the coupons before and after the corrosion tests are shown in Figure 18 and Figure 19. Just like the images of the coupons at 150°F, the coupons after the 200°F showed little damage to the surface and no signs of pitting. A Slight discoloration was observed on most of the coupons, with sample 5 showing pock marks where some of the

solid pieces of the sample had adhered to. Nevertheless, this did not affect the corrosion inhibition capabilities of the sample as seen by the low corrosion rates in Table 12.

Corrosion Tests – 250°F

The next set of corrosion tests were carried out at 250°F. At this temperature, neither the control test without additives nor that with just the intensifier was conducted successfully since the coupon completely dissolved before the end of the 6h in both cases. Furthermore due to the harsh testing conditions, 2 corrosion inhibitor intensifiers were used at 1 wt.% each. The results from these tests are shown in Table 9 and illustrated in Figure 20 below. From these results, sample 7 can be observed to have exceeded the 0.05 lb/ft^2 industrial limit while all the remaining 5 samples performed well.

Table 13: Corrosion rates of the 6 chemical containing samples at 250°F in 15 wt.% HCl over 6 hours with 1 wt.% of each corrosion inhibitor intensifier 1 and 2 added.

Sample	C.I. Concentration (wt.%)	C.I.I. #1 Conc (wt.%)	C.I.I. #2 Conc (wt.%)	Corrosion Rate (lb/ft^2)
1	2	1	1	0.00811
3	2	1	1	0.00963
4	2	1	1	0.00355
5	2	1	1	0.00151
7	2	1	1	0.07996
8	2	1	1	0.01415

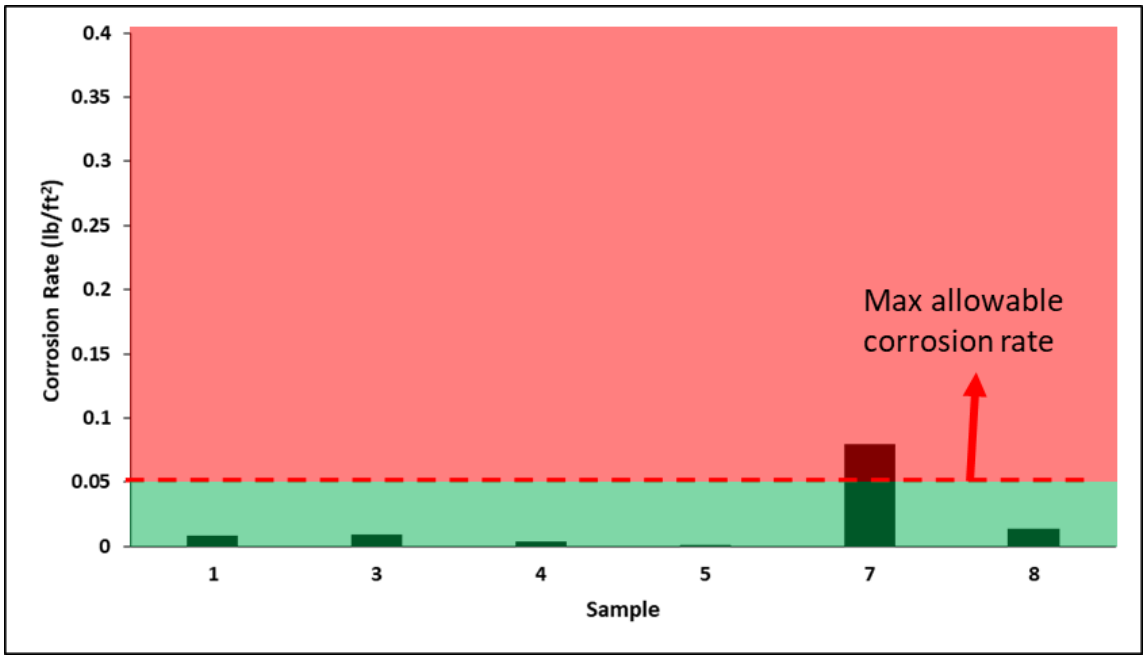

Figure 20: Illustration of corrosion test results for 6 samples in 15 wt.% HCl at 250°F over 6h with 2 wt.% corrosion inhibitor and 1 wt.% of each corrosion inhibitor intensifier. Corrosion rates lying in the green area represent successful tests.

In Figure 21, the before and after condition of the coupon with sample 7 can be seen. Even though the corrosion rate for sample 7 exceeded the 0.05 lb/ft^2 limit, it did not do so by much; hence the damage to the surface of the coupon is not as severe as that seen in Figure 12 and Figure 17. In this instance, the surface of the coupon does not appear to have suffered from severe pitting, although there is obvious roughness.

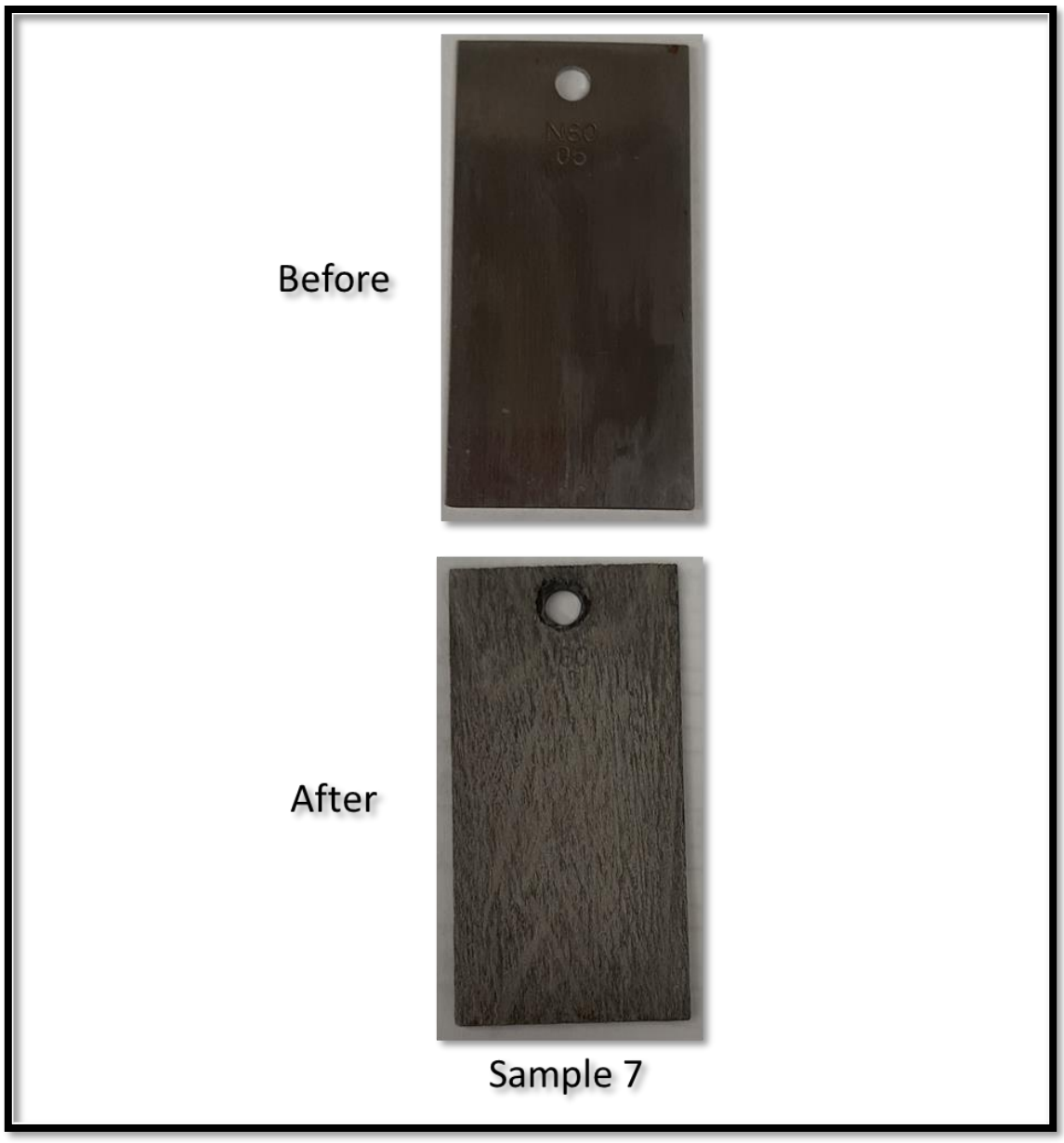

Figure 21: Pictures of N-80 coupon before and after corrosion test with 2 wt.% of sample 7 at 250°F in 15 wt.% HCl and 1 wt.% of each corrosion inhibitor intensifier for 6h.

In Figure 22 and Figure 23, it can be seen that the surface of the coupons tested with successful samples did not have significant damage. Pitting is also observed to be present

but minimal, with discoloration on the surface of the coupon being the most prominent feature after the corrosion test. Corrosion around the hole through which the coupon was suspended indicates some localized corrosion in the area of the PEEK washer attached to the coupon.

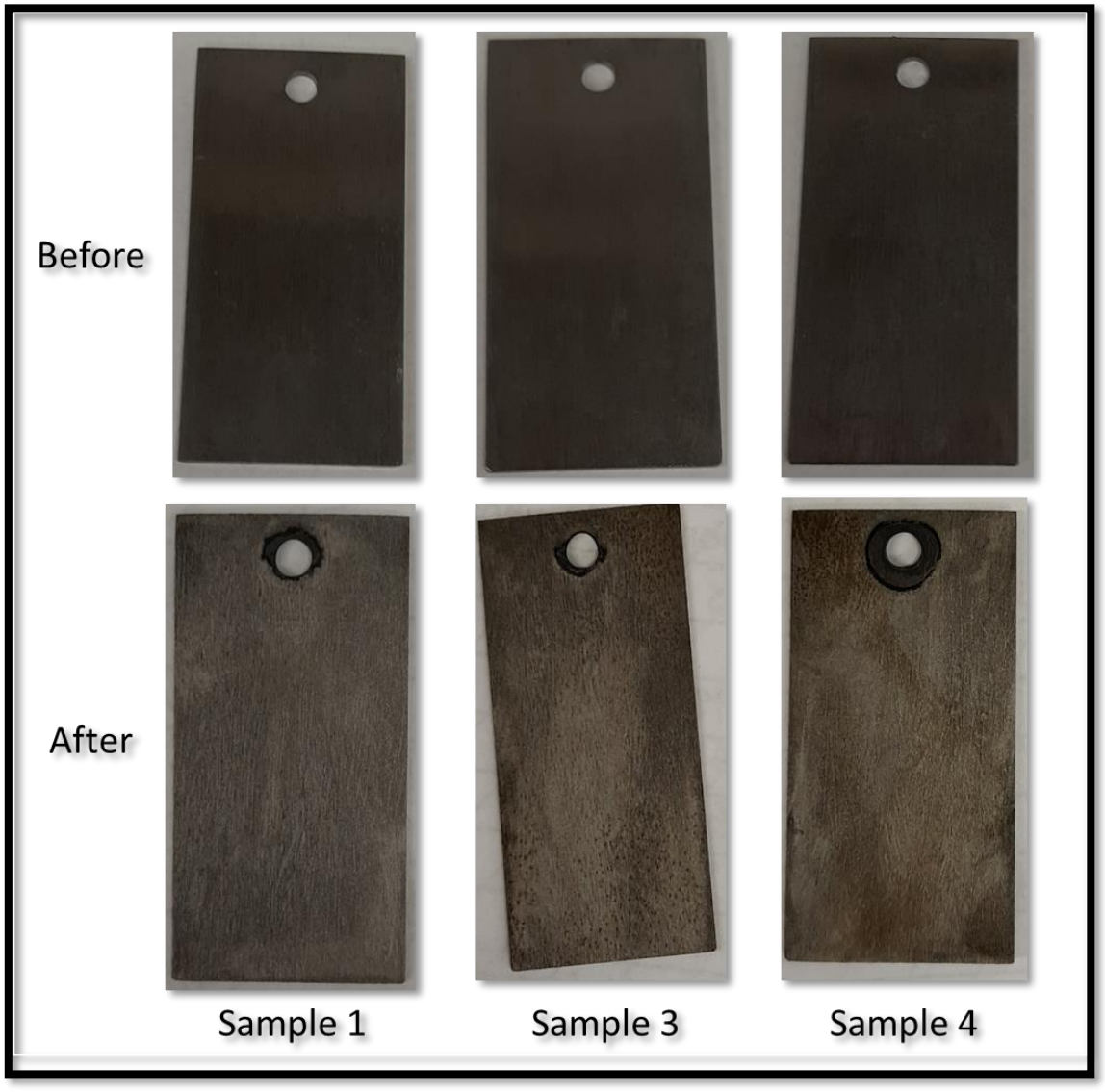

Figure 22: Pictures of N-80 coupon before and after corrosion test with samples 1, 3, and 4 at 250°F in 15 wt.% HCl and 1 wt.% of each corrosion inhibitor intensifier for 6h.

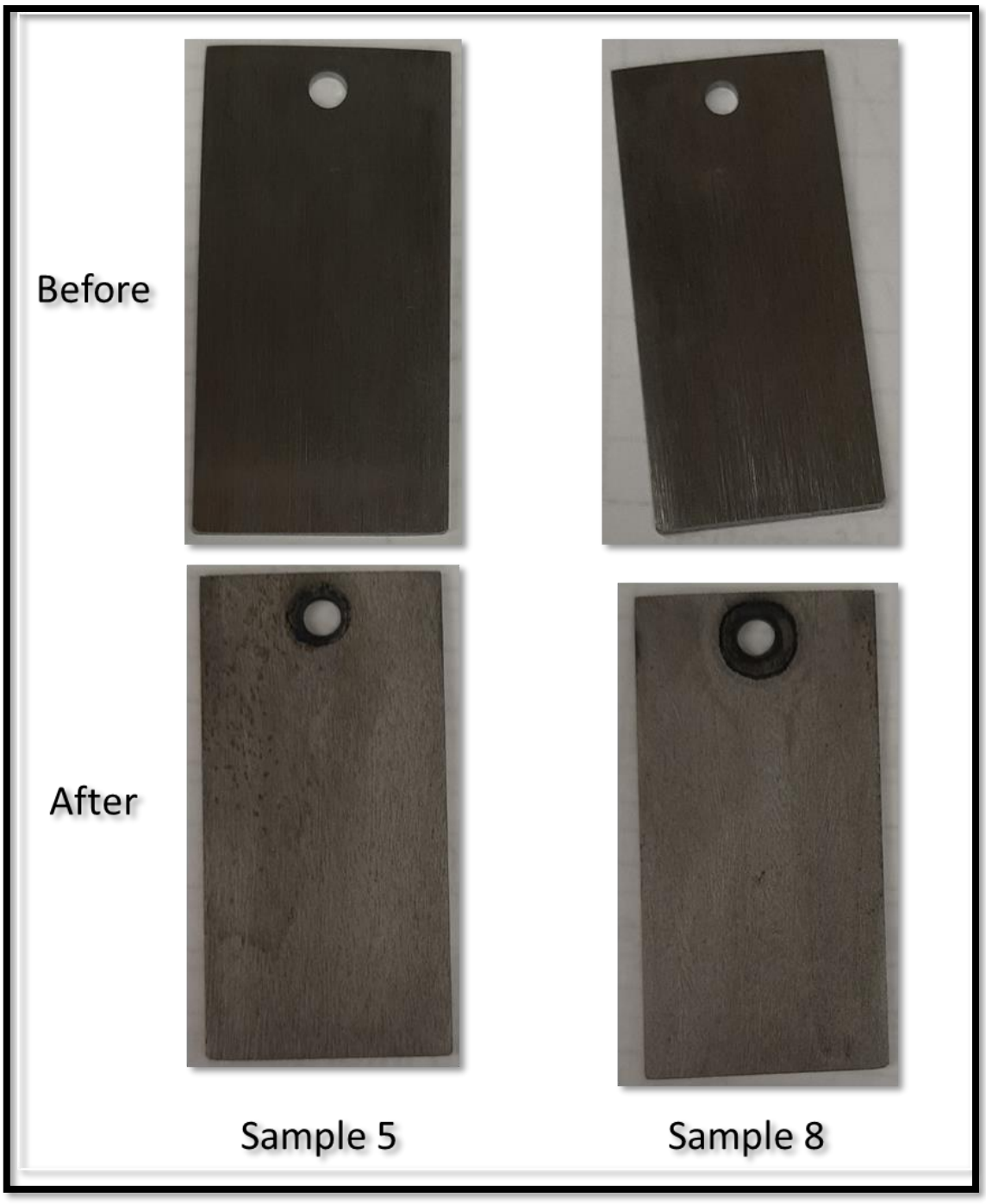

Figure 23: Pictures of N-80 coupon before and after corrosion test with samples 5 and 8 at 250°F in 15 wt.% HCl and 1 wt.% of each corrosion inhibitor intensifier for 6h.

Subsequent tests were carried out at 300°F using the 5 remaining samples. To compensate for the increase in temperature, the corrosion inhibitor intensifier concentrations used at 250°F was doubled to 2 wt.%. Despite this, at this temperature all the coupons were dissolved completely and no corrosion rates could be established. Various other types and concentrations of corrosion inhibitor intensifiers were tested but to no avail.

CHAPTER VII

CORROSION TESTS WITH CRAS

In order to control corrosion from corrosive gases such as CO_2 and H_2S, casings and tubulars made of CRAs are often used in place of LCS. CRAs are alloys that contain metals such as Cr, Mo, and Ni as these metal ions provide additional corrosion resistance. This allows CRAs to display high levels of corrosion resistance, specifically in the environment they are in, without requiring either inhibition or mitigation techniques (Petersen and Bluem 1989). CRAs typically form a layer of Cr_2O_3 in the air which confers superior resistance to CO_2 corrosion. However, despite their nomenclature as "corrosion resistant", CRAs can be corroded by concentrated HCl, resulting in damage to the base metal layer (Al-Mutairi et al. 2005). CRAs are also significantly more expensive than low carbon steel and therefore have a lower maximum allowable corrosion rate of 0.03 lb/ft^2 over 6h (Kalfayan 2008).

Corrosion Tests – 72°F

Following the corrosion test results from low carbon steel, samples that showed the greatest success in all the low carbon steel tests were tested with S13Cr to determine their effectiveness at protecting a different class of metal. These were samples 1, 3, 4, and 5. The initial tests were carried out at room temperature in 15 wt.% HCl over 6h and the success criteria was an inhibition efficiency higher than 90%, similar to that set for the low carbon steel trials before. The corrosion test results from the room temperature tests can be seen in Table 14 and were graphed as shown in Figure 24.

Table 14: Corrosion rate of samples 1, 3, 4, and 5 tested in 15 wt.% HCl over 6 hours with S13Cr at room temperature (72°F).

Sample	C.I. Concentration (wt.%)	Corrosion Rate (lb/ft^2)	Inhibition Efficiency %
Base	-	0.06835	-
1	2	0.00079	98.8
3	2	0.00229	96.6
4	2	0.00207	97.0
5	2	0.00195	97.1

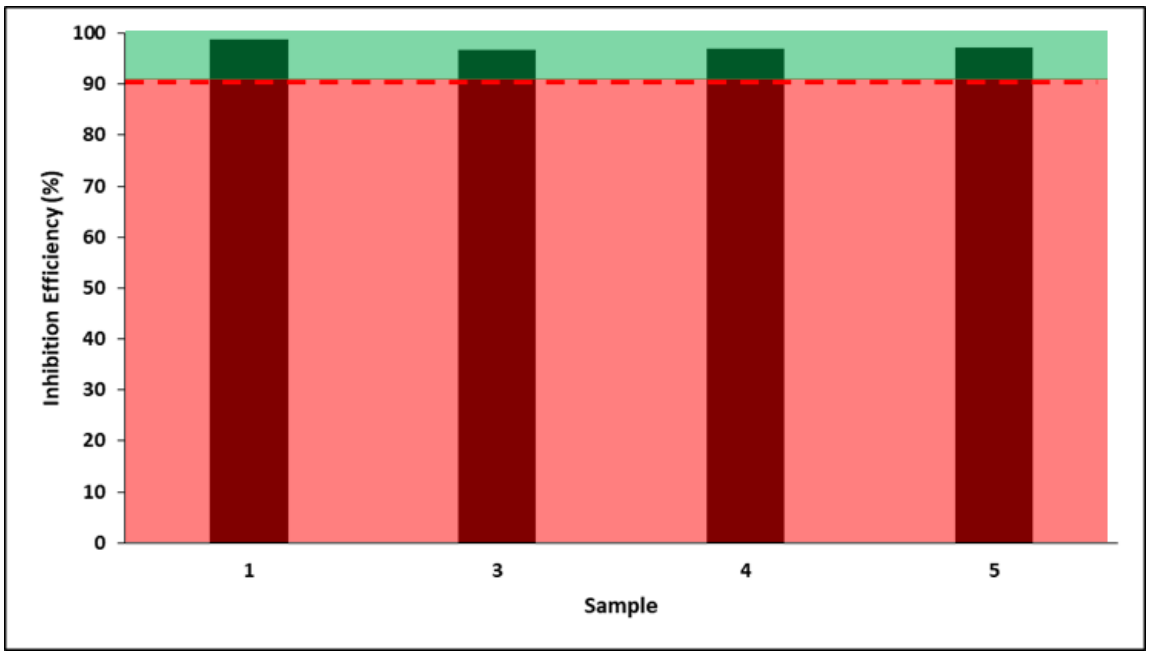

Figure 24: Illustration of corrosion test results for S13Cr with 4 samples in 15 wt.% HCl at 72°F over 6h. Corrosion rates lying in the green area represent successful tests.

Corrosion Tests – 200°F

From the results of the room temperature tests, it can be seen that the samples that were successful in the low carbon steel tests were similarly effective at protecting the S13Cr coupons. The next set of corrosion tests were carried out at 200°F to examine if these samples would retain their effectiveness at high temperatures. This temperature was

chosen instead of 250°F as emulsified acids are typically used at 250°F for stimulation treatments instead of straight HCl especially to protect the expensive CRA tubulars. As with the corrosion test at 200°F conducted before, no base corrosion rate could be obtained since the coupon was completely dissolved by the end of the experiment.

Table 15: Corrosion rate of samples 1, 3, 4, and 5 tested in 15 wt.% HCl over 6 hours with S13Cr at 200°F.

Sample	C.I. Concentration (wt.%)	C.I. Intensifier Concentration (wt.%)	Corrosion Rate (lb/ft^2)
1	2	1	0.00016
3	2	1	0.01026
4	2	1	0.00026
5	2	1	0.0074

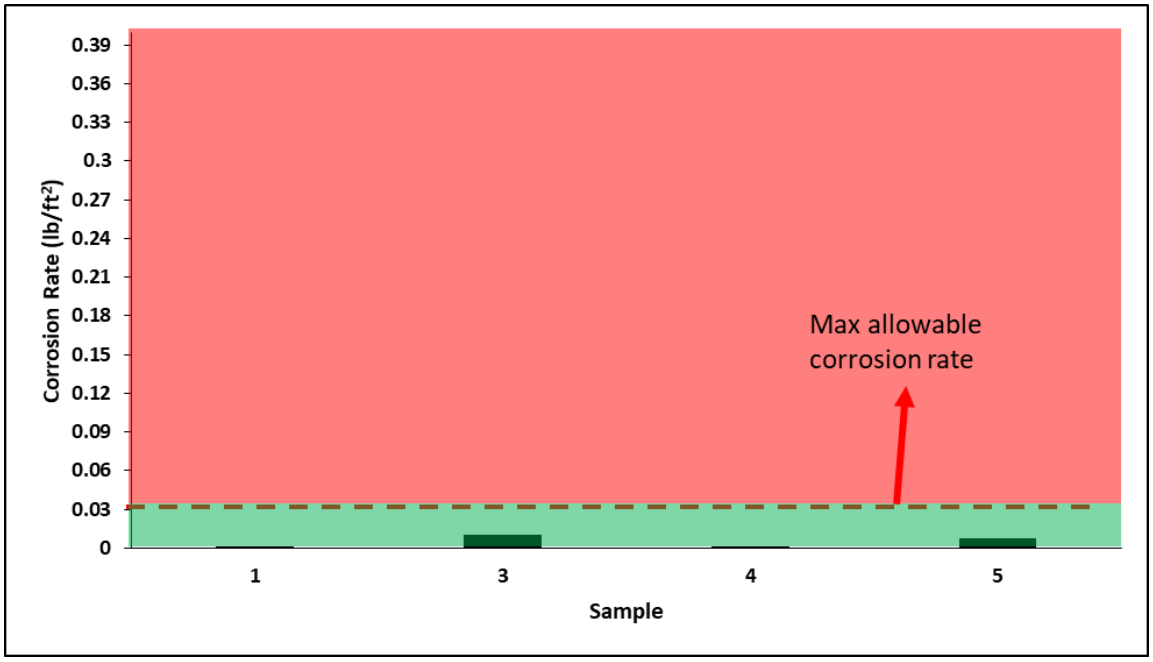

Figure 25: Illustration of corrosion test results for S13Cr with 4 samples in 15 wt.% HCl at 200°F over 6h. Corrosion rates lying in the green area represent successful tests.

The corrosion test results shown in Table 15 above show that the 4 samples tested were indeed successful at keeping the corrosion rate below the industry standard of 0.03 lb/ft^2. Figure 25 shows that for all 4 samples tested, the corrosion rates lay significantly below the 0.03 lb/ft^2 limit. Pictures of the coupons taken before and after the high-temperature test are shown below in Figure 26. From the images of the coupons, it can be observed that the appearance of the coupon was not significantly altered despite the highly corrosive environment. No pitting or stress cracking was observed to occur on any coupon, with most coupons remaining shiny after the corrosion test. These images further show that the samples tested were able to provide sufficient corrosion inhibition as well as prevent pitting from occurring to the S13Cr coupons

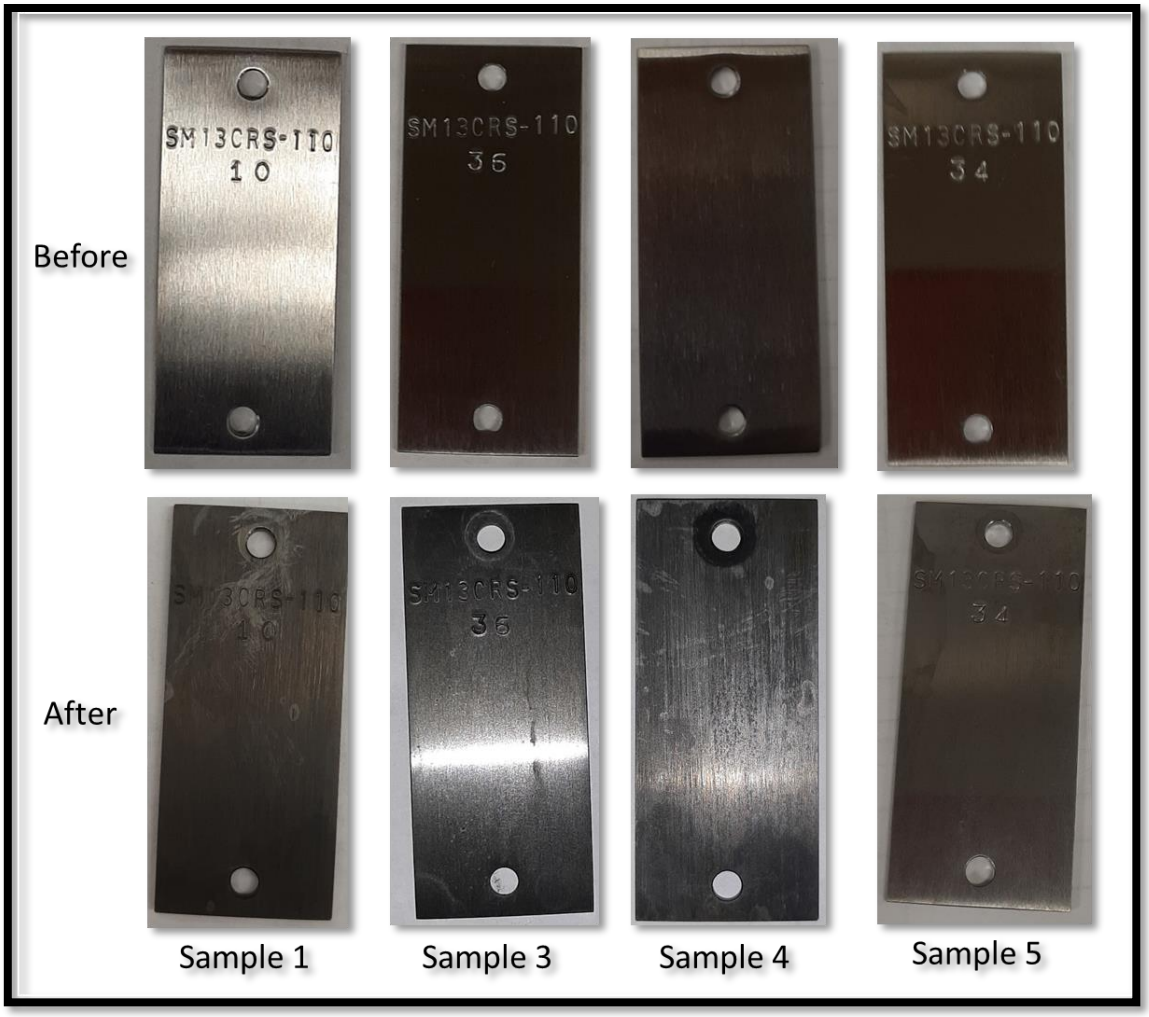

Figure 26: Before and after images of S13Cr coupons after corrosion in 15 wt.% HCl at 200F for 6h.

CHAPTER VIII

EMULSIFIED ACID

Emulsified acids are commonly used in the oil and gas temperatures to rein in the reactivity of HCl at high temperatures. They are typically used at temperatures above 250°F in order to generate wormholes since the high reactivity of HCl at this temperature will result in increased face dissolution (Cassidy et al. 2012). The formation of wormholes significantly improves the permeability of the reservoir and are thus desired over the compact dissolution of the rock (Nasr-el-Din et al. 2001). These acids involve the emulsification of the aqueous acid in an immiscible, stable organic fluid through the addition of surfactants known as emulsifiers.

Corrosion Tests – 72°F

After the emulsified acid was properly mixed, the corrosivity of the acid was determined first at room temperature. This was done in the same manner as the previous room temperature corrosion tests using samples 1, 4, and 8. The results are shown in Table 16 and graphed in Figure 27 below.

Table 16: Corrosion rate of samples tested in 15 wt.% HCl emulsified acid over 6 hours at room temperature.

Sample	C.I. Concentration (wt.%)	Corrosion Rate (lb/ft2)	Inhibition Efficiency %
Base	-	0.00221	0
1	2	0	100
4	2	0.00064	71.04
8	2	0.00086	61.09

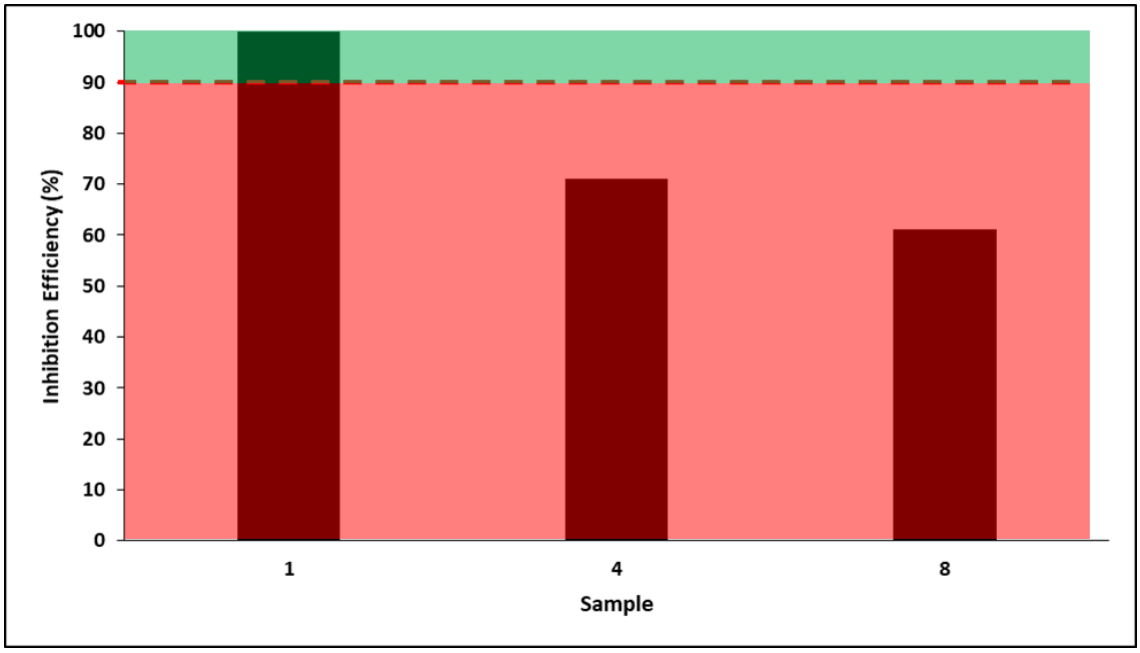

Figure 27: Inhibition efficiency of samples 1, 4, and 8 compared to the corrosion rate of the control.

Interestingly, when comparing the corrosion inhibition efficiency of the emulsified acid tests, it can be observed that samples 4 and 8 did not meet the 90% inhibition efficiency criteria as laid out previously for the other room temperature tests. This is in spite of them having shown good corrosion inhibitions at the same conditions using straight 15 wt.% HCl. However, sample 1 shows near perfect corrosion inhibition and was selected for tests at 250°F and 300°F.

Interactions with Emulsified Acid

Since corrosion inhibitor molecules are also a type of surfactant, before the tests at high temperatures were carried out, it was necessary to determine if these corrosion inhibitors would interfere with the emulsifier used. Such interference would result in

premature separation of the oil and acid phases, which would negate the benefits of injecting emulsified acids. Bottles of emulsified acid-containing samples 1, 3, and 4 were prepared using 10 gpt of emulsifier and placed in the autoclave at 250°F over 6 hours to mimic the conditions the corrosion tests would be carried out under. The before and after test results can be seen in Figure 28 below.

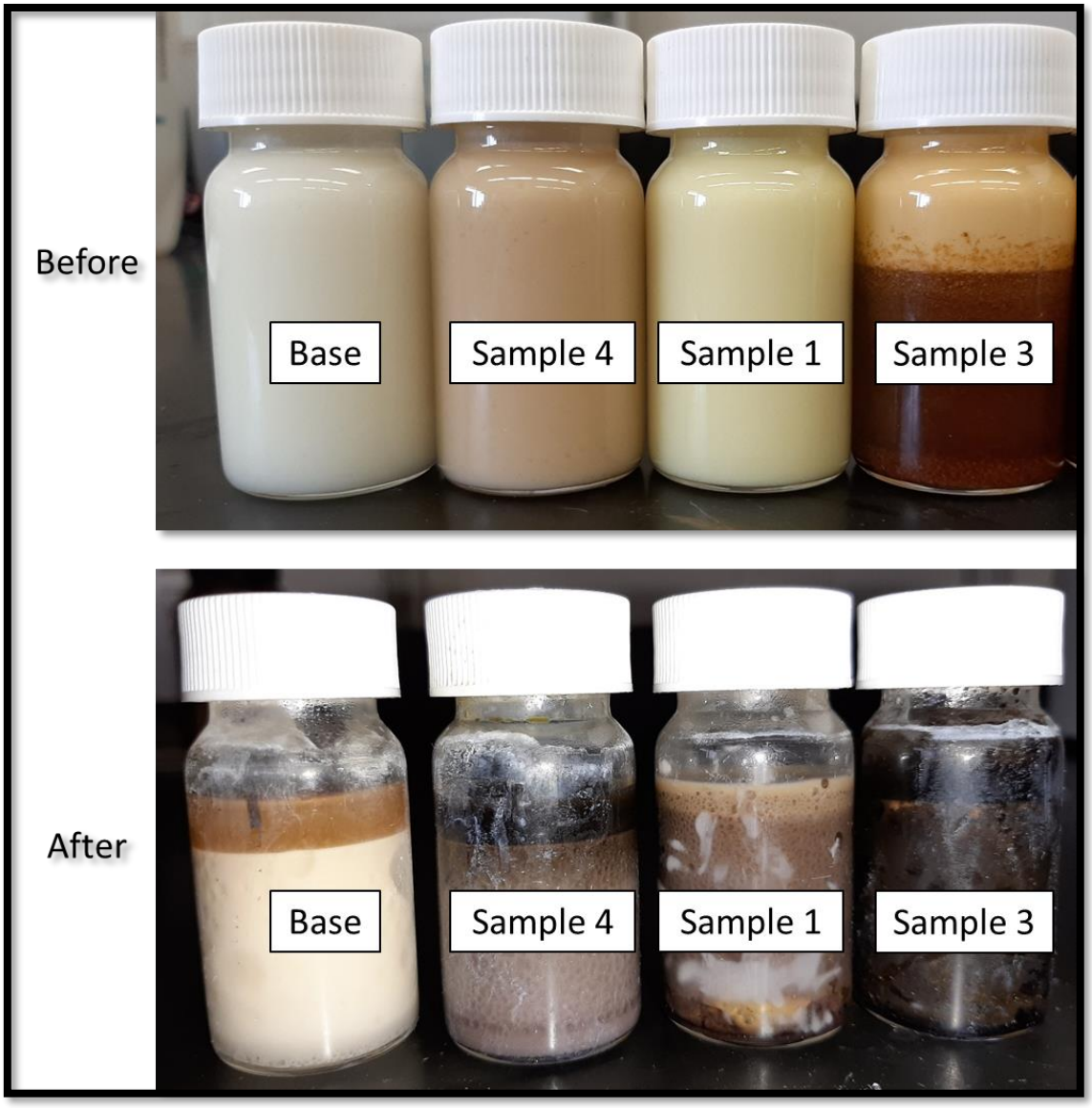

Figure 28: Before and after images of emulsified acid stability tests at 250°F over 6h.

From Figure 28a, it can be observed that sample 3 breaks the emulsion even at room temperature. The pictures were taken shortly after the addition of the samples into the bottles, indicating sample 3 could be a potential demulsifier. In Figure 28b, it can be observed that some degree of separation occurred for the base and sample 3. However, the emulsified acid containing sample 1 appears to be relatively stable, showing little signs of separation. As a result, sample 1 was selected to be tested with emulsified acid to determine if it would be able to offer sufficient corrosion inhibition.

Corrosion Tests – 250°F

The first set of tests were carried out at 250°F using sample 1 with 1 corrosion inhibitor intensifier. The choice to use 1 less intensifier than the previous tests carried out at this temperature was because the acid is now emulsified, and this has a slower rate of reaction. Therefore, it would be reasonable to assume that the acid solution should require only 1 corrosion inhibitor intensifier to achieve the desired results. The previous tests were carried out with a cationic emulsifier. During the corrosion tests, a sample of an anionic emulsifier was obtained and ran at the same conditions to determine if there was any effect of emulsifier type on the corrosion rate. The corrosion test results are shown in Table 17 below.

Table 17: Corrosion rate results using sample 1 as corrosion inhibitor for 15 wt.% HCl emulsified acid solution at 250°F.

Emulsifier Type	Emulsifier Conc. (gpt)	C.I. Conc. (wt.%)	C.I. Intensifier Conc. (wt.%)	Corrosion Rate (lb/ft^2)
Cationic	10	2	2	0.0011
	10	2	0.5	0.03453
Anionic	8	2	2	0.1025

From the results, it can be observed that the cationic and anionic surfactants had significantly different corrosion rates with the cationic emulsifier having corrosion rates approximately 100 times lower than that of the anionic surfactant. Using the cationic surfactant, the corrosion rate was found to be 0.0011 lb/ft^2 compared to the 0.1025 lb/ft^2 when the anionic emulsifier was used. Furthermore, reducing the concentration of corrosion inhibitor intensifier by 4 times resulted in an expected increase in corrosion rate to 0.03453 lb/ft^2.

The difference in corrosion rates between the cationic and anionic emulsifier suggests that the emulsified acid broke during the test. Moreover, half the coupon was observed to have been dissolved as shown by the picture taken of the retrieved coupon as shown in Figure 29 below.

Figure 29: Coupon obtained after testing with anionic emulsifier at 250°F. Half the coupon was dissolved.

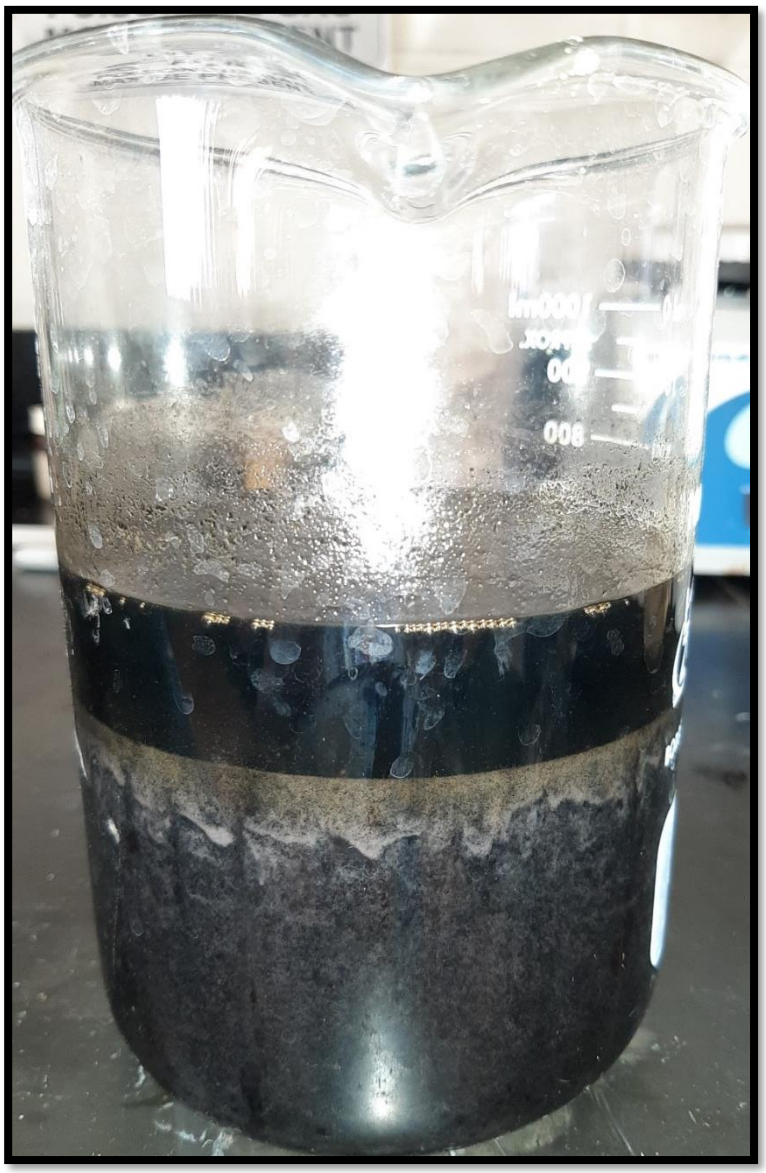

Figure 30: Broken emulsified acid after 250°F test. Anionic emulsifier was used to emulsify the acid.

The breaking of the emulsified acid was confirmed when the contents of the autoclave were emptied into a 1L borosilicate beaker, as shown in Figure 30 above. In the figure, 2 distinct layers can be seen in the fluid, with the top layer likely being the less dense organic

phase and the denser aqueous acidic phase at the bottom. Since the organic phase is non-corrosive, the top portion of the suspended coupon would not have been corroded, whereas the bottom portion that was exposed to the corrosive aqueous solution would be. This further explains the appearance of the coupon in Figure 29. Following this test, the cationic emulsifier was used to carry out the remaining emulsified acid tests at 300°F.

Corrosion Tests – 300°F

At this temperature, a second corrosion inhibitor intensifier was added to the emulsified acid. This corrosion inhibitor intensifier is an organic acid typically used in the oil and gas industry as a corrosion inhibitor intensifier and is different from the corrosion inhibitor intensifier used previously at 250°F in neat acid. The results of the corrosion test are shown in Table 18.

Table 18: Corrosion test results of emulsified acid at 300°F using sample 1 as corrosion inhibitor.

Emulsifier Conc. (gpt)	C.I. Conc. (wt.%)	C.I.I. #1 Conc (wt.%)	C.I.I. #2 Conc (gpt)	Corrosion Rate (lb/ft^2)
10	2	4	50	0.5812
15	2	4	5	0.2692
15	2	4	-	0.1212

As can be seen, none of these corrosion tests are lower than the 0.05 lb/ft^2 requirement and thus do not meet the set industry criteria. The first test carried out at 10 gpt emulsifier concentration and 50 gpt of corrosion inhibitor intensifier #2 showed extremely high rates of corrosion. This was hypothesized to be due to the interference of corrosion inhibitor intensifier #2 and the emulsifier. At this point, another stability test was carried out to determine if this hypothesis was true. For this stability test, a base emulsified acid and

another containing sample 1 were mixed and the allowed to stand. Within 30 minutes of preparation, separation in both emulsified acids was observed as shown in Figure 31 below.

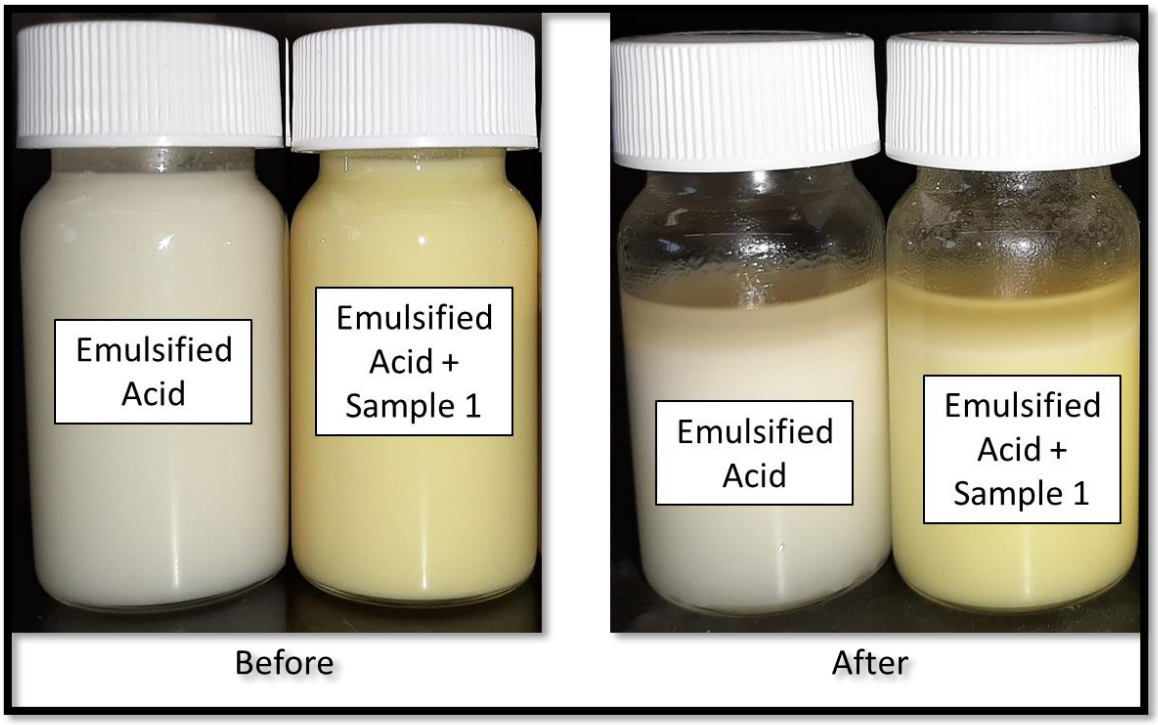

Figure 31: Before and after pictures of emulsified acid after mixing and being left to stand for 30 minutes.

Following these tests, the emulsifier concentration was increased to 15 gpt while the concentration of corrosion inhibitor intensifier #2 was reduced to 5 gpt. This adjustment saw a reduction in corrosion rate by almost half to 0.2692 lb/ft^2. Removing corrosion inhibitor intensifier #2 completely resulted in a further drop in corrosion rate to 0.1212 lb/ft^2. This shows that while corrosion inhibitor intensifier #2 is a commonly used corrosion inhibitor intensifier in most acid solutions, it did not work well with this emulsifier in generating a stable emulsified acid.

CHAPTER IX

EFFECTIVENESS OF SOLUBILIZING CORROSION INHIBITORS

The solubility of extracts 1 and 3 was tested. Examples of solvents tested were formic acid, acetic acid, acetone, ethanol, methanol, isopropyl alcohol, and hydrochloric acid. Water was not used since alkaloids are often insoluble in water. This was to examine realistic methods of application of these extracts in the field as the extracts were obtained as dried powders. In order to determine the effect of solvents on the performance of the corrosion inhibitor, a known excess of sample 1 was first dissolved in isopropyl alcohol, acetone, methanol, and ethanol. Subsequently, the undissolved sample 1 was filtered out from each solvent, dried, and subsequently weighed to determine the mass of sample 1 that dissolved. The final solutions containing the dissolved sample 1 are shown in Figure 32 below. As can be observed from the picture, no precipitation was observed and therefore sample 1 was fully dissolved in each solvent.

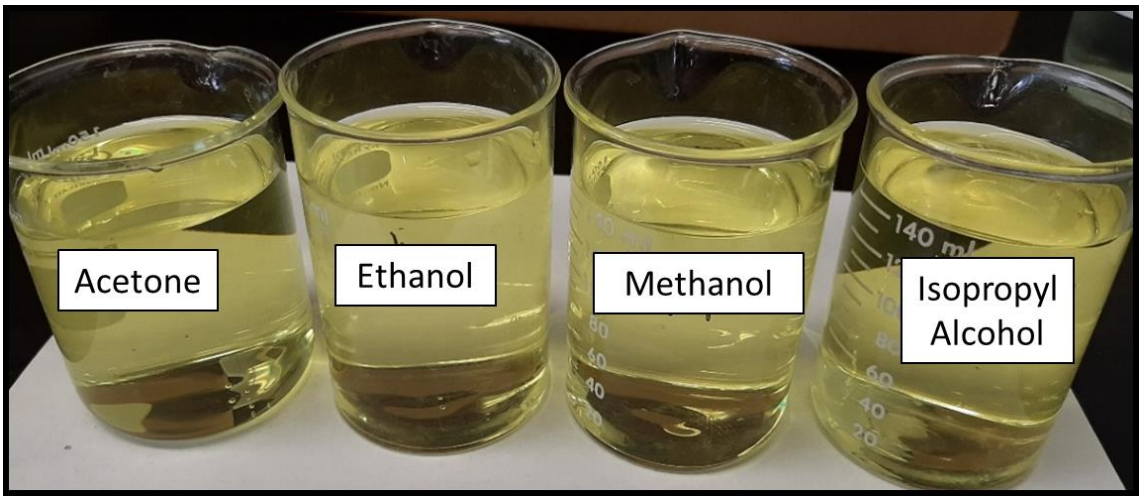

Figure 32: Sample 1 dissolved in various solvents including acetone, ethanol, methanol, and isopropyl alcohol.

Corrosion Tests – 72°F

These solvents were then used to introduce sample 1 into the 15 wt.% HCl solution so that sample 1 would constitute a concentration of 0.2 wt.% in the acid solution. Corrosion tests were then carried out using these solutions at room temperature over 6h and the results are shown in Table 19. The results indicate that aside from methanol, the choice of solvent had no significant influence on the inhibition efficiency of sample 1.

Table 19: Corrosion test results comparing the effect of each solvent on the performance of sample 1 at room temperature in 15 wt.% HCl over 6h.

Sample	C.I. Concentration (wt.%)	Corrosion Rate (lb/ft^2)	Inhibition Efficiency %
Base	-	0.0142	-
Isopropyl Alcohol	0.2	0.00002	99.86
Acetone	0.2	0.00009	99.37
Methanol	0.2	0.00028	98.03
Ethanol	0.2	0.00009	99.37

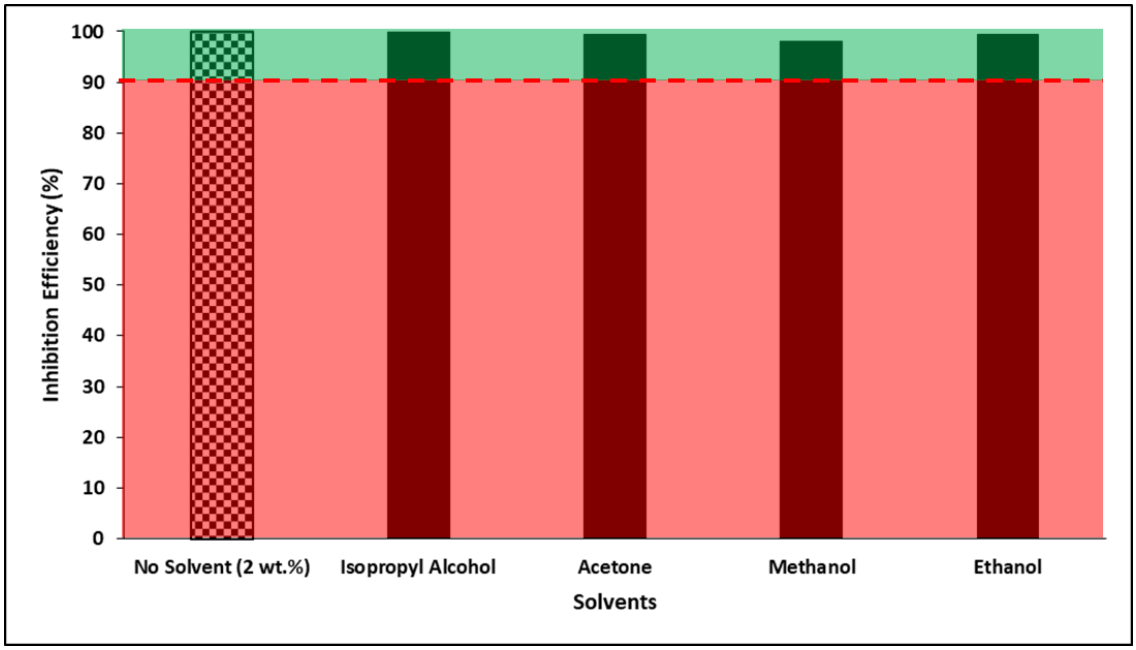

Figure 33: Illustration of corrosion test results for 4 different solvents used to dissolve sample 1 in 15 wt.% HCl at 72°F over 6h. Corrosion rates lying in the green area represent successful tests.

Corrosion Tests – 150°F

Eventually, it was found that the best method was to dissolve the extracts in ethanol which could then be mixed in with the 15 wt.% HCl solution. Corrosion tests at 150°F

with 15 wt.% HCl were carried out using these extract solutions resulting in 0.2 wt.% of each extract dissolved in the final solution. The results are shown in Table 20 below.

Table 20: Corrosion test results for extract solution tests carried out at 150°F in 15 wt.% HCl over 6h.

Sample	C.I. Concentration (wt.%)	Corrosion Rate (lb/ft^2)	Inhibition Efficiency %
Base	-	0.371	-
1	0.2	0.00499	98.7
3	0.2	0.03731	89.9

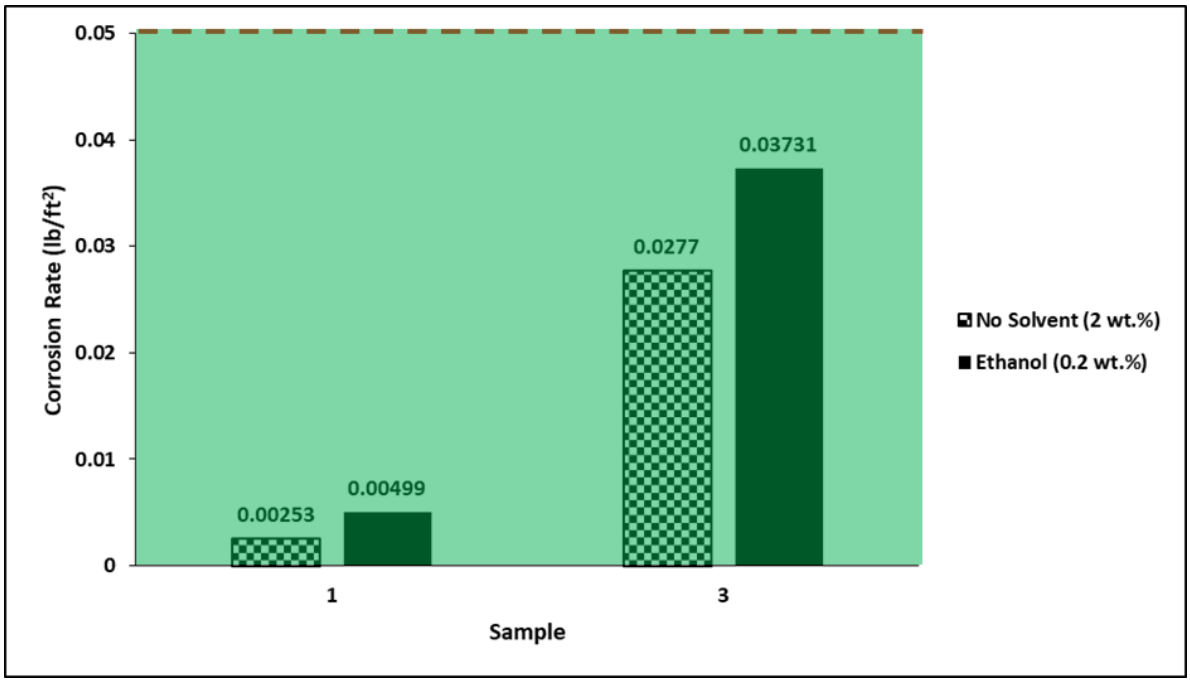

Figure 34: Illustration of corrosion test results solvated samples 1 and 3 in 15 wt.% HCl at 72°F over 6h. Corrosion rates lying in the green area represent successful tests.

Comparing the results with Table 19, it can be seen that while only 10% of the each sample was used, the inhibition efficiency only decreased by 0.6% for sample 1 and 2.6%

for sample 3. Furthermore, both samples are still below the industry required corrosion rate maximum of 0.05 lb/ft^2.

CHAPTER X

MULTIPURPOSE NATURE OF CORROSION INHIBITORS

Demulsifier Tests

As mentioned previously, when sample 3 was mixed with emulsified acid, it was found to be able to instantaneously separate the acid from the diesel emulsifying it. This led to the possibility that this sample could be used as an environmentally friendly, non-toxic demulsufier. Current demulsifiers used in the oil and gas industry are known to be toxic to marine life and humans, and are also harmful to the environment (Henderson et al. 1999; Yaacob and Sulaimon 2017). Common examples of demulsifiers include acid catalyzed phenol-formaldehyde resins, polyethyleneimines, and polyamines.

As its name suggests, demulsifiers are surfactants that are used to break oil-water emulsions. Such emulsions are formed when emulsifiers migrate to the oil-water interface and stabilize it by reducing the interfacial tension between the two liquids. This is due to the presence of hydrophilic and hydrophobic functional groups on the emulsifiers that allow these surfactants to adsorb to the interface of both immiscible liquids. Demulsifiers disrupt the arrangement of emulsifiers at the interface, thereby breaking the emulsion. Raya et al. (2020) states that emulsions of water-soluble demulsifiers are used to destabilize oil-in-water emulsions while oil-soluble demulsifiers are used to break water-in-oil emulsions. Since sample 3 is more oil-soluble than water-soluble, it is an ideal candidate to break the common water-in-oil emulsions present in the oil and gas industry.

These water-in-oil emulsions are especially common in crude oil containing polar components such as asphaltene as it readily forms emulsions when mixed with acidic or iron-containing solutions (Almubarak et al 2020). Since sample 3 has been shown to provide excellent corrosion inhibition at temperatures up to 250°F, if it is able to be used simultaneously as a demulsifier, it would eliminate the need for additional chemicals during acid treatment.

In order to test the demulsifying properties of sample 3, Alaskan crude with an API of 41 was used to create an emulsion with 15 wt.% HCl solution. Equal volumes of crude oil and HCl were added to a 20 ml glass bottle as shown in Figure 35a below. In this figure, the less dense crude oil floats on top of the denser acid, and as can be seen, a clear interface exists between the two liquids. This shows that there is no miscibility at all between the liquids.

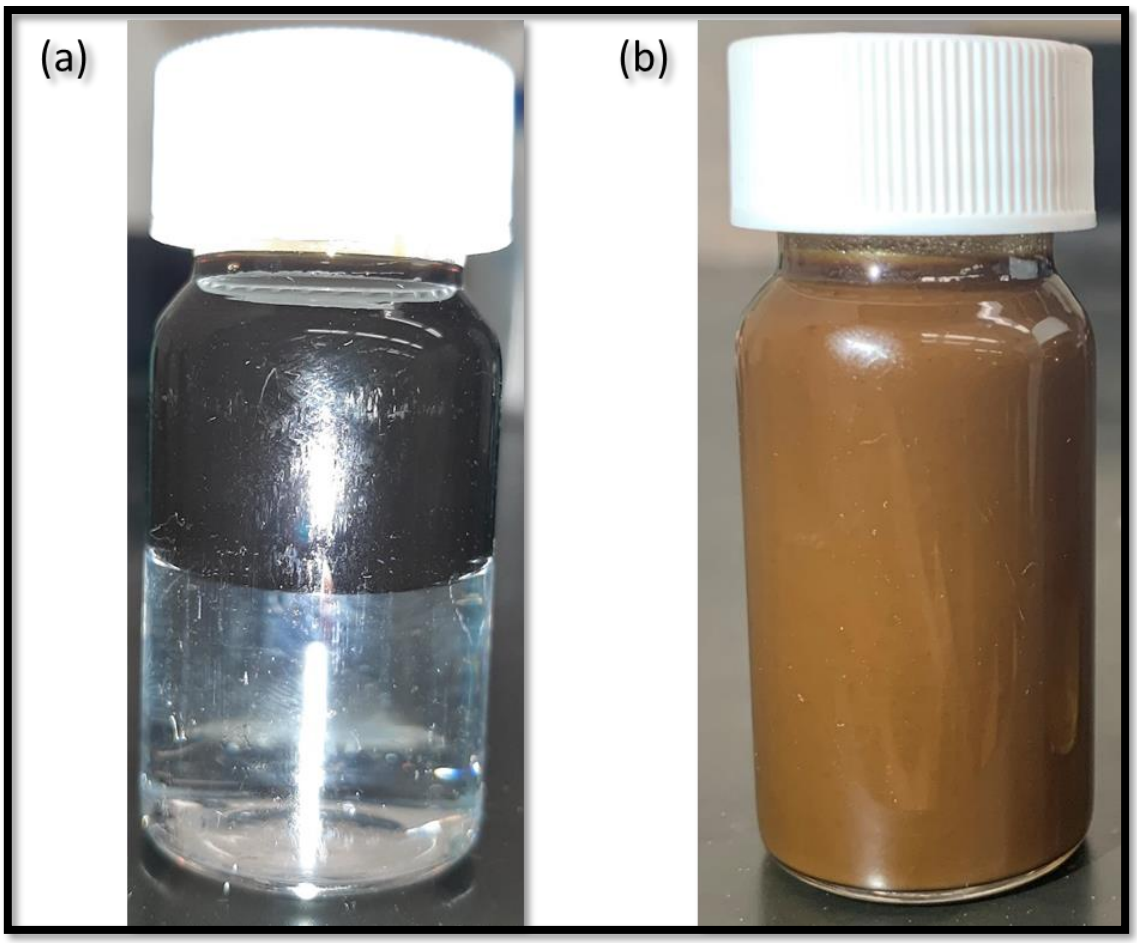

Figure 35: Picture of acid-oil emulsion. (a) Acid and oil before vigorous shaking. (b) Acid and oil emulsion formed after vigorous shaking.

Figure 35b shows the emulsion formed after the bottle was shaken vigorously by hand for approximately 10 minutes. A second bottle containing the same acid and crude oil mixture was prepared and shaken for a similar duration to the first bottle described above. 1 gram of sample 3 was then added to the second bottle and shaken again to dissolve sample as much of sample 3 in the emulsion as possible.

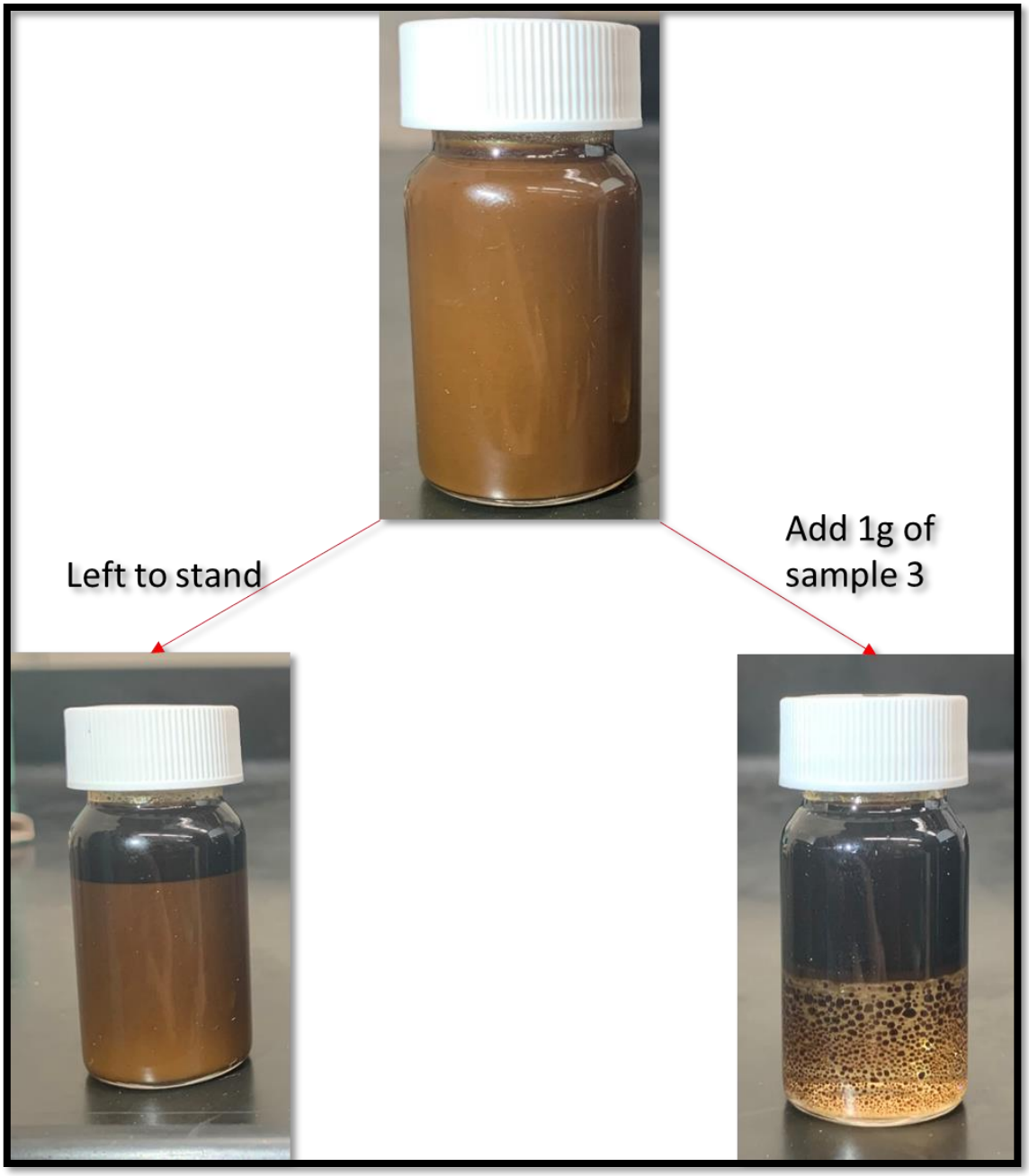

Figure 36: Emulsion after being left to stand and after the addition of 1g of sample 3.

The results of the test can be seen in Figure 36 above where the emulsion in bottle 1 can be observed to undergo partial separation due to the formation of the black layer of

crude oil near the top of the bottle. However, when 1g of sample 3 was added to bottle 2 and shaken, it can be observed that the emulsion breaks almost instantaneously and the emulsion separates into the distinct crude oil and water layers as shown in Figure 36. The interface between the separated acid and oil phases still shows a thin layer of emulsion remaining but compared to bottle 1, the emulsion is almost completely broken. From these results, sample 3 shows that it has strong demulsifying properties and can be used as a potential green demulsifier in the field.

Emulsifier Tests

The previous work showed how sample 3 was able to act as a demulsifier and break emulsions of crude oil and acid. This was due to sample 3 being able to displace and interfere with the arrangement of surfactants on the oil-water interface. By extension, it is possible that sample 3 could act as an emulsifier as well.

To test the emulsifying properties of sample 3, a 20 ml bottle containing acid and diesel was prepared. The bottle contained 10 ml of each liquid as shown in Figure 37a and no emulsifier was added initially to determine the stability of an emulsion formed between acid and diesel in the absence of an emulsifier. The bottle was then vigorously shaken for several minutes in order to form an emulsion as can be seen in Figure 37b. After the emulsion was observed, the bottle was left to stand for 10 minutes. Due to the absence of an emulsifier, the emulsion separated as expected and the final separated solution can be seen in Figure 37c. Comparing Figure 37a to Figure 37c, it can be seen that the height of acid is similar, indicating that the emulsion had separated completely.

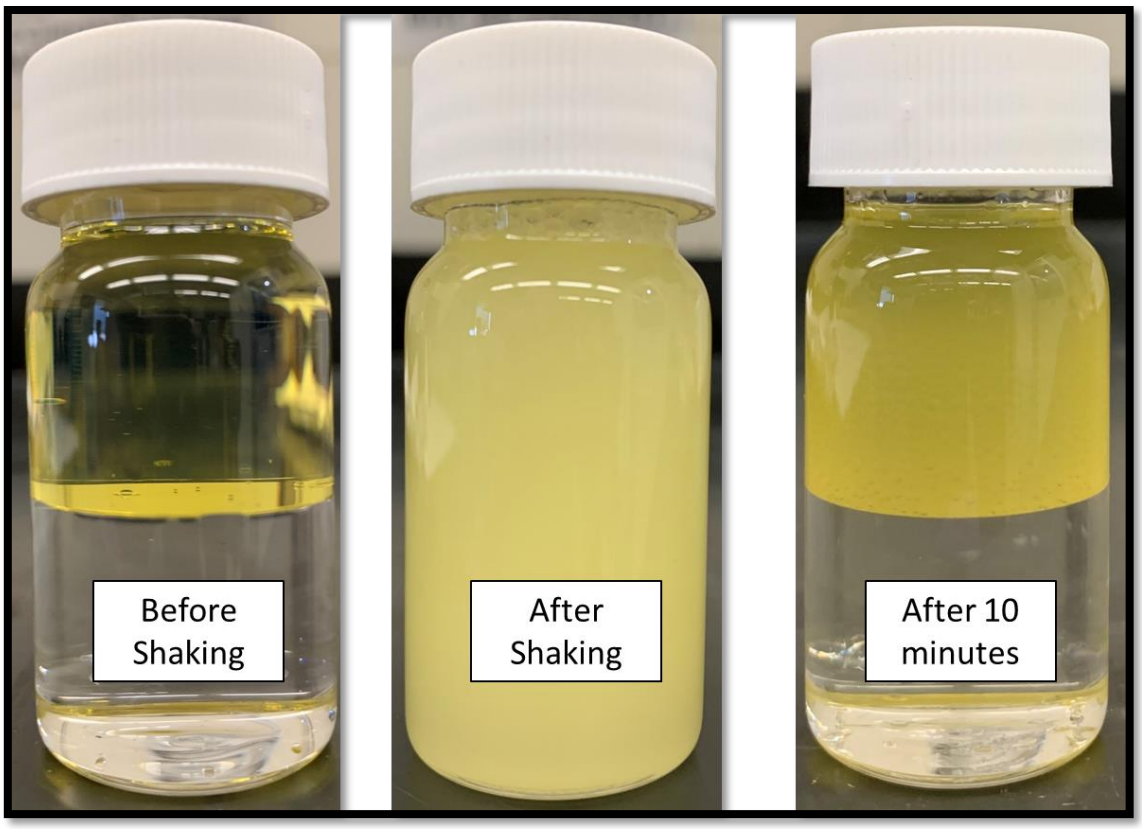

Figure 37: 10 ml of 15 wt.% HCl with 10 ml of diesel.

Following this test, 2 wt.% of sample 3 was added to 6 ml to diesel before 14 ml of 15 wt.% HCl solution was added to the bottle. This was to create the 70:30 acid to diesel ratio that is commonly used to prepare emulsified acids in the oil and gas industry. Figure 38 shows the images of the mixture before and after it was shaken. In Figure 38b, it can be seen that the emulsion formed is more stable than that between diesel and acid alone (Figure 37c), indicating that sample 3 was indeed fulfilling its role as an emulsifier.

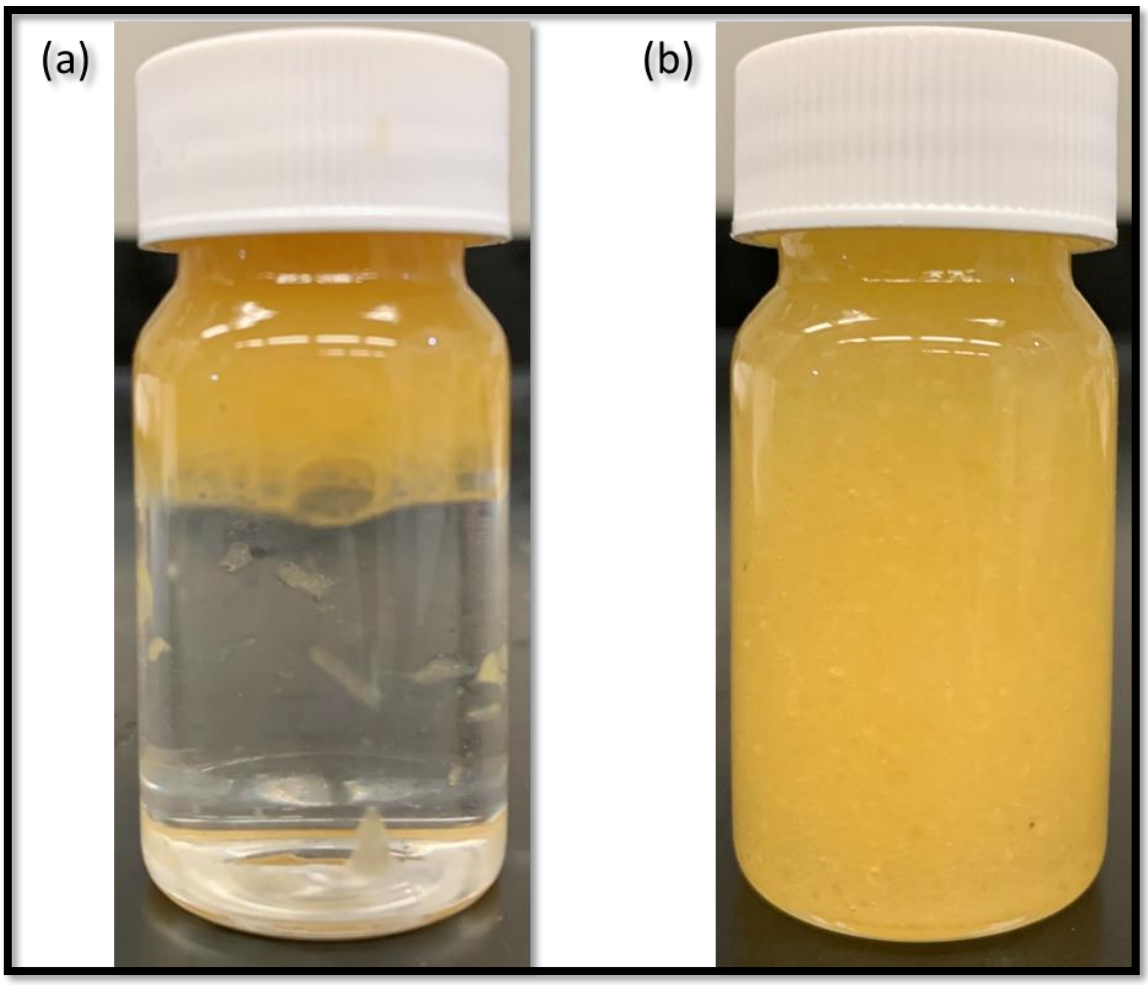

Figure 38: 20 ml bottle containing 6 ml diesel mixed with 2 wt.% sample 3 and 14 ml of 15 wt.% HCl solution (a) before shaking, (b) after shaking and left to stand for 10 minutes.

Subsequently, the stability of the sample 3 emulsified acid was determined by adding it dropwise into a jar of water using a 1 ml syringe. As can be observed in Figure 39, addition of the emulsified acid to the jar of water caused distinct droplets of acid to be formed in the water. The droplets did not break upon contact with the water and appear to be able to maintain their shape to a large extent. This indicates that the emulsion formed was indeed a water-in-oil emulsion as desired and the phases had not reversed.

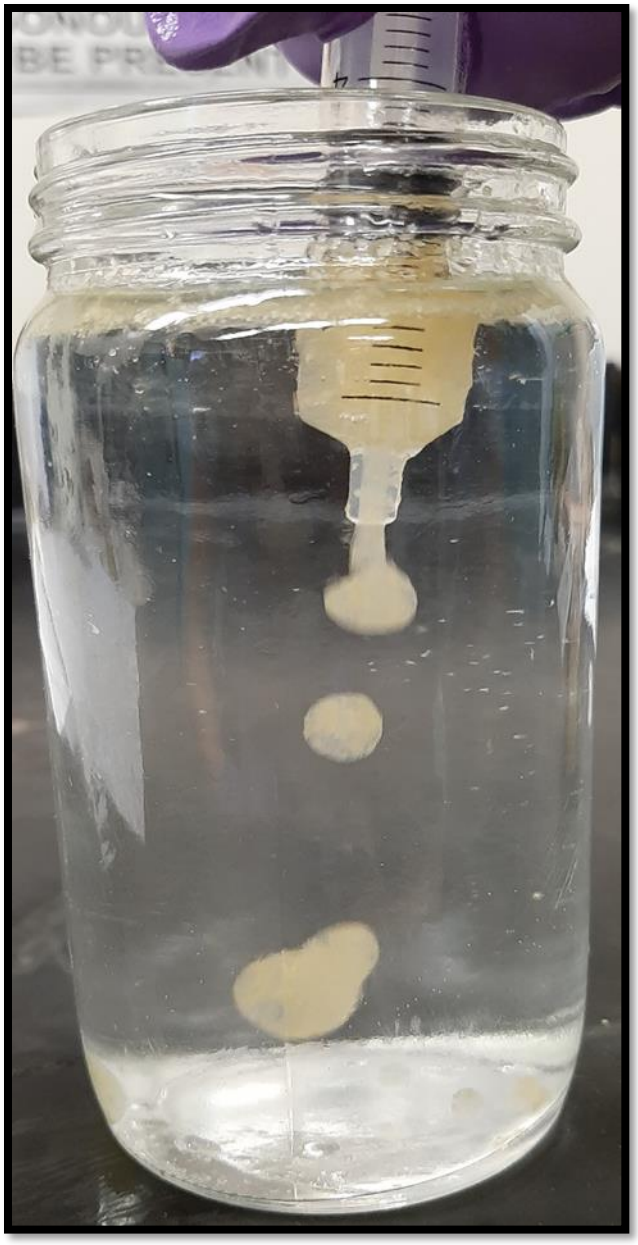

Figure 39: Drop test of emulsified acid into jar of water. Distinct droplets of emulsified acid are formed upon addition into water and sink to the bottom.

Furthermore, the emulsified acid was observed to sink to the bottom of the jar. This is consistent with the 70:30 acid to diesel ratio that was used to create the emulsified acid, indicating the emulsion was properly mixed and carried the correct amount of acid.

Finally, a conductivity test was carried out and determined that the conductivity of the emulsified acid solution was close to 0 S/m. This further showed that the acid had been emulsified in the oil phase and the emulsion was stable since no aqueous component was present.

CHAPTER XI

CHEMICAL ANALYSIS AND INTERPRETATION

Sample 1

Following the corrosion and demulsifier tests, chemical analysis of the extracts of samples 1 and 3 were carried out using H-NMR and LC-MS to attempt to determine the decomposition products and the structure of the samples used. Furthermore, these methods would also show the thermal stability of the tested samples and serve to highlight any possibility that the decomposition products could play a role in corrosion inhibition of the metal.

The NMR spectra results for the extract of sample 1 are shown in Figure 40 to Figure 42 below. Figure 40 shows the NMR result of sample 1 in $CDCl_3$ solvent prior to degradation. Analysis of the spectra matched the hydrogens on the molecule to those detected by the spectra, thereby confirming the identity of sample 1. As can be observed from the spectra, the distinct peaks recorded indicate that the sample used for the tests were very pure, with the peak at 1.22 ppm showing the presence of a small amount of impurities present in the sample.

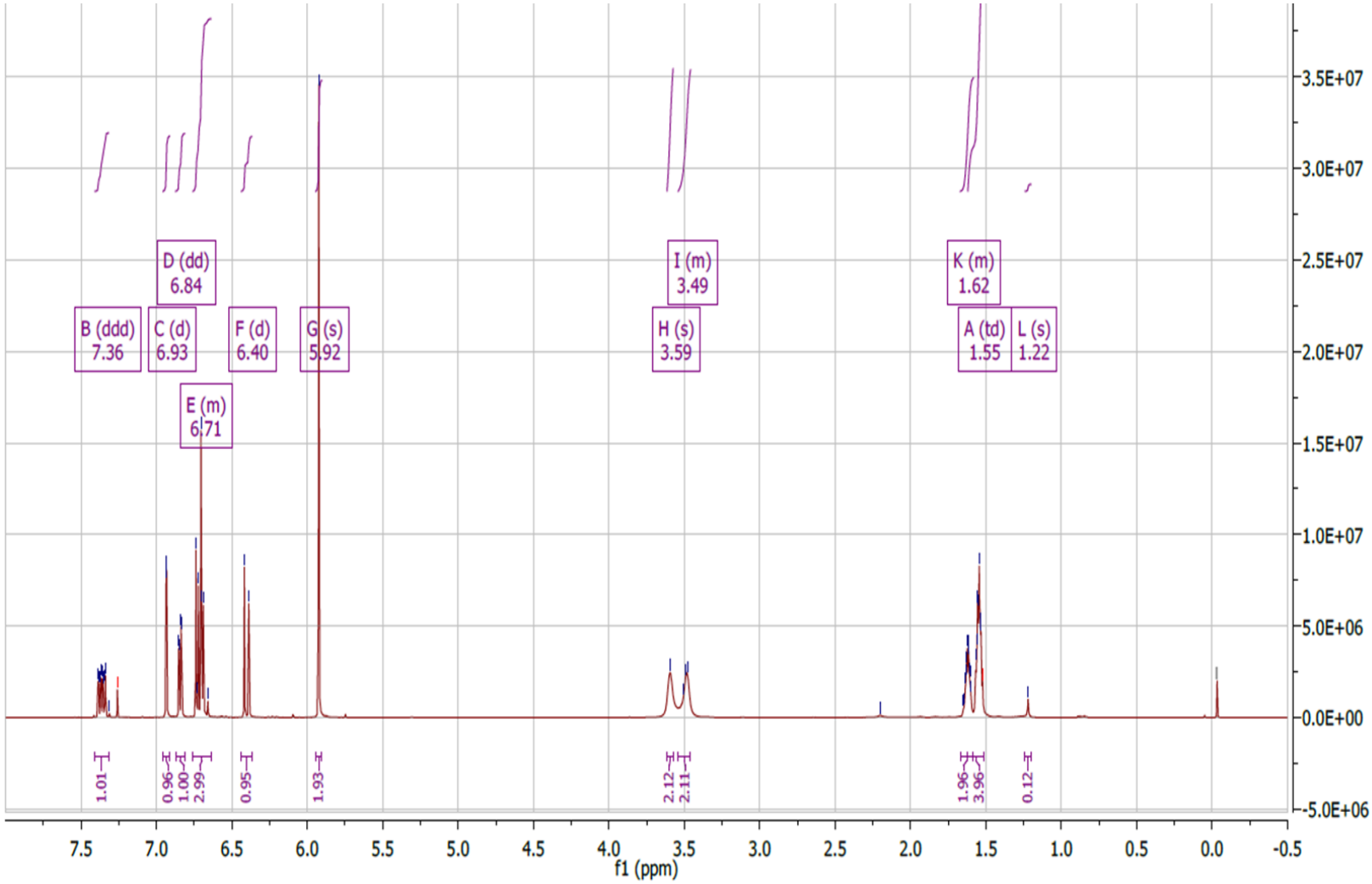

Figure 40: NMR results for sample 1 using $CDCl_3$ solvent.

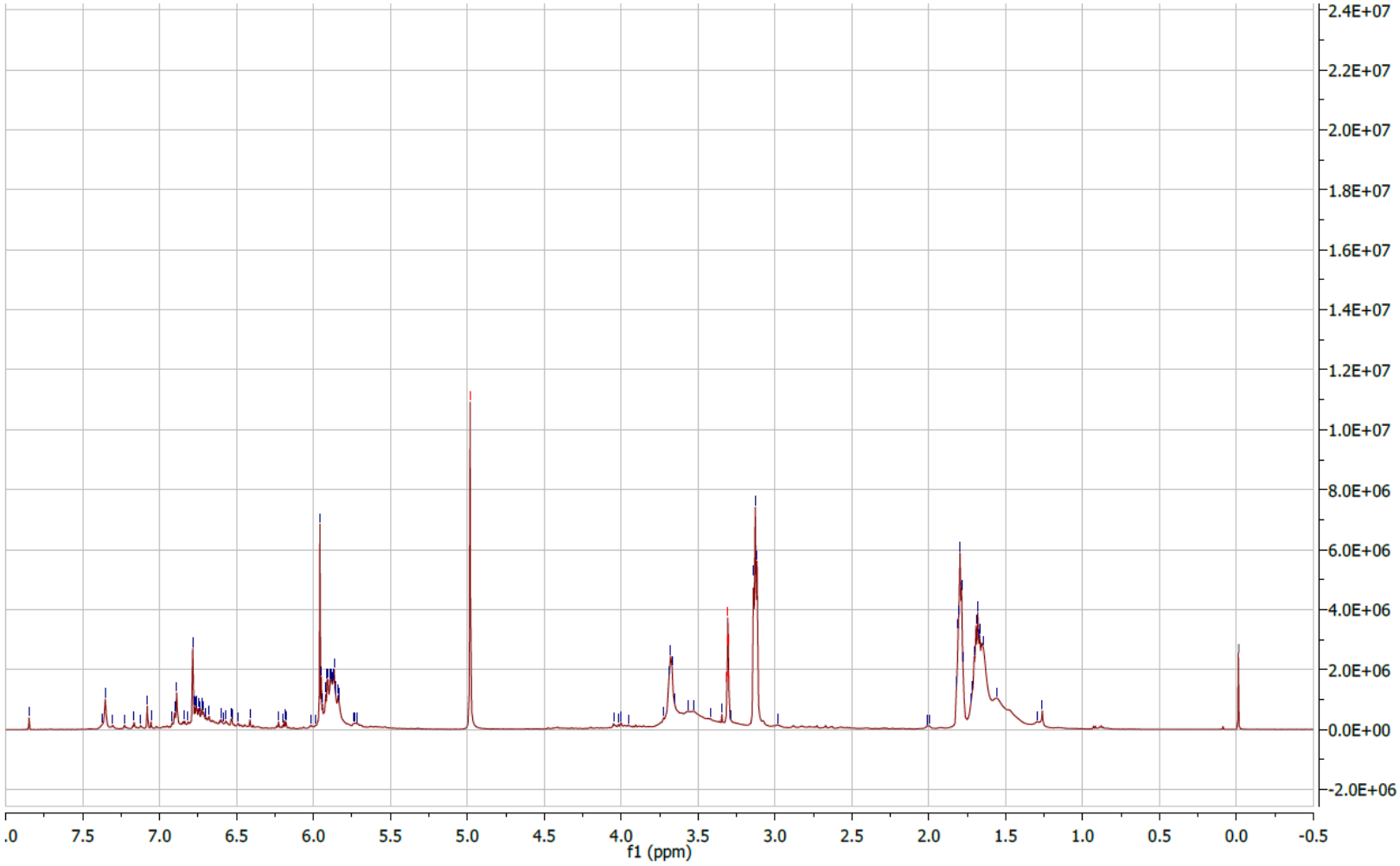

Figure 41: NMR results for decomposition products of sample 1 in 15 wt.% DCl for 6h at 200°F.

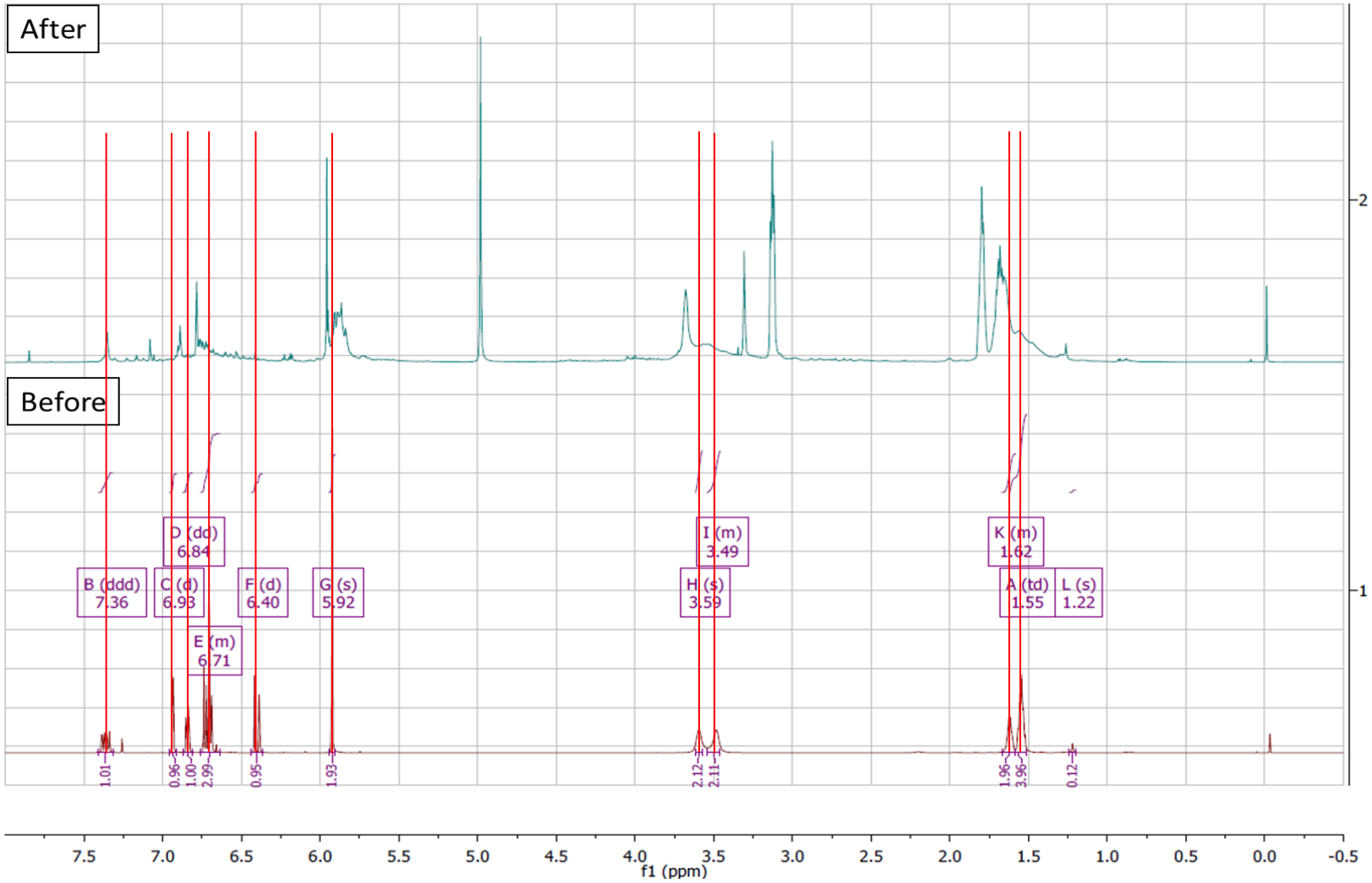

Figure 42: Combined NMR results for sample 1 and its decomposition products in 15 wt.% DCl for 6h at 200°F.

Decomposition of sample 1 was carried out in 15 wt.% DCl solution to mimic the acidic conditions of the corrosion tests. This decomposition was carried out in an oven preheated to 200°F and the decomposition products re-dissolved in MeOD before the NMR test. Figure 41 shows the NMR analysis of these decomposition products while Figure 42 shows the comparison between the before and after analysis of sample 1. By comparing the NMR spectra for sample 1 and its decomposition products via the red lines on the spectra, it can be observed that sample 1 was completely decomposed by the end of 6h. The disappearance of the peaks at 1.62, 3.49, 3.59, 6.40, 6.71, 6.84, and 6.93 ppm as shown in Figure 42 are the main indicators of this. Furthermore, the appearance of a prominent new singlet at 4.95 ppm as well as the other new peaks confirms the production of a new molecule during the degradation process. However, as can be observed in Figure 41, many of these peaks are poorly resolved, such as those spanning 5.75 to 6.0 ppm, 3.0 to 3.75 ppm, and 1.25 to 2.0 ppm. This makes determination of the decomposition products extremely difficult. In order to confirm the complete degradation of sample 1, LC-MS was carried out.

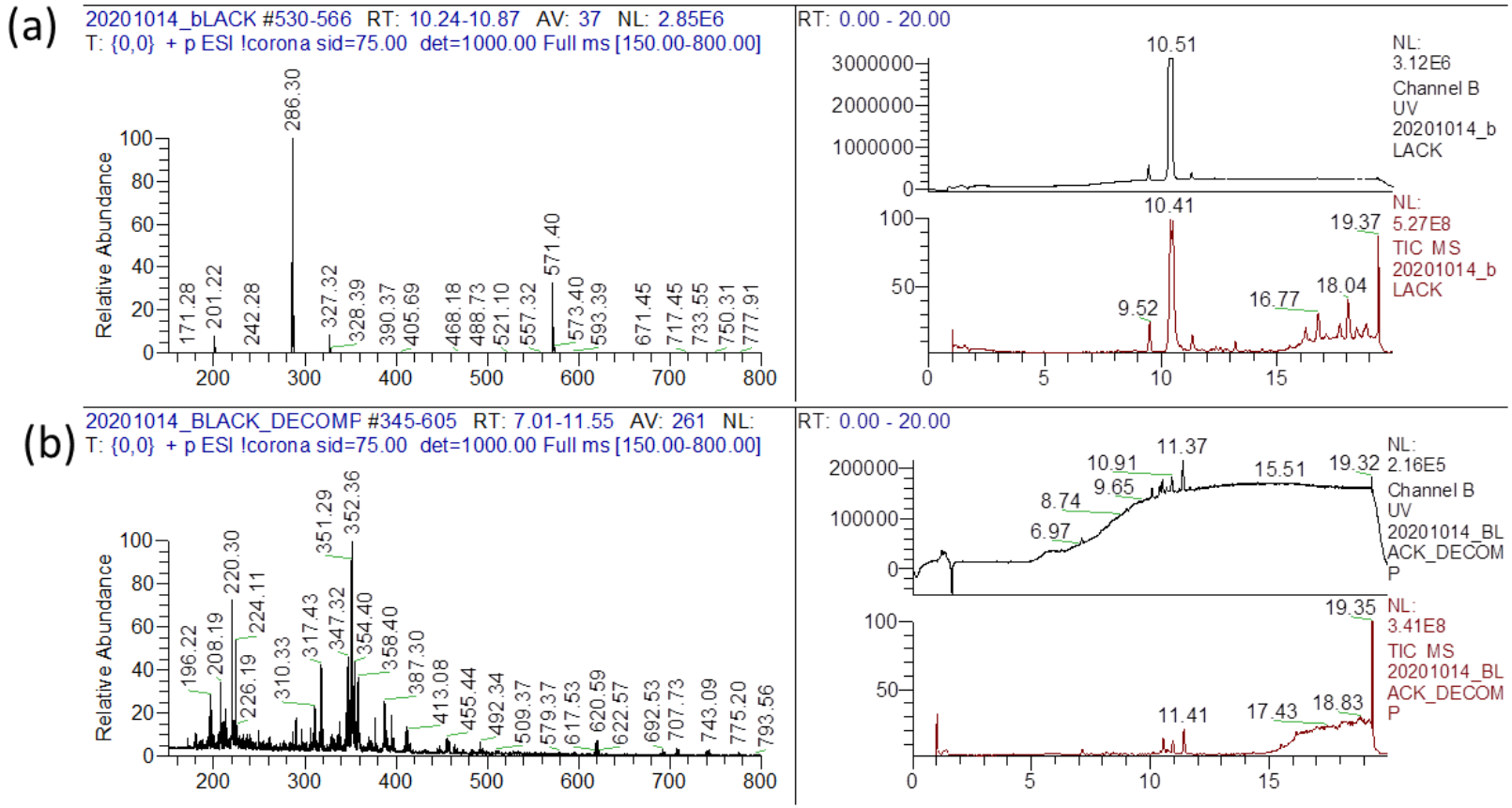

Figure 43: LC-MS of sample 1 (a) before degradation and (b) after degradation at 200°F

The LC-MS results are shown in Figure 43 above. Similar to the NMR results, Figure 43a shows that sample 1 had a high purity with distinct peaks at m/z of 201.22, 286.30, 327.32, and 571.40 with the higher molecular weights belonging to a dimerized form of sample 1. The products resulting from the degradation are shown in Figure 43b. Similar to Figure 41, a multitude of decomposition products can be observed with none of the initial 4 distinct peaks remaining. This indicates that sample 1 was completely degraded under these conditions and is in agreement with the results shown from the NMR tests.

Interestingly, despite the complete degradation of sample 1 at this temperature, the corrosion test results have shown that it was able to confer strong corrosion resistance to the metal coupon. This would imply that the decomposition of sample 1 was essential in creating a corrosion-resistant layer on the surface of the coupon and that this cocktail of decomposition products are responsible for the corrosion resistance shown in the tests above.

Figure 44 to Figure 46 shows the NMR results for sample 3. As with sample 1, Figure 44 shows the NMR result of sample 3 dissolved in $CDCl_3$ solvent. Comparing this NMR spectra to known H-NMR spectra of sample 3, it can be observed that the peaks at 5.81, 1.49, and 1.13 ppm are likely impurities in the sample. However, their intensity suggests that they do not constitute a significant proportion of sample 3 and thus should not have influenced the surfactant and inhibiting properties of sample 3. These impurities are likely a result of the extraction process.

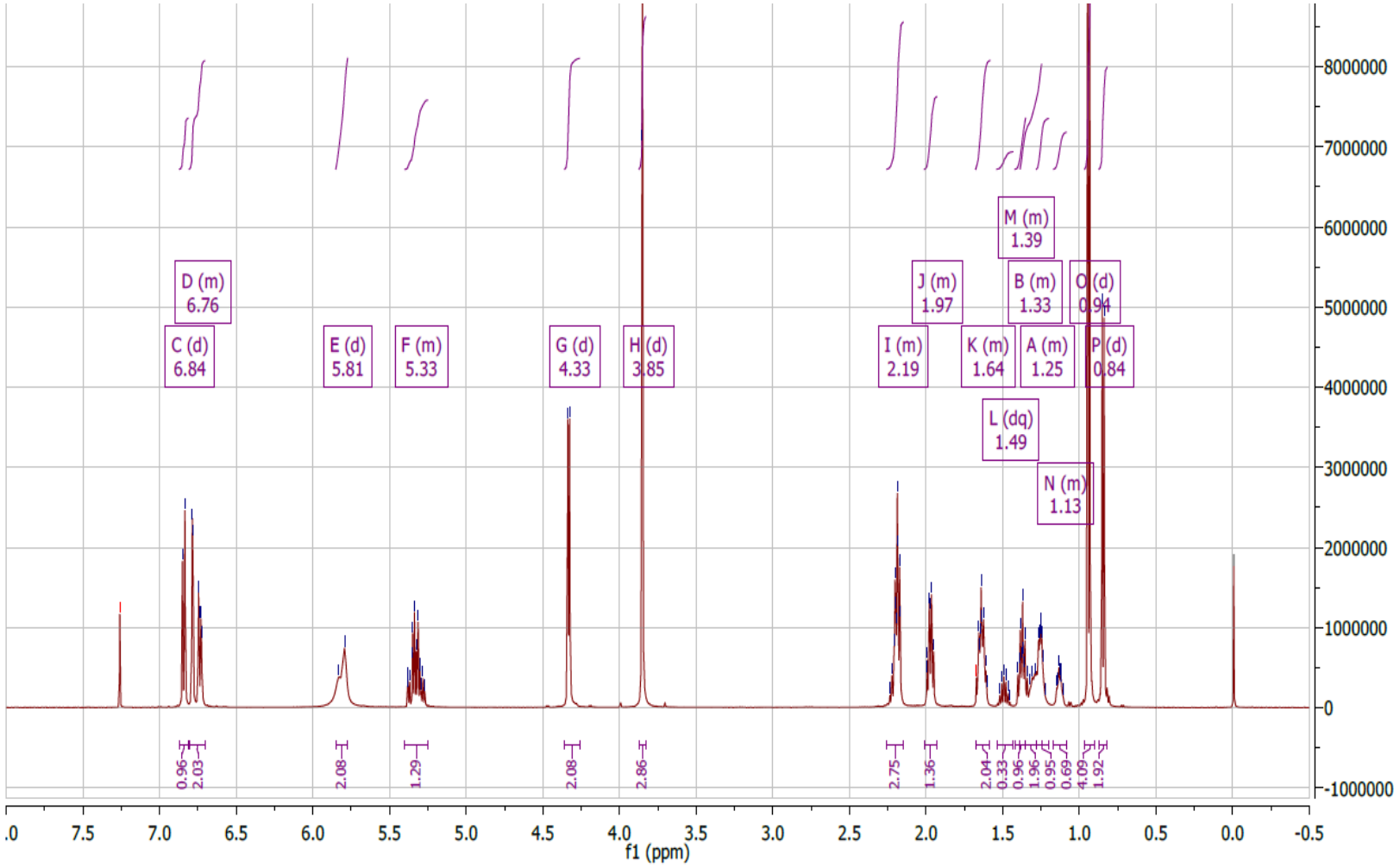

Figure 44: NMR results for sample 3 using $CDCl_3$ solvent.

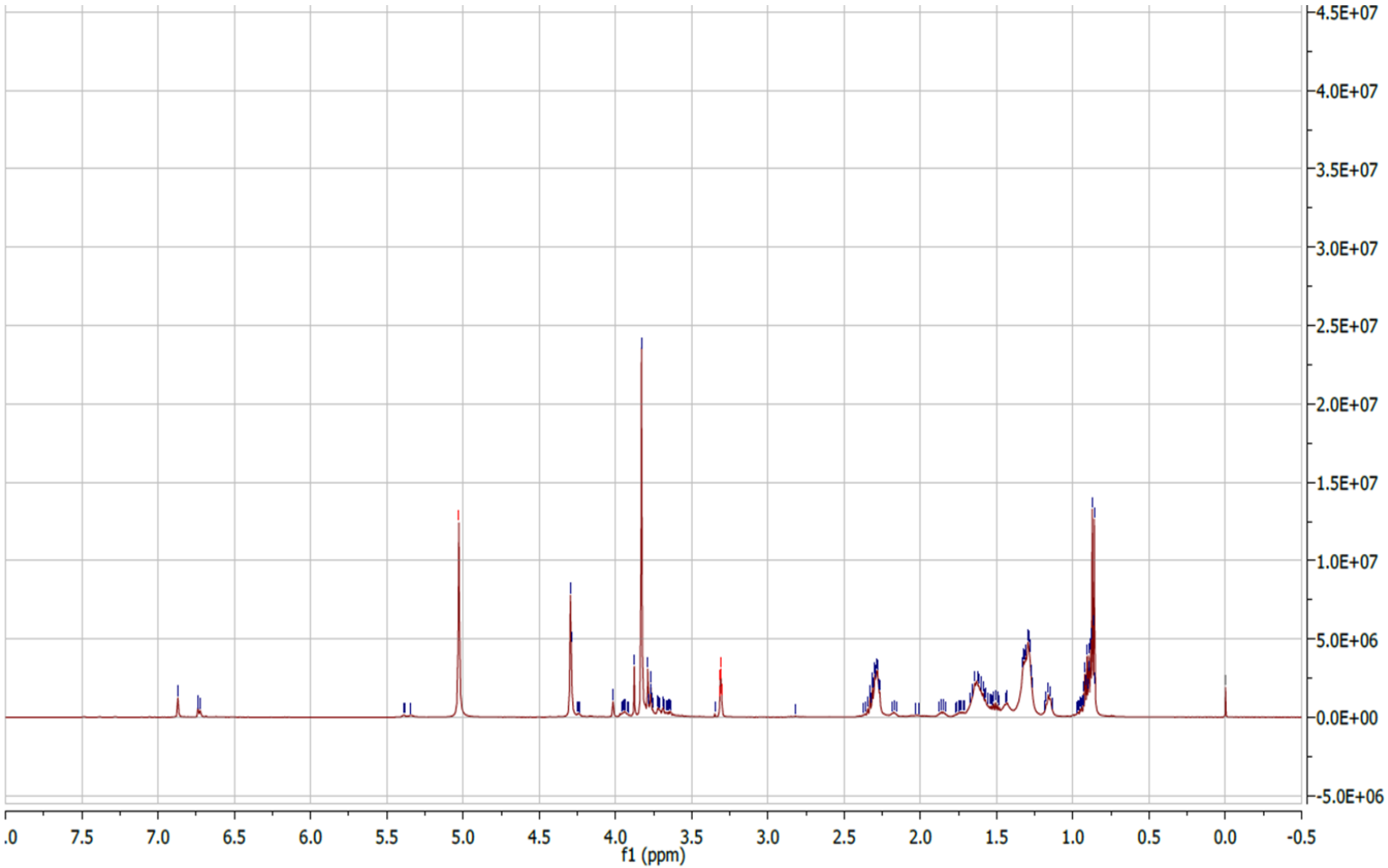

Figure 45: NMR results for decomposition products of sample 3 in 15 wt.% DCl for 6h at 200°F.

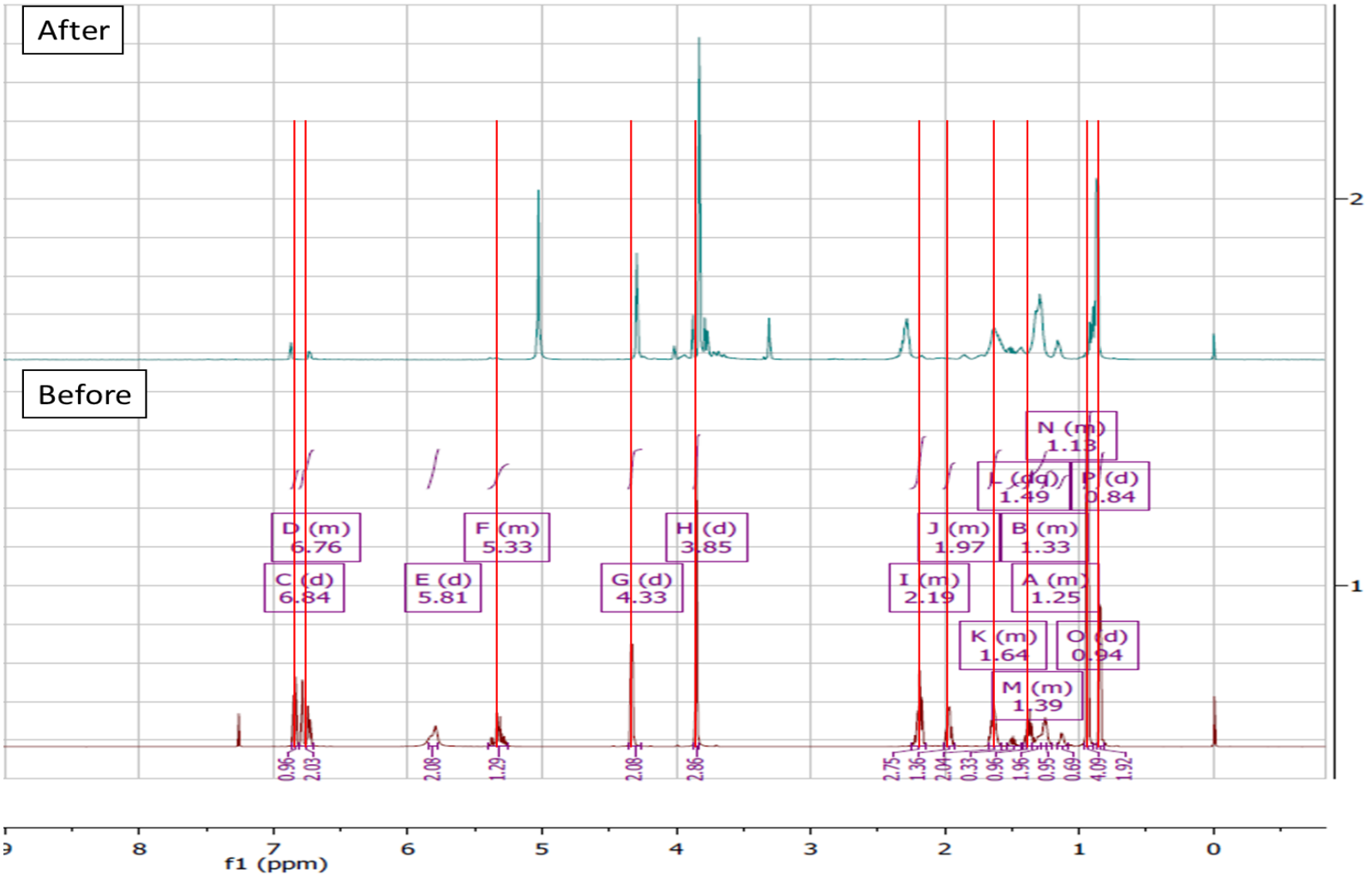

Figure 46: Combined NMR results for sample 3 and its decomposition products in 15 wt.% DCl for 6h at 200°F.

Sample 3

Like sample 1, decomposition of sample 3 was carried out in 15 wt.% DCl solution to mimic the acidic conditions of the corrosion tests. This decomposition was also carried out in an oven preheated to 200°F and the decomposition products dissolved in MeOD before the NMR test. The NMR results of the degraded sample are shown in Figure 45 with the before and after comparisons shown in Figure 46. By examining the red lines that represent the important peaks defining sample 3, it can be observed that, like sample 1, several peaks that were present before the decomposition were absent after the decomposition was completed. However, unlike sample 1, there appear to be peaks that remained even after the decomposition. Examples of these include peaks at 0.94, 1.64, 3.85, 4.33, 6.76, and 6.84 ppm. This would suggest that while sample 3 did decompose at 200°F, its decomposition products retained similar functional groups to that of sample 3. This would imply that the initial decomposition products of sample 3 are thermally stable and did not further breakdown like those of sample 1. In order to confirm these results, LC-MS was also carried out on sample 3 and is shown in Figure 47 below.

The spectrum of sample 3 prior to degradation shown in Figure 47a shows major peaks at m/z values of 182.36, 306.36, 347.33, 611.57, and 612.56. These values correspond to those of sample 3, as shown in literature regarding this molecule with the larger molecular weights indicating the formation of dimers. This confirms the NMR results which indicate that sample 3 is a pure substance. After decomposition, it can be observed from Figure 47b that many new products were formed. Furthermore, the peaks

indicating the presence of sample 3 are no longer present, confirming that sample 3 was decomposed completely as indicated by the NMR results.

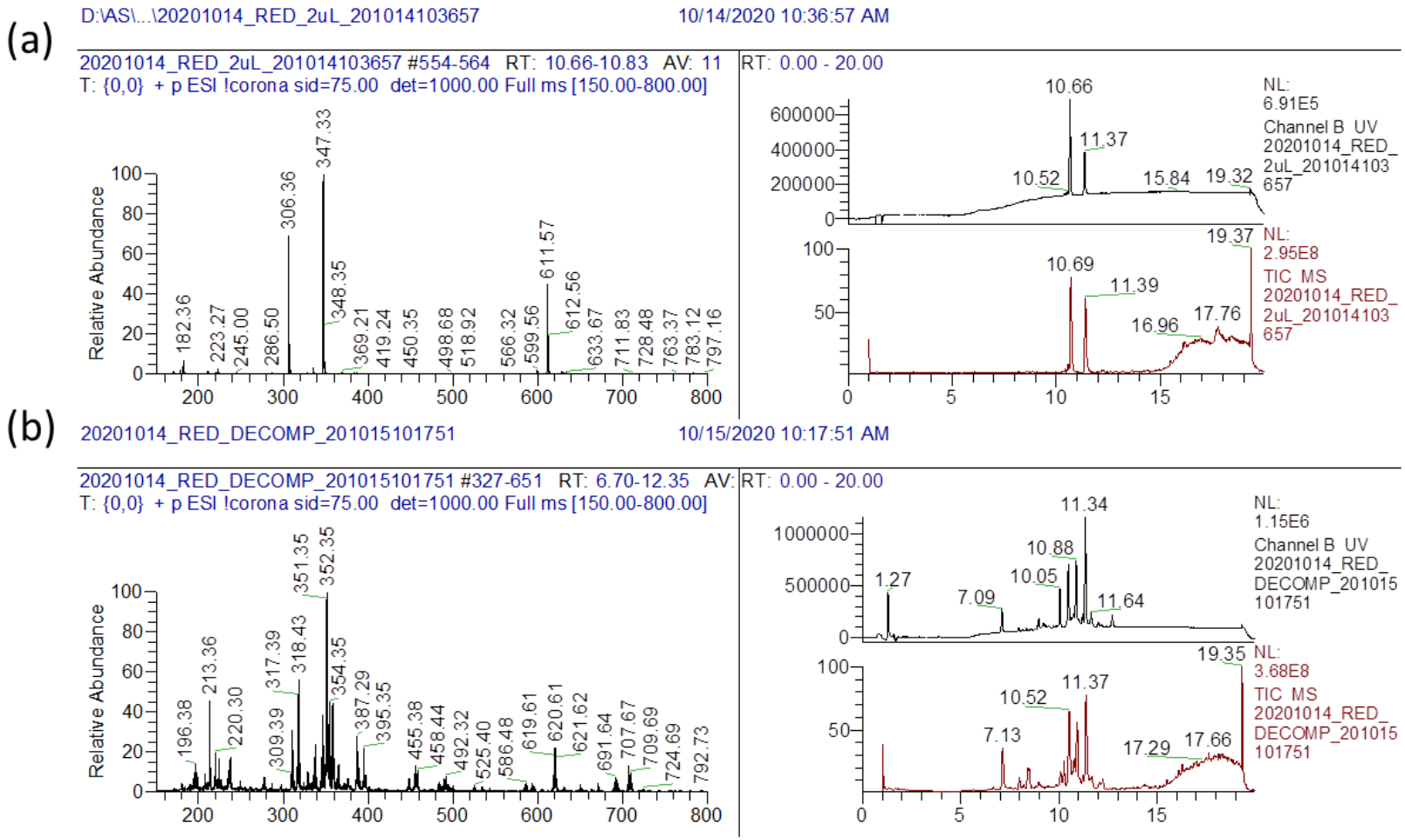

Figure 47: LC-MS of sample 3 (a) before degradation and (b) after degradation at 200°F.

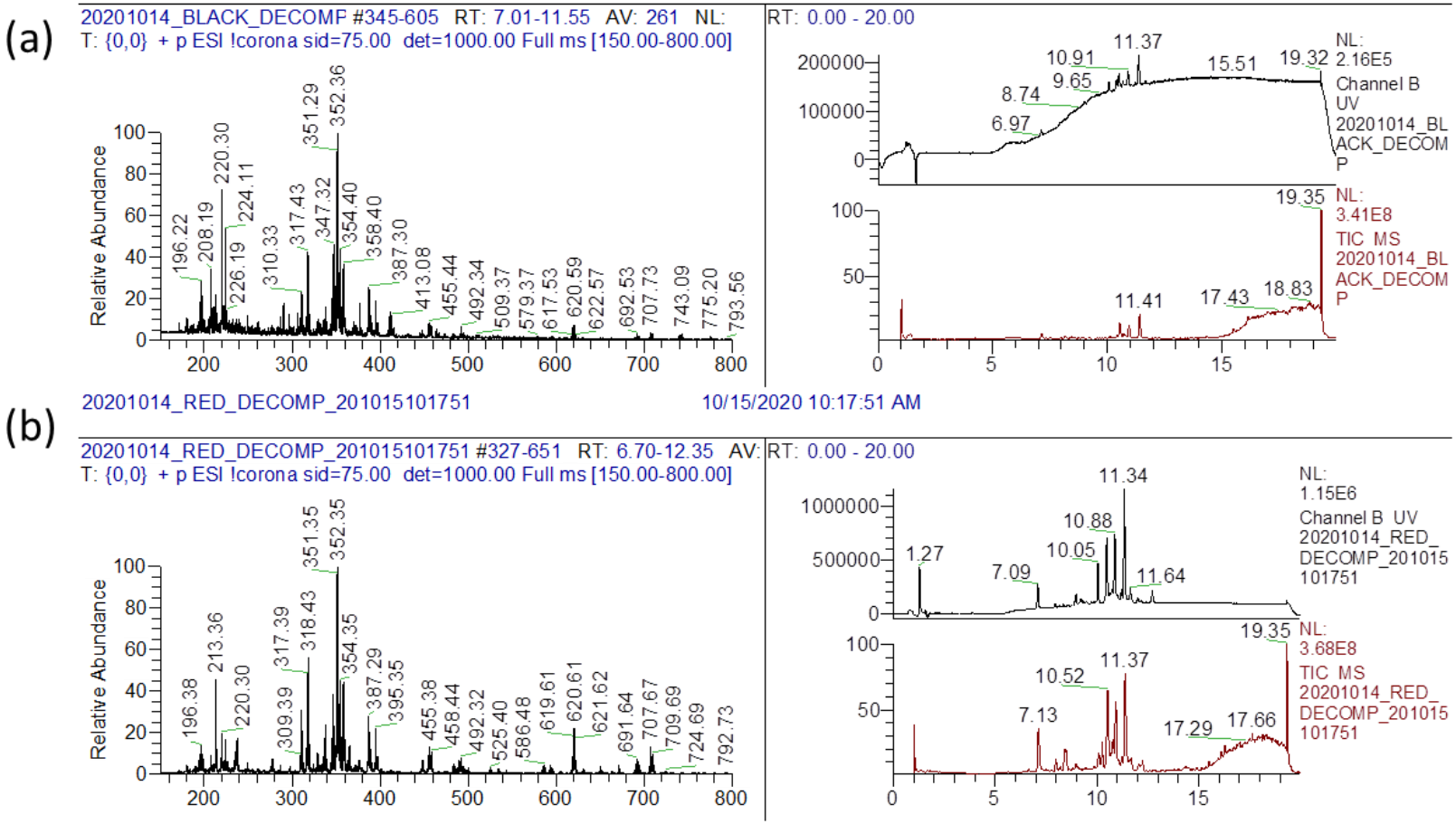

Figure 48: Comparison between the decomposition LC-MS results of (a) sample 1 and (b) sample 3.

Comparing the LC-MS products of both samples 1 and 3 using Figure 43b and Figure 47b respectively yields some interesting results. When placed side by side as in Figure 48, it can be seen that there are many similarities between the decomposition products. Many similar peaks exist between the decomposition products including m/z values at 196, 220.30, 317, 351, 352, 354, 387.30, 455, and 620. While the structures of these decomposition products cannot be determined by the m/z values alone, the presence of these similar peaks in both products indicates that samples 1 and 3 form common decomposition products that could be responsible for providing the strong corrosion inhibition observed in the corrosion tests. Future work will involve identifying and isolating these decomposition products to determine the compound that is responsible for the corrosion inhibiting properties.

CHAPTER XII

DISCARDED CIGARETTES

Going back to the miscellaneous results obtained in Table 8, one of the environmentally friendly corrosion inhibitors tested was material obtained from used cigarettes. The world buys roughly 6 trillion cigarettes each year. Most of the cigarette is wrapped with paper that can burn and disintegrate. However, a portion of the cigarette known as the “cigarette butt” is made of plastic called cellulose acetate. This kind of material does not get burned. It acts as a filter to reduce that burned cigarette smoke goes through prior to inhalation. This process results in the accumulation of harmful chemicals in the cigarette butt, which causes it to change in color from white to the yellow brownish color typically seen in cigarette remains. Trillions of these cigarette butts make it to the trash, however, the majority of the cigarette butts are just flung on the streets and into the environment causing damage to the surrounding plant and animal life.

Many recent studies have shown that cigarette buts hurt plant growth and eventually go to the water drainage and start hurting the ocean life. Used cigarettes butts have been known to be a major source of pollution due to their poor biodegradability, the ability to leach highly toxic chemicals such as nicotine and heavy metals into aquatic environments (Slaughter et al. 2011, Selmar et al. 2018), and their unsightliness.

The inability of cigarette butts to degrade causes them to be consumed by unsuspecting wildlife or remain in the ground or water for extended periods of time, allowing the toxic leachate to permeate into the animal or the water body exposed to the cigarette butt. 1 cigarette butt soaked in 1L of water for 4 days was shown to produce enough toxic leachate

to kill test fish (Benavente et al. 2019). Therefore, the opportunity to reuse such an environmentally harmful waste product resulted in the corrosion testing of cigarette butts to examine their ability to act as a corrosion inhibitor.

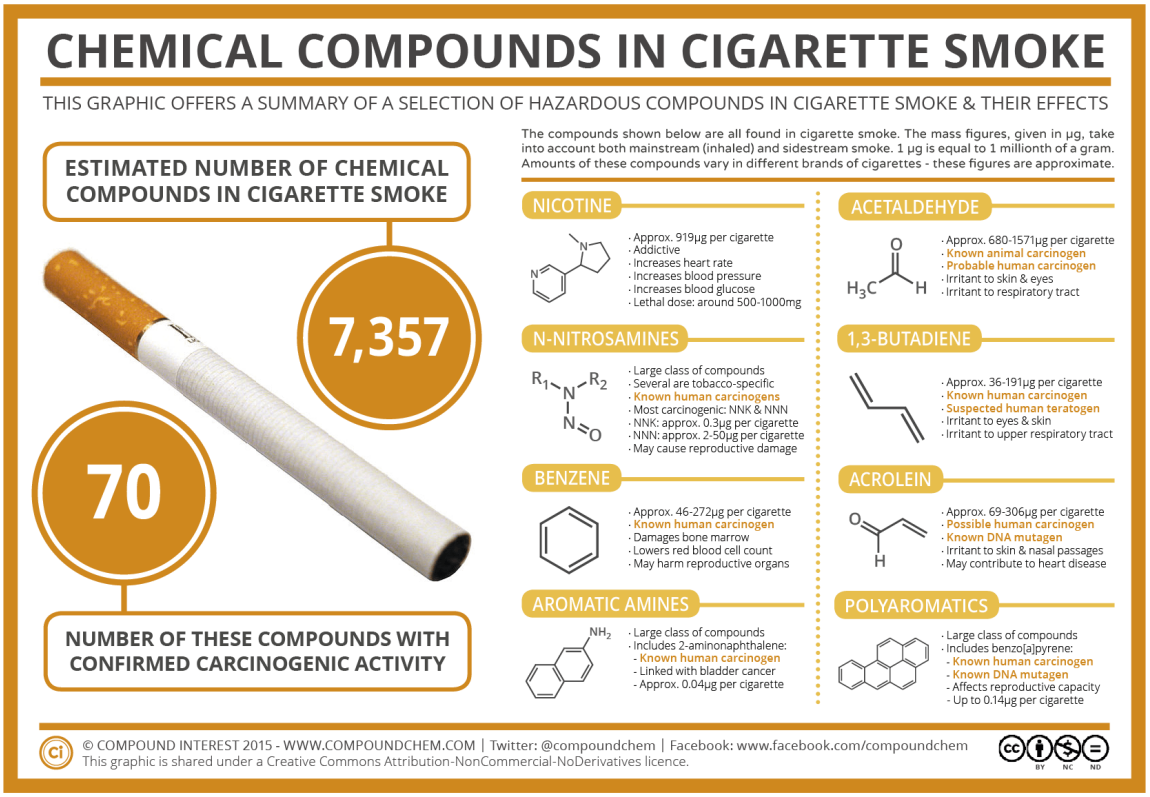

Figure 49: Infographic of chemicals present in cigarette smoke (Compound Interest 2014)

Figure 49 shows the major components present in cigarette smoke. From these components, it can be seen that many of the byproducts in used cigarettes contain aromatic groups such as benzene, and other aromatic amines and polyaromatic hydrocarbons. While these components are present in cigarette smoke, some of them should remain in the cigarette butt in the form of residue. The presence of the electron ring in benzene structures

is known to allow adsorption of the molecule onto the surface of metal and therefore, these structures could possibly provide some corrosion inhibition.

To determine the effect of these chemicals on corrosion inhibition, used cigarette butts from the cigarette disposal area were allowed to soak in 15 wt.% HCl for 15 minutes prior to the corrosion test in order to allow for extraction of these organic compounds into the solution. The coupon was then immersed into the solution. This is shown in Figure 50 below.

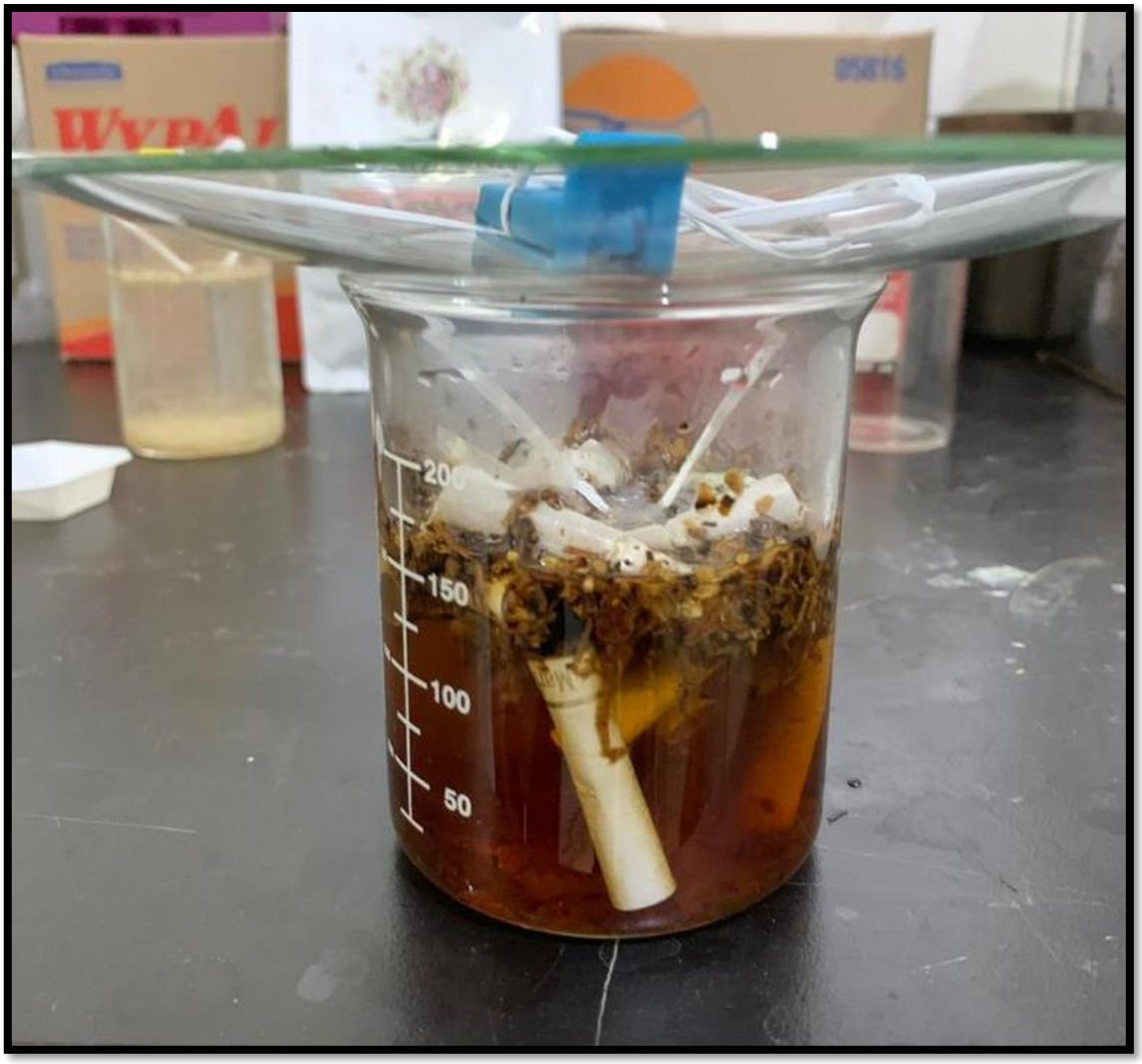

Figure 50: Room temperature corrosion test using used cigarette butts in 15 wt.% HCl over 6h.

Unlike the other controlled room temperature corrosion tests, this test acted as a precursor to determine if cigarette butts possessed any corrosion inhibiting compounds and therefore a strict weight requirement of the corrosion inhibitors was not adhered to. Furthermore, the concentration of such inhibiting compounds could not be accurately calculated prior to the test. From the corrosion test results, the cigarette butts achieved an

inhibition efficiency of 97.9%, indicating that corrosion inhibiting compounds were present in cigarette butts. However, due to the onset of the SARS-COV-2 virus, further collection of used cigarette butts was too dangerous and would be pursued in future studies. The picture of the coupon used before and after the corrosion evaluation test at room temperature is seen in Figure 51.

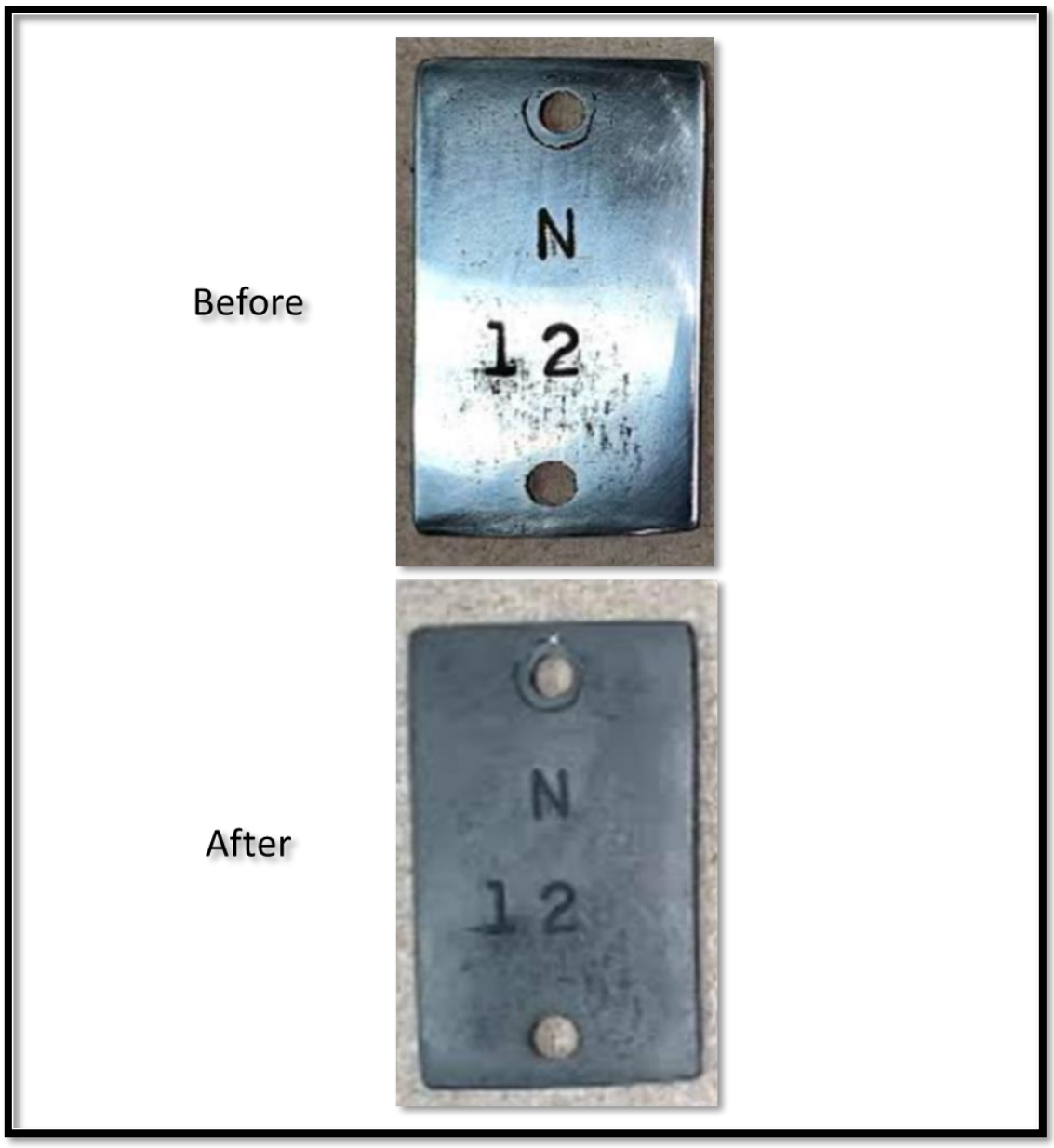

Figure 51: Before and after images of N-80 coupon after corrosion tests with cigarette butts in 15 wt.% HCl at 72°F for 6h.

CHAPTER XIII

EXPIRED MEDICATION

In addition to the recycling efforts of using discarded cigarette butts, corrosion tests using expired medication was carried out. The demand for pharmaceutical products has been increasing every year. However, many of these products are not completely used by patients, leading to the expiration of large quantities of these drugs (Ayele and Mamu 2018). Since a law was passed in 1979, pharmaceutical drug manufacturers were required to place an expiration date on their products. This was to give the consumers some sense of safety regarding the drug potency and effectiveness. Many studies from the food and drug administration showed that more than 90% of expired drugs still contain their active ingredients after the marked expiration date for both over the counter or prescription medication. They noted that the active ingredients were still present and fully functional even after a period of almost 15 years.

These marked expired drugs are typically discarded by garbage or by flushing down the toilet by consumers, causing them to end up in landfills and waterways respectively (Sasu et al. 2012, Wang et al. 2016). These drugs then leach into the nearby water sources and cause accidental poisoning to humans and wildlife as well as damage to the environment (Insani et al. 2020). As a result, it was decided to determine if some of these expired medication could be utilized as corrosion inhibitors.

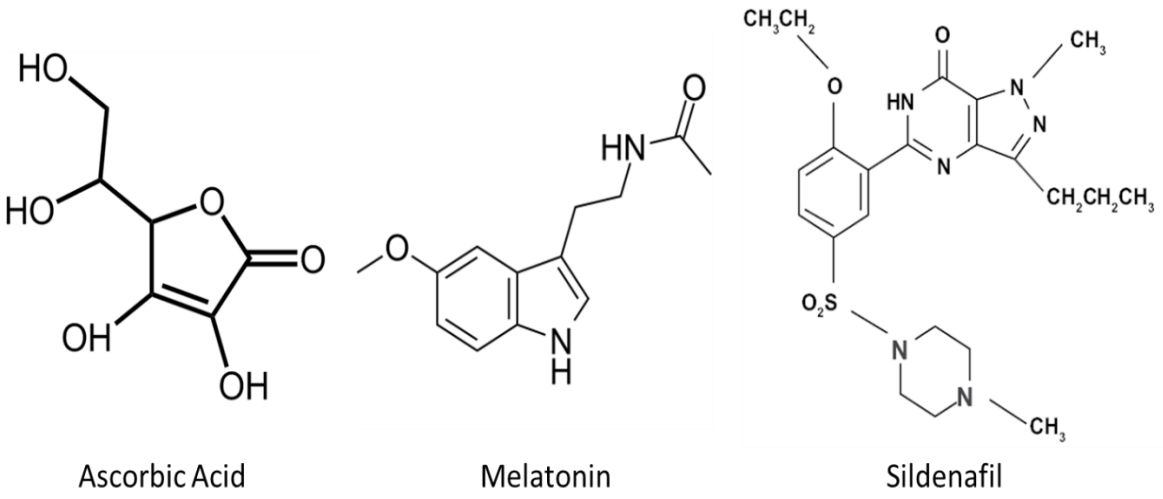

Figure 52: Chemical structures of expired medication tested.

In this work, expired medication used were picked based on the population consumption quantity. Medication related to disorders such as insomnia, allergy, pain, lack of nutrition, energy boosters, anxiety and depression are very common and faced by a significant portion of the population worldwide. For that reason, patients get access to pain medications that contain paracetamol or ibuprofen as the active compounds. They also tend to get access to stronger pain relievers that are typically opioids such as morphine, tramadol and oxycodone. In addition, allergy medications that contain compounds such as loratadine, fexofenadine, and cetirizine are very commonly used. Sleep medications will include compounds such as melatonin, Temazepam, Triazolam, Ramelteon, and Zolpidem. Antidepressants include compounds such as trazadone, fluoxetine, and sertraline. Nutrient enhancing supplements such as vitamins as also heavily bought and unfortunately discarded, sometimes even prior to their expiration

dates. Two heavily bought are ascorbic acid and cholecalciferol, which are commonly known as vitamin C and vitamin D, respectively.

What most of these structure have in common are the benzene rings, nitrogen atoms, and hydrophobic segments. These specific structures all lead to favorable adsorption to the metals in oil and gas well and they have the potential to achieve corrosion inhibition through impermeable layer formation or by sterically hindering and impeding the H^+ attacks from the acids used in the oilfield treatments.

After looking at all these expired chemical options and weighing in the ease of obtaining them for testing, three molecules were chosen as an initial experiment. The molecules chosen were melatonin (6), ascorbic acid (8), and Sildenafil (9). The chemical structures of these compounds are shown in Figure 52 above. All the 3 chemical structures contain combinations of benzene rings, and electron donating groups such as nitrogen and oxygen atoms which allow for adsorption onto the metal surface. Like all the other samples tested, these expired medication were grinded into fine powder before being added to 15 wt.% HCl solution. At room temperature conditions, the 3 samples showed a corrosion inhibition efficiency of 97.5%, 2.4%, and 67.1% respectively. This data is represented in Figure 53 below.

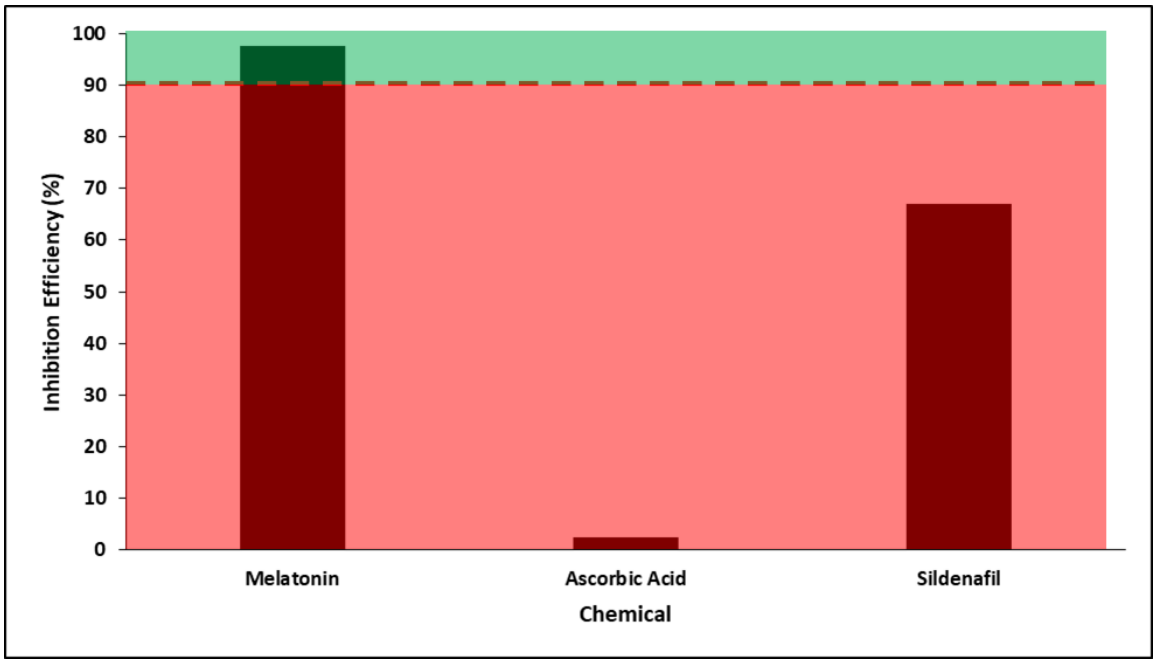

Figure 53: Illustration of corrosion test results for expired medication tests in 15 wt.% HCl at room temperature (72°F) over 6h. Corrosion inhibition efficiencies lying in the green area represent successful tests.

Melatonin performed the best out of the 3 tested samples and had a corrosion inhibition efficiency greater than 90%. Therefore, it was subsequently further tested at 150°F to determine if it would work at high temperatures. In the absence of any corrosion inhibitor intensifier, the corrosion rate was found to be 0.0548 lb/ft^2, exceeding the maximum corrosion rate of 0.05 lb/ft^2 for low carbon steels.

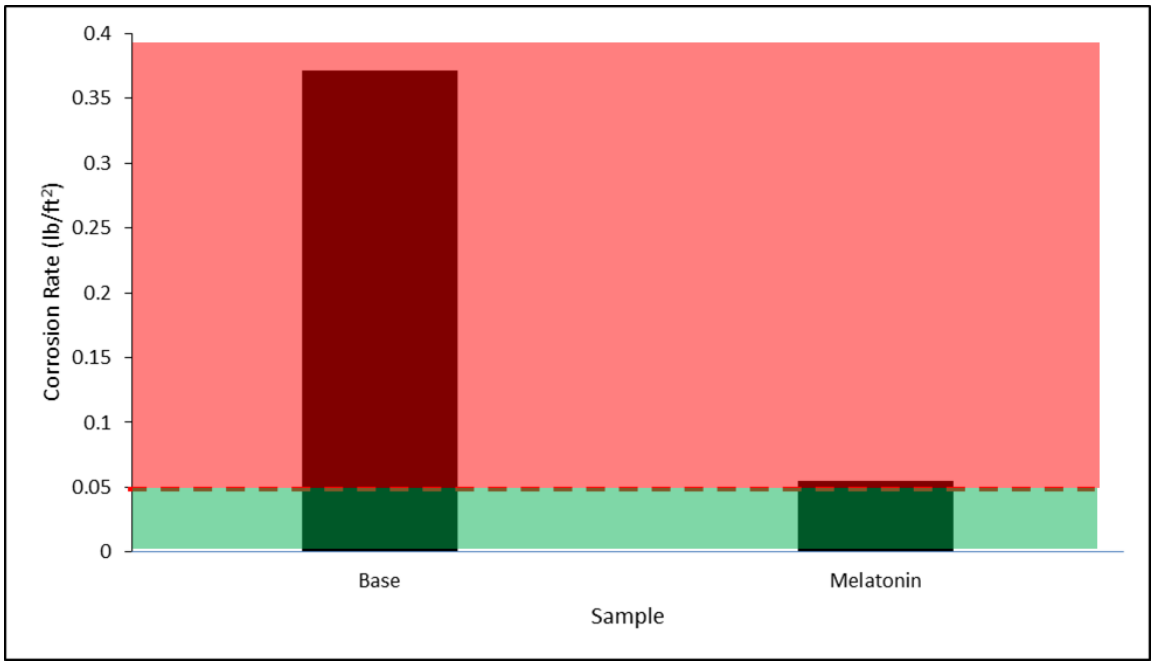

Figure 54: Illustration of corrosion test results for melatonin vs control test in 15 wt.% HCl at 150°F over 6h. Corrosion rates lying in the green area represent successful tests.

In Figure 54, it can be seen that despite the elevated temperature conditions, melatonin is still able to provide 85.2% corrosion inhibition efficiency compared to the control test at this temperature. However, it is still inadequate in terms of the corrosion rate standard. This shows that expired medication has the potential to be used as corrosion inhibitors although more work regarding their concentrations and pairing corrosion inhibitors are required. The before and after images of the coupon can be seen in Figure 55 below. Since the corrosion rate of melatonin is not significantly higher than the maximum limit, the coupon does not appear seriously damaged. This is similar to sample 7 as shown in Figure 21. No significant pitting is observed on the coupon after the test.

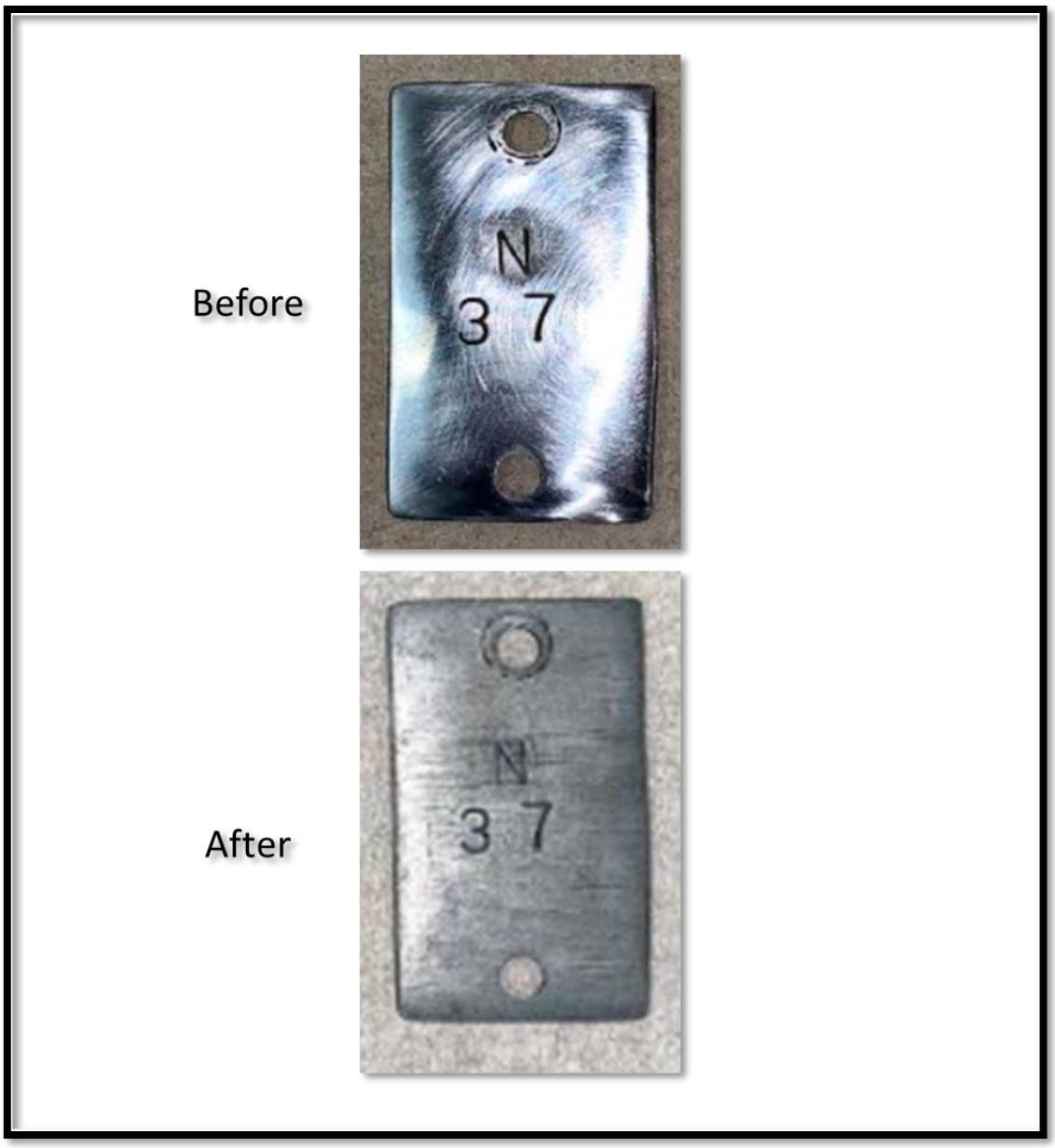

Figure 55: Before and after images of N-80 coupon after the corrosion test with melatonin in 15 wt.% HCl at 150°F for 6h.

CHAPTER XIV

DISCUSSION AND RECOMMENDATIONS

From the results obtained, it can be observed that of the initial 9 samples tested, only 6 samples were effective at temperatures above 150°F. This could be due to the type of decomposition products formed on the surface of the coupon. As shown in the NMR analyses of samples 1 and 3, despite complete degradation at the tested temperature, they are still able to provide sufficient corrosion inhibition to protect the coupon. Therefore, these corrosion inhibitors can be used in low temperature wells as a substitute for traditional corrosion inhibitors.

Sample 1 has been shown to be effective when used at temperatures of 200°F and 250°F in 15 wt.% HCl with low carbon steel coupons. Sample 1 was has also been shown to be effective at protecting CRAs up to temperatures of 200°F. This can be observed from the corrosion rate of sample 1 recorded for low carbon steel at 200°F was 0.0013 lb/ft^2 while that for CRAs was 0.00016 lb/ft^2 at the same temperature. These corrosion rates also show that sample 1 is able to protect CRAs almost 10 times better than low carbon steels, though it should be noted that both these corrosion rate values are well below the 0.05 lb/ft^2 standard that is required for low carbon steel and the 0.03 lb/ft^2 standard required for CRAs. Furthermore, sample 1 was shown to be the only one capable of maintaining a stable emulsion when a cationic emulsifier was used. This is an extremely important property as many commercial corrosion inhibitors have been known to interfere with the emulsifier, causing the emulsion to break prematurely. This would separate the diesel from the aqueous phase giving it full capability to corrode the tubular at high rates. This can be

extreme and can cause the loss of the tubular completely as was seen in the coupon completely dissolving upon separation in the tests. Furthermore, it can be mixed directly into the diesel phase during preparation. This will serve to simplify the preparation of the emulsified acid in the field since no additional mixing units or equipment would be needed. Lastly, sample 1 was able to be solubilized in organic solvents, allowing for the development of a proper liquefied corrosion inhibitor that will prevent the deposition of solid particles in the formation. This property reduces damage to the formation and ensures safety while pumping and reducing the hazard of having to unplug the pumps during the operation. Therefore, sample 1 appears to be the most versatile of the 6 naturally occurring corrosion inhibitors at temperatures up to 250°F.

Sample 3 was also observed to perform well in 15 wt.% HCl solution with low carbon steel coupons at 150, 200, and 250°F. The corrosion rate with low carbon steel was 0.0277 lb/ft^2, 0.01725 lb/ft^2, and 0.00963 lb/ft^2 respectively. It was also observed to perform well when the coupon was changed to the more expensive CRA with a corrosion rate of 0.01026 lb/ft^2. These values were also well below the 0.05 lb/ft^2 standard that is required for low carbon steel and the 0.03 lb/ft^2 standard required for CRAs. Compared to sample 1 however, sample 3 had a higher corrosion rate and is therefore less effective as a corrosion inhibitor. The advantage of sample 3 is its multi functionality. Sample 3 is a surfactant based molecule. It has been shown to not only possess corrosion inhibiting properties, but also demulsifying and emulsifying acid and oil mixtures. This can be especially useful in reducing required additives during acidizing jobs. When dealing with oil sensitive formation demulsifiers are typically required in the formula. However, as

seen from the results, if properly mixed sample 3 can act as both a corrosion inhibitor and a demulsifier. However, this strong demulsifying capability prevents it from being used in conjunction with emulsified acids. Mixing sample 3 to create a proper emulsion is not feasible at the moment and will cause issues in the field operation. The preparation is extremely sensitive and is not as stable as the commercially available emulsifier. So as of writing this dissertation, more work is required towards either enhancing the emulsifying properties to expand it to field application or towards finding an alternative emulsifier that is able to work well with sample 3. Therefore, sample 3 should be used in straight acid solutions only.

Sample 4 showed good performance in the corrosion tests with low carbon steel and CRAs with corrosion rates nearly equaling those of sample 1 at most temperatures. Sample 4 has showed good performance at temperatures of 150, 200, and 250°F. Sample 4 was able to achieve a corrosion rate of 0.00355 lb/ft^2 when used with low carbon steel at 250°F. It was also able to achieve a corrosion rate of 0.00026 lb/ft^2 when used with corrosion resistant alloys at 200°F. These rates are also well below the 0.05 lb/ft^2 standard that is required for low carbon steel and the 0.03 lb/ft^2 standard required for CRAs However, sample 4 appeared to have a mild negative effect on the stability of emulsified acids as witnessed in Figure 28. Unlike sample 3, the emulsified acid solution did not break quickly when sample 4 was added to it which indicates that sample 4 does not react instantly with the emulsifier. This would likely allow it to be able to work with other emulsified acids with different emulsifiers.

Samples 5 was tested with both low carbon steel and CRAs and was shown to provide good corrosion inhibition for both grades of metal. When used with low carbon steel, sample 5 was observed to provide acceptable corrosion rates at 0.0171 lb/ft^2, 0.00878 lb/ft^2, and 0.00151 lb/ft^2 at 150°F, 200°F, 250°F respectively. These rates are one of the lowest compared to the other samples at similar temperatures. With CRAs, the corrosion rate remains relatively similar at 0.0074 lb/ft^2, well below the 0.03 lb/ft^2 limitation for CRAs. Therefore sample 5 can be used with any straight HCl solution on any type of metal up to 250°F.

Samples 7 and 8 were tested with low carbon steel coupons and showed good results for temperatures up to 200°F. However at 250°F, sample 7 exceeded the 0.05 lb/ft^2 limit with a corrosion rate of 0.07996 lb/ft^2. At this temperature, sample 8 had the highest corrosion rate across all of the other successful samples at a corrosion rate of 0.01415 lb/ft^2. Therefore, while sample 7 can only be used up to temperatures of 200°F, sample 8 can be employed at temperatures of up to 250°F.

The initial concentrations used in all the tested samples were 2 wt.%. However, when extracts of the plants were used, a smaller concentration of extract was required to achieve adequate corrosion inhibition properties. The recommended concentration to use is between 0.05-2 wt.% although this will depend on the temperature of the well.

The type of metal will also control the amount of corrosion inhibitor required to use. It will also depend on the duration of pumping and type of treatments being applied in the field. The tests conducted in this work only span 6 hours of metal exposure. If improper placement and chemical flushing was done during the field operation, the tubulars would

be exposed to the acid for much longer periods that can span days or weeks depending on the time the facilities are able to handle the well flowing back. As seen from the discussion above, CRAs are more expensive than low carbon steel and thus typically require higher corrosion inhibitor concentration to reduce the potential damage to the tubular and save cost.

In regards to the recycling initiative towards achieving more environmentally friendly corrosion inhibitors, the tests involving discarded cigarette butts and expired medication show very promising results. Extracting the chemical compounds available in disposed cigarette butts provides inhibition of over 95% towards low carbon steel tubulars. Testing was halted due to the SARS-COV-2 virus making it dangerous to acquire virus-free samples for further testing.

In addition, expired medication such as melatonin, Sildenafil, and ascorbic acid were tested. Out of the three compounds tested, melatonin showed the most promising results, maintaining over 90% corrosion inhibition efficiency at room conditions. Further testing was done and showed that melatonin was able to achieve boarder-line acceptable results at 150°F. The recommendation for using melatonin as environmentally friendly corrosion inhibitors shows initial success at concentrations of 2 wt.% and temperatures up to 150°F for melatonin.

CHAPTER XV

CONCLUSIONS AND FUTURE WORK

Corrosion inhibitors have had a key role in the oil and gas industry by protecting tubular and equipment from the corrosive nature of many commonly used acids commonly. However due to their environmentally unfriendliness and toxicity, newer green alternatives have to be developed. The problem with the previously developed green alternatives is the possibility of them being toxic to humans and to the wildlife. Whereas, the non-toxic alternatives have issues of degradation and failing to provide sufficient metal protection at higher temperatures. This work shows that environmentally friendly and non-toxic corrosion inhibitors can be developed from various plant parts. Some of these samples have been shown to be extremely effective at preventing corrosion at temperatures of 150°F, 200°F, and even 250°F in straight HCl as well as in emulsified acids. These are the conditions that are typically associated with acid treatments worldwide. Furthermore, some of these corrosion inhibitors are also able to serve additional roles as emulsifiers and demulsifiers. This unique property allows for reduction in needed chemicals, eliminated incompatibility with these specific functional chemicals, thus, easing the mixing and pumping operation on the field and ultimately reducing the cost of the operation.

However, it has also been shown that in spite of reducing the reactivity of the acid solution through the use of emulsified acids or the addition of multiple corrosion inhibitor intensifiers, these environmentally friendly corrosion inhibitors still failed to provide sufficient protection to the metal coupons at very high temperature of 300°F and above.

These temperatures are rare, but testing should still aim to overcome this boundary as we continue to explore deeper and high temperature formations. This highlights the need further advancements in emulsifier technology that would allow for the creation of a stable emulsion in the presence of other surfactants. Corrosion inhibitors have also been known to negatively impact many surfactants commonly used in the oil and gas industry since corrosion inhibitors are also surfactant based. These new corrosion inhibitors are no exception as can be seen from the demulsifying and emulsifying properties of sample 3. Therefore they need to be adequately tested with the pumped solution to determine if there are any possible interactions.

In future work, more plant parts such as sample 5, 7 and 8 will require testing with emulsified acids. These samples have the potential to work well with emulsified acids as initial compatibility tests were positive, however, high temperature tests were not conducted due to limitation in equipment availability at the time. More plant parts will be tested via the same procedure to discover additional naturally occurring sources of corrosion inhibitors. There are hundreds of plant parts that are being produced annually but are not likely to be seen in the local grocery stores. Some of these exotic produces can contain corrosion inhibiting molecules that can potentially work at oil and gas field conditions.

In addition, more chemical analyses will be carried out to determine the identity of the degraded chemical common to sample 1 and 3. These molecules are likely responsible for the corrosion inhibition properties as shown in the tests. Determining these molecules and being able to identify the corrosion inhibition mechanisms is a study that will help

identify other molecules capable of surviving the harsh oil and gas environments. Moreover, commercial emulsifiers, acid retarders, and new corrosion inhibitor intensifiers are continuously being developed, newer technologies will be tested in order to create a stable emulsion and a working acid solution at 300°F and above.

In regard to expired medications, compounds such as melatonin almost passed the criteria required without the presence of corrosion inhibitor intensifiers. Further testing should be conducted in the presence of intensifiers to evaluate its effectiveness at a temperature of 150 and 200°F. Additionally, compatibility with emulsified acid should be evaluated as emulsified acids are more commonly used and melatonin could provide acceptable performance in emulsified acid form. These tests show that environmentally friendly approaches can be achieved through recycling wasted products from the environment. These recycled products are cheap since they don't require manufacturing. The only cost associated with using them would be the waste gathering and separation cost.

Additional testing would also be required for all corrosion inhibitor samples if treatments are to be conducted in long horizontal oil and gas wells. Horizontal well acidizing jobs can have a much higher concentration than what was tested, typically a concentration of almost 28 wt.% HCl would be used and that needs to be evaluated for each corrosion inhibitor. This high concentration can cause issues of compound degradation and emulsified acid separation, which would ultimately lead to extreme corrosion rates especially at high temperatures conditions.

Lastly, in an effort to protect food resources and in an attempt to reduce cost, once the working molecules are confirmed, partnerships with chemical companies can be utilized to produce these molecules via synthetic pathways, which would be much cost effective than extracting these molecules from produces being consumed by the population worldwide.

REFERENCES

Al-Katheeri, M., Nasr-El-Din, H., Taylor, K. et al. 2002. Determination and Fate of Formic Acid in High Temperature Acid Stimulation Fluids. Presented at the International Symposium and Exhibition on Formation Damage Control, Lafayette, Louisiana, 20-21 February. SPE-73749-MS. https://doi.org/10.2118/73749-MS.

Almubarak, T., Alkhaldi, M., Ng, J. H. et al. 2020. Matrix Acidizing: A Laboratory and Field Investigation of Sludge Formation and Removal of Oil-Based Drilling Mud Filter Cake. *SPE Drill & Compl*. **Preprint** (Preprint): SPE-178034-PA. https://doi.org/10.2118/178034-PA.

Almubarak, T., Alkhaldi, M., Ng, J. H. et al. 2020. Matrix Acidizing: A Laboratory and Field Investigation of Sludge Formation and Removal of Oil-Based Drilling Mud Filter Cake. *SPE Drill & Compl*. **Preprint** (Preprint): SPE-178034-PA. https://doi.org/10.2118/178034-PA.

Almubarak, T., Ng, J. H. and Nasr-El-Din, H. 2017. Chelating Agents in Productivity Enhancement: A Review. Presented at the SPE Oklahoma City Oil and Gas Symposium, Oklahoma City, Oklahoma, USA, 27–31 March. SPE-185097-MS. https://doi.org/10.2118/185097-MS.

Al-Mutairi, S. H, Nasr-El-Din, H. A., Al-Muntasheri, G. A. et al. 2005. Corrosion Control During Acid Fracturing of deep Gas Wells: Lab Studies and Field cases. Presented at the SPE International Symposium on Oilfield Corrosion held in Aberdeen, UK, 13 May. SPE 94639.

Al-Taq, A. A., Ali, S. A., Al-Haji, H. et al. 2012. Performance of Synthesized Amine-based Corrosion Inhibitors in Concentrated HCl Acid Solutions: Effect of Intensifier. Presented at the SPE International Conference & Workshop on Oilfield Corrosion, Aberdeen, UK, 28-29 May. SPE-154957-MS. https://doi.org/10.2118/154957-MS.

API SPEC 5CT, Petroleum and natural gas industries—Steel pipes for use as casing or tubing for wells, eighth edition. 2005. Washington, D.C.: API.

Ayele, Y. and Mamu, M. 2018. Assessment of knowledge, attitude and practice towards disposal of unused and expired pharmaceuticals among community in Harar city, Eastern Ethiopia. *Journal of Pharmaceutical Policy and Practice*. **11** (1): 27. http://dx.doi.org/10.1186/s40545-018-0155-9.

Barmatov, E., Hughes, T. and Nagl, M. 2015. Performance of Organic Corrosion Inhibitors on Carbon Steels and High Alloys in 4M Hydrochloric Acid. Presented at the CORROSION 2015, Dallas, Texas, 15-19 March. NACE-2015-5893.

Benavente, M., Caballero, M., Silvero, G. et al. 2019. Cellulose Acetate Recovery from Cigarette Butts. *Proceedings*. **2** (20): http://dx.doi.org/10.3390/proceedings2201447.

Bockris, J. 1991. The Mechanism of Corrosion Inhibition of Iron in Acid Solution by Acetylenic Alcohols. Journal of The Electrochemical Society. 138 (8): http://dx.doi.org/10.1149/1.2085956.

Buijse, M., Boer, P. d., Breukel, B. et al. 2004. Organic Acids in Carbonate Acidizing. SPE Prod & Fac 19 (03): 128 - 134. SPE-82211-PA. https://doi.org/10.2118/82211-PA.

Cassidy, J. M., McNeil, R. I. and Kiser, C. 2007. Understanding Formic Acid Decomposition as a Corrosion Inhibitor Intensifier in Strong Acid Environments. Presented at the International Symposium on Oilfield Chemistry, Houston, Texas, U.S.A., 28 February-2 March. SPE-106185-MS. https://doi.org/10.2118/106185-MS.

Cassidy, J. M., Wadekar, S. and Pandya, N. K. 2012. A Unique Emulsified Acid System with Three Intensifiers for Stimulation of Very High Temperature Carbonate Reservoirs. Presented at the SPE Kuwait International Petroleum Conference and Exhibition, Kuwait City, Kuwait, 10-12 December. SPE-163308-MS. https://doi.org/10.2118/163308-MS.

Chang, F. F., Nasr-El-Din, H. A., Lindvig, T. et al. 2008. Matrix Acidizing of Carbonate Reservoirs Using Organic Acids and Mixture of HCl and Organic Acids. Presented at the SPE Annual Technical Conference and Exhibition, Denver, Colorado, USA, 21-24 September. SPE-116601-MS. https://doi.org/10.2118/116601-MS.

Chen, H. J., Jepson, W. P. and Hong, T. 2000. High Temperature Corrosion Inhibition Performance of Imidazoline and Amide. Presented at the CORROSION 2000, Orlando, Florida, 26-31 March. NACE-00035.

Chigondo, M. and Chigondo, F. 2016. Recent Natural Corrosion Inhibitors for Mild Steel: An Overview. Journal of Chemistry. 2016: 1-7. http://dx.doi.org/10.1155/2016/6208937.

Compound Interest. 2014. The Chemicals in Cigarette Smoke & Their Effects, https://www.compoundchem.com/2014/05/01/the-chemicals-in-cigarette-smoke-their-effects/ (accessed 16 January 2021)

Craig, B. D. and Smith, L. 2001. *Corrosion Resistant Alloys (CRAs) in the oil and gas industry – selection guidelines update*, 3rd edition, North Carolina: Nickel Institute Technical Series.

da Rocha, J., da Cunha Ponciano Gomes, J., and D'Elia, E. 2010. Corrosion inhibition of carbon steel in hydrochloric acid solution by fruit peel aqueous extracts. Corrosion Science 52 (7): 2341-2348. http://dx.doi.org/10.1016/j.corsci.2010.03.033.

Durnie, W., Auty, L., Gough, M. et al. 2002. Characterization, Isolation and Performance Characteristics of Imidazolines. Presented at the CORROSION 2002, Denver, Colorado, 7-11 April. NACE-02301.

El Dahan, H., Mohamed, T., and Abo El-Enin, S. 1999. Efficient quaternary ammonium salt as corrosion inhibitor for steel pickling in sulphuric acid media. Anti-Corrosion Methods and Materials 46 (5): 358-363. http://dx.doi.org/10.1108/00035599910295571.

Elewady, G. and Mostafa, H. 2009. Ketonic secondary Mannich bases as corrosion inhibitors for aluminium. Desalination. 247: 573-582. http://dx.doi.org/10.1016/j.desal.2008.08.006.

Elmsellem, H., Youssouf, M., Aouniti, A. et al. 2014. Adsorption and inhibition effect of curcumin on mild steel corrosion in hydrochloric acid. Russian Journal of Applied Chemistry 87 (6): 744-753. http://dx.doi.org/10.1134/s1070427214060147.

Fidrusli, A. and Mahmood, M. 2018. Ginger extract as green corrosion inhibitor of mild steel in hydrochloric acid solution. IOP Conference Series: Materials Science and Engineering 290 http://dx.doi.org/10.1088/1757-899x/290/1/012087.

Finsgar, M. and Jackson, J. 2014. Application of corrosion inhibitors for steels in acidic media for the oil and gas industry: A review. Corrosion Science 86 (1): 17-41. http://dx.doi.org/10.1016/j.corsci.2014.04.044.

Fontana, M. and Greene, N. 1967. Corrosion Engineering, first edition, New York: Mc-Graw Hill.

Foster, G. L., Oakes, B. D. and Kucera, C. H. 1959. Acetylenic Corrosion Inhibitors. Ind. Eng. Chem. 51 (7): 825-828. https://doi.org/10.1021/ie50595a027.

Hegazy, M., Abdallah, M., Awad, M. et al. 2014. Three novel di-quaternary ammonium salts as corrosion inhibitors for API X65 steel pipeline in acidic solution. Part I: Experimental results. Corrosion Science 81: 54-64. http://dx.doi.org/10.1016/j.corsci.2013.12.010.

Henderson, S., Grigson, S., Johnson, P. et al. 1999. Potential Impact of Production Chemicals on the Toxicity of Produced Water Discharges from North Sea Oil Platforms. *Marine Pollution Bulletin* **38** (12): 1141-1151. http://dx.doi.org/10.1016/s0025-326x(99)00144-7.

Insani, W., Qonita, N., Jannah, S. et al. 2020. Improper disposal practice of unused and expired pharmaceutical products in Indonesian households. *Heliyon*. **6** (7): e04551. http://dx.doi.org/10.1016/j.heliyon.2020.e04551.

Kalfayan, L. 2008. Production Enhancement with Acid Stimulation, p. 5. Tulsa, Oklahoma: PennWell Corporation.

Khadom, A., Abd, A., and Ahmed, N. 2018. Potassium Iodide as a Corrosion Inhibitor of Mild Steel in Hydrochloric Acid: Kinetics and Mathematical Studies. Journal of Bio- and Tribo-Corrosion. 4 (2): 17. http://dx.doi.org/10.1007/s40735-018-0133-4.

Khamis E., and Alandis, N. 2002. Herbs as new type of green inhibitors for acidic corrosion of steel. Materialwissenschaft und Werkstofftechnik 33 (9): 550-554. http://dx.doi.org/10.1002/1521-4052(200209)33:9<550::AID-MAWE550>3.0.CO;2-G

Kurek, J. 2019. Alkaloids - Their Importance in Nature and for Human Life, 1st Edition. : IntechOpen.

Mahmoud, M. A., Nasr-El-Din, H. A., Wolf, C. D. et al. 2010. Stimulation of Carbonate Reservoirs Using GLDA (Chelating Agent) Solutions. Presented at the Trinidad and Tobago Energy Resources Conference, Port of Spain, Trinidad, 27-30 June. SPE-132286-MS. https://doi.org/10.2118/132286-MS.

Marway, J., Anderson, G., Miell, J. et al. 1996. Application of proton NMR spectroscopy to measurement of whole-body RNA degradation rates: effects of surgical stress in human patients. Clinica Chimica Acta 252 (2): 123-135. http://dx.doi.org/10.1016/0009-8981(96)06300-0.

Nasr-El-Din, H., Solares, J., Al-Mutairi, S. et al. 2001. Field Application of Emulsified Acid-Based System to Stimulate Deep, Sour Gas Reservoirs in Saudi Arabia. Presented at the SPE Annual Technical Conference and Exhibition, New Orleans, Louisiana, 30 September-3 October. SPE-71693-MS. https://doi.org/10.2118/71693-MS.

Ng, J. H., Almubarak, T. and Nasr-El-Din, H. A. 2018. Low-Carbon-Steel Corrosion at High Temperatures by Aminopolycarboxylic Acids. SPE Prod & Oper 33 (01): 131 - 144. SPE-188007-PA. https://doi.org/10.2118/188007-PA.

Parthipan, P., Elumalai, P., Narenkumar, J. et al. 2018. Allium sativum (garlic extract) as a green corrosion inhibitor with biocidal properties for the control of MIC in carbon steel and stainless steel in oilfield environments. International Biodeterioration & Biodegradation. 132: 66-73. http://dx.doi.org/10.1016/j.ibiod.2018.05.005.

Petersen, C. W. and Bleum, M. F. 1989. Requirements for Corrosion-Resistant Alloy (CRA) Production Tubing. Presented at the SPE Annual Technical Conference and Exhibition, San Antonio, Texas, 8-11 October. SPE-19727-MS. https://doi.org/10.2118/19727-MS.

Rafie, M., Said, R., Al-Hajri, M. et al. 2014. The First Successful Multistage Acid Frac of an Oil Producer in Saudi Arabia. Presented at the SPE Saudi Arabia Section Technical Symposium and Exhibition, Al-Khobar, Saudi Arabia, 21-24 April. SPE-172224-MS. https://doi.org/10.2118/172224-MS.

Raja, P. and Sethuraman, M. 2008. Natural products as corrosion inhibitor for metals in corrosive media — A review. Materials Letters 62 (1): 113-116. http://dx.doi.org/10.1016/j.matlet.2007.04.079.

Ramanathan, R. S., Nasr-El-Din, H. A. and Zakaria, A. S. 2020. New Insights into the Dissolution of Iron Sulfide Using Chelating Agents. SPE J.. Preprint (Preprint): SPE-202469-PA. https://doi.org/10.2118/202469-PA.

Rani, B. and Basu, B. 2012. Green Inhibitors for Corrosion Protection of Metals and Alloys: An Overview. International Journal of Corrosion. 2012: 1-15. http://dx.doi.org/10.1155/2012/380217.

Raya, S., Mohd Saaid, I., Abbas Ahmed, A. et al. 2020. A critical review of development and demulsification mechanisms of crude oil emulsion in the petroleum industry. *Journal of Petroleum Exploration and Production Technology* **10** (4): 1711-1728. http://dx.doi.org/10.1007/s13202-020-00830-7.

Rostami, A. and Nasr-El-Din, H. 2009. Review and Evaluation of Corrosion Inhibitors Used in Well Stimulation. Presented at the SPE International Symposium on Oilfield Chemistry, The Woodlands. Texas, 20-22 April, SPE-121726-MS, https://doi.org/10.2118/121726-MS.

Sasu, S., Kümmerer, K., and Kranert, M. 2012. Assessment of pharmaceutical waste management at selected hospitals and homes in Ghana. *Waste Management & Research* **30** (6): 625-630. http://dx.doi.org/10.1177/0734242x11423286.

Sedik, A., Lerari, D., Salci, A. et al. 2020. Dardagan Fruit extract as eco-friendly corrosion inhibitor for mild steel in 1 M HCl: Electrochemical and surface morphological studies. Journal of the Taiwan Institute of Chemical Engineers 107: 189-200. http://dx.doi.org/10.1016/j.jtice.2019.12.006.

Selmar, D., Radwan, A., Abdalla, N. et al. 2018. Uptake of nicotine from discarded cigarette butts – A so far unconsidered path of contamination of plant-derived commodities. *Environmental Pollution*. **238**: 972-976. http://dx.doi.org/10.1016/j.envpol.2018.01.113.

Singh, W., and Bockris, J. 1996. Toxicity Issues of Organic Corrosion Inhibitors: Applications of QSAR Model. Presented at the CORROSION 96, Denver, Colorado, 24-29 March. NACE-96225.

Slaughter, E., Gersberg, R., Watanabe, K. et al. 2011. Toxicity of cigarette butts, and their chemical components, to marine and freshwater fish. *Tobacco Control*. **20**: 25-. http://dx.doi.org/10.1136/tc.2010.040170.

Son, A. J. 2007. Developments In The Laboratory Evaluation Of Corrosion Inhibitors: A Review. Presented at the CORROSION 2007, Nashville, Tennessee, 11-15 March. NACE-07618.

Tang, J., Wang, H., Jiang, X. et al. 2018. Electrochemical behavior of jasmine tea extract as corrosion inhibitor for carbon steel in hydrochloric acid solution. International Journal of Electrochemical Science, 13, (4):, 3625 - 3642. http://dx.doi.org/10.20964/2018.04.41.

Tang, M., Li, J., Li, Z. et al. 2019. Mannich Base as Corrosion Inhibitors for N80 Steel in a CO2 Saturated Solution Containing 3 wt % NaCl. Materials. 12 (3): 449 – 464 http://dx.doi.org/10.3390/ma12030449.

Umoren, S., Obot, I., Gasem, Z. et al. 2015. Experimental and Theoretical Studies of Red Apple Fruit Extract as Green Corrosion Inhibitor for Mild Steel in HCl Solution. Journal of Dispersion Science and Technology 36 (6): 789-802. http://dx.doi.org/10.1080/01932691.2014.922887.

Wang, X., Howley, P., Ba Boxall, A. et al. 2016. Behavior, preferences, and willingness to pay for measures aimed at preventing pollution by pharmaceuticals and personal

care products in China. *Integr Environ Assess Manag*, **12**, (4):, 793-800. . http://dx.doi.org/10.1002/ieam.1746.

Yaakob, A. and Sulaimon, A. 2017. Performance Assessment of Plant Extracts as Green Demulsifiers. *Journal of the Japan Petroleum Institute* **60** (4): 186-193. http://dx.doi.org/10.1627/jpi.60.186.

Yang, J., Gao, L., Liu, X. et al. 2016. A Highly Effective Corrosion Inhibitor by Use of Gemini Imidazoline. SPE J. 21 (05): 1,743 - 1,746. SPE-173777-PA. https://doi.org/10.2118/173777-PA.

Yaro, A., Khadom, A., and Ibraheem, H. 2011. Peach juice as an anti‐corrosion inhibitor of mild steel. Anti-Corrosion Methods and Materials 58 (3): 116-124. http://dx.doi.org/10.1108/00035591111130497.

Zhao, A., Sun, H., Chen, L. et al. 2019. Electrochemical studies of bitter gourd (Momordica charantia) fruits as ecofriendly corrosion inhibitor for mild steel in 1 M HCl solution. Int. J. Electrochem. Sci. 14 (7): 6814-6825. http://dx.doi.org/10.20964/2019.07.75

Zucchi, F. and Omar, I. 1985. Plant extracts as corrosion inhibitors of mild steel in HCl solutions. Surface Technology 24 (4): 391-399. http://dx.doi.org/10.1016/0376-4583(85)90057-3.